ENGINEERED VASCULAR TISSUE GENERATED BY CELLULAR SELF-ASSEMBLY
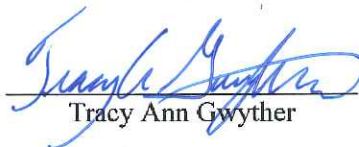
A Dissertation

Submitted to the Faculty of the
WORCESTER POLYTECHNIC INSTITUTE

in partial fulfillment of the requirements for the

Degree of Doctorate of Philosophy
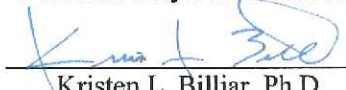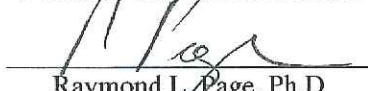in Biomedical Engineering

January 13, 2012

By

Tracy Ann Gwyther

Marsha W. Rolle, Ph.D
Assistant Professor, Advisor
Biomedical Engineering Department
Worcester Polytechnic Institute

Kristen L. Billiar, Ph.D
Associate Professor
Biomedical Engineering Department
Worcester Polytechnic Institute

Raymond L. Page, Ph.D
Assistant Professor
Biomedical Engineering Department
Worcester Polytechnic Institute

Tanja Dominko, DVM, Ph.D
Associate Professor
Biology and Biotechnology Department
Worcester Polytechnic Institute

Stelios T. Andreadis, Ph.D
Professor
Chemical and Biological Engineering
SUNY at Buffalo

Acknowledgements

I would like to thank my advisor, Marsha Rolle, for all of her guidance and support over the years.

I would also like to thank my committee members for their feedback, discussions, and guidance throughout this project.

I am grateful to all of my fellow graduate students, collaborators, and undergraduate students who have helped me throughout the years. I appreciate all of the support and the positive reinforcement.

I would like to especially thank the people who have helped me with this project; Jason Hu, Sharon Shaw, Alex Christakis, Jeremy Skorinko, Funmi Adebayo, Jenn Mann, Michelle Tran, Bethany Almeida, Brittany Alphonse, and Zoe Reidinger.

I would like to thank Chris Malcuit, Tanja Dominko, and Ray Page of Cell Thera, Inc. for their use and assistance with the polarized light microscope. I would also like to thank both Sakthi Ambady and Chris Malcuit for their assistance with molecular biology.

I would like to thank Jason Hu and Matt Phaneuf from BioSurfaces, Inc. for generously donating electrospun material for tube fusion studies. Also, I would like to thank Drs. John Keaney and Siobhan Craige at UMMS for their assistance with myography. Additionally, we would like to thank Dr. Thomas Wight of Benaroya research institute for their generous donation of rat aortic smooth muscle cells.

I also would not have been able to complete this project without expert technical assistance from Jack Ferraro, Neil Whitehouse, and Sia Najafi. Thank you!

I would like to give special thanks to my family and friends for loving and supporting me through this process. A special thank you to my husband, Steve Hookway - I would never have been able to get through this experience without you.

Table of Contents

Table of Figures

Table of Tables

Abbreviations

ANOVA – Analysis of variance
ANG II – Angiotensin II
DMEM – Dulbecco's modified eagle medium
CALP – Calponin
CDM – Cell-derived matrix
ECs – Endothelial cells
ECM – Extracellular matrix
EGF – Epidermal growth factor
FBS – Fetal bovine serum
FGF – Fibroblast growth factor
GAG – Glycosaminoglycans
H&E – Hematoxylin & Eosin
hMSC – Human mesenchymal stem cells
hTERT – Human telomerase reverse transcriptase
IGF – Insulin-like growth factor
KPSS – Potassium rich – physiological salt solution
MMPs – Matrix metalloproteinases
MSCGM – Mesenchymal stem cell growth medium
MTM – Maximum tangent modulus
PBS – Phosphate buffered saline
PCI – Percutaneous coronary intervention
PCNA – Proliferating cell nuclear antigen
PDGF – Platelet derived growth factor
PDMS – Polydimethylsiloxane
PGA – Polyglycolic Acid
PSS – Physiological salt solution
RFL-6 – Fetal rat lung fibroblasts
SMA – Smooth muscle alpha-actin
SMC – Smooth muscle cells
SPG – Sulfated proteoglycans
SmGM-2 – Smooth muscle cell growth medium
TEBV – Tissue engineered blood vessels
TGFβ – Transforming growth factor beta
UTS – Ultimate tensile strength
VEGF – Vascular endothelial growth factor

Abstract

Small diameter vascular grafts comprised entirely from cells and cell-derived extracellular matrix (ECM) have shown promise in clinical trials and may have potential advantages as *in vitro* vascular tissue models. A challenge with current cell-derived tissue engineering approaches is the length of time required to generate strong, robust tissue. There is a lack of alternative methods to rapidly assemble cells into a 3D format without the support of a scaffold. Toward the goal of engineering a new approach to rapidly synthesizing vascular tissue constructs entirely from cells, we have developed and characterized a strategy for creating cell-derived tissue rings by cellular self-assembly. The focus of this thesis was to develop the system to rapidly generate engineered tissue rings, and to evaluate their structural and functional properties.

To generate tissue rings, rat smooth muscle cells (SMCs) were seeded into round-bottomed, ring-shaped agarose wells with varying inner post diameters (2, 4, and 6 mm). Within 24 hours of seeding, cells aggregated, contracted, and formed robust tissue that could be removed from their wells and handled. If kept in culture, the thickness of these tissue rings increased with time. Mechanical analysis of the tissue showed that it was stronger after only 8 days in culture than engineered tissues generated by other approaches (such as seeding cells in biopolymer gels) cultured and tested at similar time points. Histological staining of the tissue rings revealed high cell densities throughout, along with the presence of glycosaminoglycans and some collagen. We also found that we could use the tissue rings as building blocks to generate larger tubular structures. Briefly, tissue rings were removed from the agarose wells and transferred onto silicone tubing mandrels. Once the rings were placed in contact with each other on the mandrel, they were cultured to allow the rings to fuse together. We found that the ability of tissue rings to fuse decreased with increasing ring "pre-culture" duration, and that we were able to generate fully fused tissue tubes in as little as 8 days (with only one day of ring pre-culture and seven days of fusion).

In the last section of this thesis, we established the feasibility of using primary human SMCs to generate self-assembled tissue rings, similar to the self-assembled rings generated with rat SMCs. Compared to the rat SMC rings, human SMC rings were stronger, stiffer and appeared to contain increased levels of collagen. These data showed that human SMCs are capable of self-assembling into tissue rings similar to rat SMCs, and may therefore be used to create engineered human vascular tissue.

Overall, we have developed a platform technology that can be used to screen the effects of culture parameters on the structure, mechanics, and function of vascular tissue. We anticipate that through the use of this technology, we can further improve vascular grafts by better understanding factors which promote ECM synthesis and SMC contraction. We can use these results directly toward the generation of vascular grafts by fusing self-assembled cell rings together to form tissue tubes. These novel bioengineered vascular tissues may also serve as a method to produce *in vitro* models to help further our understanding of vascular diseases, as well as facilitate pre-clinical screening of vascular tissue responses to pharmacologic therapies.

Chapter 1: Overview

1.1 Introduction

Cardiovascular disease is one of the leading causes of morbidity and mortality in the United States. According to American Heart Association statistics, 16 million Americans have been diagnosed with coronary heart disease and over 8 million of these people have had a myocardial infarction.[1] In 2004, 408,000 coronary artery bypass grafting (CABG) procedures were performed to restore blood flow to myocardial tissue where blood flow had been compromised by occluded or partially occluded coronary arteries.[1] The standard of care in CABG is to use the patients' own (autologous) vessels, most commonly the internal mammary artery, radial artery, or saphenous vein, as the donor vessel for the bypass procedure.[2,3] However, in approximately one third of these patients, such as those with advanced peripheral vascular disease or those undergoing a second CABG procedure, there is insufficient availability of autologous vessel material. As the number of patients needing CABG procedures rises due to the increasing age of the U.S. population and prevalence of obesity, there is a need to develop alternative grafting materials. Synthetic grafts have been used widely for vascular surgery to replace large vessels (> 6 mm diameter) such as the abdominal aorta, but small diameter synthetic grafts (< 5 mm diameter) fail due to thrombosis or intimal hyperplasia.[4-7] Alternative graft materials include allogeneic or xenogeneic grafts, but the use of these materials requires life-long immunosuppression therapy, and they will eventually fail.[8-10] As such, there is a great need for strong vascular grafts that can remain patent as small diameter vessel replacements without the need for immunosuppressive or anticoagulant therapy. To meet this need, tissue engineering has been explored as a promising approach to generating vascular grafts that have similar mechanical and biological properties to those of native arteries.

The concept of creating tissue engineered blood vessels was first explored in the 1980's with the innovative approach of encapsulating vascular cells in tubular collagen gels and allowing the cells to remodel the gel during culture *in vitro*.[11] While the field has advanced considerably since then, the basic principle of adding cells to either natural biopolymer[12-14] or synthetic polymer[15,16] scaffolds remains the primary method for generating tissue-engineered vascular grafts. In fact, a co-polymer of lactic acid and ε-caprolactone seeded with autologous bone marrow cells has been used clinically for pediatric cardiovascular surgery.[17-19] More recently, clinical trials have been conducted with vascular grafts made

entirely out of autologous patient cells and the extracellular matrix (ECM) the cells produce (without exogenous scaffold material).[20] With all approaches to vascular graft development, researchers have improved on many aspects, including increased burst pressure strengths,[21,22] increased ECM synthesis,[23,24] and improved biocompatibility and patency.[25-27] Together, the combination of these improved characteristics has progressed the field considerably; giving rise to many promising approaches toward solving the clinical need for small-diameter vascular conduits.

Despite the advances in the field of vascular tissue engineering over the past three decades, many challenges still remain. For example, most vascular tissue engineering approaches have yielded grafts with low cell densities,[15,28] low compliance,[29] and limited physiological contraction when compared to native arteries.[15] The use of scaffold materials as the structural foundation of most tissue engineered grafts may be partially responsible for these limitations. Scaffold materials dominate graft mechanical properties and have been shown to limit cell-seeding densities,[15,28] which can lead to limited vascular contraction. To address these shortcomings, cell-derived approaches to vascular tissue engineering have been developed.[20,21,30-34] Cell-derived tissues have much higher cell densities and improved compliance.[31,35]

However, two challenges of cell-derived vascular tissue engineering are the quantity of cells and the long culture times required to generate tissue constructs. The production options are either to expand cells in culture in advance and use high initial cell seeding densities to generate tissues, or to seed lower initial densities and allow the cells to proliferate and generate ECM to build the tissue over time. In either approach, there are a variety of culture parameters which need optimization (such as culture duration, cell source, media supplementation, etc.) to produce functional vascular grafts. Due to the large quantity of cells and the long culture times required for cell-derived vascular graft generation, evaluating and optimizing culture conditions on full-sized tubular constructs would be an expensive, reagent-, and time-consuming process. Therefore, there is a need for a method to rapidly generate 3D tissue constructs, which would use fewer cells, require less culture time, and could be used to "screen" the effects of a variety of culture conditions on the mechanical, functional, and structural properties of vascular tissue. The information obtained throughout this screening process could then be applied to the generation of transplantable vascular grafts from cells and cell-derived ECM.

1.2 Summary of thesis objectives

To address some of the current challenges in vascular graft tissue engineering, the overall objective of this project was to develop a system to rapidly generate cell-derived, scaffold-free vascular tissue constructs from self-assembled cells. To do this, we placed smooth muscle cells into round-bottomed, annular wells and allowed them to aggregate and generate ring-shaped tissues. We utilized these tissue rings to assess the structural and functional properties of cell-based engineered tissues. In addition, we showed that cell-derived tissue rings can be stacked together in culture, and that the rings remodeled and fused to form tissue tubes. Based on this observation, we then investigated parameters such as the length of time rings were "pre-cultured" prior to being stacked together as a means of controlling their fusion into tissue tubes. Finally, we evaluated whether this system of tissue self-assembly, which we developed and assessed using rat smooth muscle cells (SMCs), could be translated to generate tissue constructs from primary human SMCs, which proliferate at a much lower rate in culture.

Objective 1: Create and validate a novel scaffold-free 3D vascular tissue model system based on cellular self-assembly.

To address the need for rapid generation of vascular tissue, the first objective of this thesis was to develop a scaffold-free, cell-derived ring model system which we used to evaluate the function and structure of tissue formed using this technique. To do this, a mold was developed that contained non-adhesive, round-bottomed, annular agarose wells which allowed cell aggregation, thus self-assembly into ring-shaped tissues. Tissue rings were made with different diameters (2, 4, and 6 mm inner diameter) and cultured for various lengths of time (7 – 14 days). We utilized uniaxial tensile testing combined with histology and light microscopy to examine how these different culture parameters affected tissue biomechanics and morphology. Our results indicated that cell-derived, self-assembled tissue rings were significantly stronger than tissues formed using the SMCs in gels approach, cultured over a similar time period.[36,37] Additionally, we demonstrated that generating tissue rings through the use of SMC self-assembly yields tissue constructs with a high cell density and evidence of ECM deposition compared to the same "SMCs in gels" tissues. Finally, to demonstrate that the tissue ring system can be translated into fabricating tubular tissues of clinically useful sizes, tissue rings cultured for seven days were stacked together on silicone mandrels and investigated for their ability to form cell-derived tissue tubes by fusion of individual rings. Together, these studies suggest that this self-assembled ring system can be used to assess structure and function of vascular tissue, and that the information gained from manipulation of this system can then be directly applied to the fabrication of tissue engineered vascular grafts. *Gwyther, T.A.,*

Hu, J.Z., Christakis A.G., Skorinko J.K., Shaw S.M., Billiar K.L., Rolle M.W. "Engineered vascular tissue fabricated from aggregated smooth muscle cells." Cells Tissue Organs, 194(1):13-24, 2011.[38]

Objective 2: Identify culture parameters that lead to enhanced fusion of aggregated cell rings to create vascular tissue tubes.

Above, we explore the potential use of self-assembled cell rings as building blocks with which to generate tube-shaped tissue constructs. Although some degree of fusion between stacked rings was observed, complete fusion to a morphologically homogeneous tissue tube was not observed in our studies. In this second thesis objective, we evaluated whether the duration of ring culture affects remodeling and fusion of tissue rings into viable, cohesive tissue tubes. To do this, rat SMC rings were pre-cultured for various lengths of time before they were stacked together to form tissue tubes, and tissue ring fusion kinetics were measured. We found that the fusion of the rings into tubes was improved by removing the tissue rings from culture at earlier time points before stacking together, which ultimately resulted in fully fused tissue tubes in as short a time as 8 days. We utilized a custom burst pressure testing device to evaluate the mechanical strength of the resulting fused ring-derived tissue tubes. Finally, we explored the spatial retention of cell position within the tissue tubes after ring fusion, as well as application of the fused ring method to create more complex structures, such as branched vessels. To complete the structural analysis of these studies, a combination of fluorescent cell tracking, histology, light and fluorescent microscopy were used. These results suggest that the fused ring method offers an alternative approach to generating completely cell-derived vascular tissue constructs more rapidly than previously described and allows for the generation of branched vessels which may be useful for modeling areas of the vasculature which are susceptible to disease. *Gwyther, T.A., Rolle, M.W. Fabrication of cell-derived vascular tissue tubes using a modular tissue engineering approach. Manuscript in preparation.*

Objective 3: Evaluate the translation of cellular self-assembly and tissue fusion to primary human smooth muscle cells for the generation of human vascular tissue constructs.

The goal of this section of the thesis was to demonstrate that cellular self-assembly is not unique to rat SMCs, but can be applied for use with primary human SMCs. Human SMCs were seeded into our custom agarose molds and allowed to aggregate to form tissue rings. Human tissue rings were then cultured for 14 days prior to mechanical and histological analysis. The ultimate tensile strength, as determined by uniaxial tensile testing, was found to be higher than similarly cultured rings generated from rat SMCs. Similar to our previous observations with rat SMC rings, human SMC rings contained a high

cell density but exhibited greater amounts of collagen deposition. Also, similar to rat SMCs, we found that human SMC rings were able to fuse and remodel into tissue tubes.

Due to the lower proliferation rate of the human SMCs (doubling time ~ 6 days compared to <1 day for rat SMCs), obtaining large quantities of cells to perform experiments takes a long time. Therefore, we investigated the feasibility of reducing the critical cell number required for aggregation and tissue ring formation by modifying our original agarose mold design to decrease the dimensions of the seeding wells. This design change resulted in a decrease in the number of human SMCs required to create tissue rings from 750,000 to 300,000 cells per ring. This modification makes the method of creating cell-derived rings more "high-throughput", which is particularly important when studying tissue generated from primary cells with low proliferative indices and limited replicative life-spans. In all, we demonstrated that primary human SMCs are capable of self-assembling into strong, scaffold-free tissue in a short amount of time. Further, primary human SMC tissue rings are capable of remodeling and fusing to form tissue tubes. Finally, we improved the overall utility of the aggregated cell ring system by reducing the critical number of cells required to make tissue rings, which will ultimately reduce the amount of time required to fabricate cell-derived tissue tubes. *Gwyther, T.A., Rolle, M.W. Spontaneous aggregation and self-assembly of human smooth muscle cells to create engineered vascular tissues. Manuscript in preparation.*

1.3 Conclusions

This thesis describes the development and validation of a system in which we can rapidly generate 3D vascular tissue constructs in a format which is conducive to quantitative structural, mechanical, and functional analysis. We demonstrated that cell-derived tissue rings can be used to evaluate culture parameters to optimize tissue growth, and can also be fused together to generate tissue tubes. This suggests that any information we obtain about culture parameters from ring studies may directly translate to tissue tube generation. Further, the tissues rings are derived entirely from cells and the ECM that they produce, which enables direct quantitative assessment of the contributions of cells and/or the ECM to vascular structure and function (without the confounding effects of exogenous scaffold materials). Finally, we demonstrated that this system can be translated to primary human smooth muscle cells, allowing us to more directly model native human vessels. This cell-aggregated ring system can therefore serve as a platform technology to study vascular tissue engineering and regenerative biology.

1.4 References

1. Roger VL, Go AS, Lloyd-Jones DM, Adams RJ, Berry JD, Brown TM, Carnethon MR, Dai S, de Simone G, Ford ES and others. Heart disease and stroke statistics--2011 update: a report from the American Heart Association. Circulation 2011;123(4):e18-e209.
2. Goldman S, Zadina K, Moritz T, Ovitt T, Sethi G, Copeland JG, Thottapurathu L, Krasnicka B, Ellis N, Anderson RJ and others. Long-term patency of saphenous vein and left internal mammary artery grafts after coronary artery bypass surgery: results from a Department of Veterans Affairs Cooperative Study. J Am Coll Cardiol 2004;44(11):2149-56.
3. Khot UN, Friedman DT, Pettersson G, Smedira NG, Li J, Ellis SG. Radial artery bypass grafts have an increased occurrence of angiographically severe stenosis and occlusion compared with left internal mammary arteries and saphenous vein grafts. Circulation 2004;109(17):2086-91.
4. L'Heureux N, Dusserre N, Marini A, Garrido S, de la Fuente L, McAllister T. Technology insight: the evolution of tissue-engineered vascular grafts--from research to clinical practice. Nat Clin Pract Cardiovasc Med 2007;4(7):389-95.
5. Klinkert P, Post PN, Breslau PJ, van Bockel JH. Saphenous vein versus PTFE for above-knee femoropopliteal bypass. A review of the literature. Eur J Vasc Endovasc Surg 2004;27(4):357-62.
6. Haruguchi H, Teraoka S. Intimal hyperplasia and hemodynamic factors in arterial bypass and arteriovenous grafts: a review. J Artif Organs 2003;6(4):227-35.
7. Herring M, Baughman S, Glover J, Kesler K, Jesseph J, Campbell J, Dilley R, Evan A, Gardner A. Endothelial seeding of Dacron and polytetrafluoroethylene grafts: the cellular events of healing. Surgery 1984;96(4):745-55.
8. Lamm P, Juchem G, Milz S, Schuffenhauer M, Reichart B. Autologous endothelialized vein allograft: a solution in the search for small-caliber grafts in coronary artery bypass graft operations. Circulation 2001;104(12 Suppl 1):I108-14.
9. Augelli NV, Lupinetti FM, el Khatib H, Sanofsky SJ, Rossi NP. Allograft vein patency in a canine model. Additive effects of cryopreservation and cyclosporine. Transplantation 1991;52(3):466-70.
10. Sebesta P, Stádler P, Sedivý P, Bartík K. The seven-year' secondary patency of a fresh arterial allograft in the femorocrural position in a heart transplant recipient. Ann Vasc Surg 2010;24(7):953.e7-953.e10.
11. Weinberg CB, Bell E. A blood vessel model constructed from collagen and cultured vascular cells. Science 1986;231(4736):397-400.
12. Liu JY, Swartz DD, Peng HF, Gugino SF, Russell JA, Andreadis ST. Functional tissue-engineered blood vessels from bone marrow progenitor cells. Cardiovasc Res 2007;75(3):618-28.
13. Long JL, Tranquillo RT. Elastic fiber production in cardiovascular tissue-equivalents. Matrix Biol 2003;22(4):339-50.
14. Ross JJ, Tranquillo RT. ECM gene expression correlates with in vitro tissue growth and development in fibrin gel remodeled by neonatal smooth muscle cells. Matrix Biol 2003;22(6):477-90.
15. Niklason LE, Gao J, Abbott WM, Hirschi KK, Houser S, Marini R, Langer R. Functional arteries grown in vitro. Science 1999;284(5413):489-93.
16. Hibino N, Shin'oka T, Matsumura G, Ikada Y, Kurosawa H. The tissue-engineered vascular graft using bone marrow without culture. J Thorac Cardiovasc Surg 2005;129(5):1064-70.
17. Matsumura G, Hibino N, Ikada Y, Kurosawa H, Shin'oka T. Successful application of tissue engineered vascular autografts: clinical experience. Biomaterials 2003;24(13):2303-8.
18. Shin'oka T, Imai Y, Ikada Y. Transplantation of a tissue-engineered pulmonary artery. N Engl J Med 2001;344(7):532-3.
19. Shin'oka T, Matsumura G, Hibino N, Naito Y, Watanabe M, Konuma T, Sakamoto T, Nagatsu M, Kurosawa H. Midterm clinical result of tissue-engineered vascular autografts seeded with autologous bone marrow cells. J Thorac Cardiovasc Surg 2005;129(6):1330-8.
20. L'Heureux N, McAllister TN, de la Fuente LM. Tissue-engineered blood vessel for adult arterial revascularization. N Engl J Med 2007;357(14):1451-3.
21. L'Heureux N, Pâquet S, Labbé R, Germain L, Auger FA. A completely biological tissue-engineered human blood vessel. FASEB J 1998;12(1):47-56.

22. Dahl SL, Rhim C, Song YC, Niklason LE. Mechanical properties and compositions of tissue engineered and native arteries. Ann Biomed Eng 2007;35(3):348-55.
23. Schutte SC, Chen Z, Brockbank KG, Nerem RM. Cyclic strain improves strength and function of a collagen-based tissue-engineered vascular media. Tissue Eng Part A 2010;16(10):3149-57.
24. Peng HF, Liu JY, Andreadis ST, Swartz DD. Hair follicle-derived smooth muscle cells and small intestinal submucosa for engineering mechanically robust and vasoreactive vascular media. Tissue Eng Part A 2011;17(7-8):981-90.
25. He W, Nieponice A, Soletti L, Hong Y, Gharaibeh B, Crisan M, Usas A, Peault B, Huard J, Wagner WR and others. Pericyte-based human tissue engineered vascular grafts. Biomaterials 2010;31(32):8235-44.
26. Hashi CK, Zhu Y, Yang GY, Young WL, Hsiao BS, Wang K, Chu B, Li S. Antithrombogenic property of bone marrow mesenchymal stem cells in nanofibrous vascular grafts. Proc Natl Acad Sci U S A 2007;104(29):11915-20.
27. Watanabe T, Kanda K, Yamanami M, Ishibashi-Ueda H, Yaku H, Nakayama Y. Long-term animal implantation study of biotube-autologous small-caliber vascular graft fabricated by in-body tissue architecture. J Biomed Mater Res B Appl Biomater 2011;98(1):120-6.
28. Ziegler T, Nerem RM. Tissue engineering a blood vessel: regulation of vascular biology by mechanical stresses. J Cell Biochem 1994;56(2):204-9.
29. de Valence S, Tille JC, Mugnai D, Mrowczynski W, Gurny R, Möller M, Walpoth BH. Long term performance of polycaprolactone vascular grafts in a rat abdominal aorta replacement model. Biomaterials 2012;33(1):38-47.
30. Gauvin R, Ahsan T, Larouche D, Lévesque P, Dubé J, Auger FA, Nerem RM, Germain L. A novel single-step self-assembly approach for the fabrication of tissue-engineered vascular constructs. Tissue Eng Part A 2010;16(5):1737-47.
31. Konig G, McAllister TN, Dusserre N, Garrido SA, Iyican C, Marini A, Fiorillo A, Avila H, Wystrychowski W, Zagalski K and others. Mechanical properties of completely autologous human tissue engineered blood vessels compared to human saphenous vein and mammary artery. Biomaterials 2009;30(8):1542-50.
32. Norotte C, Marga FS, Niklason LE, Forgacs G. Scaffold-free vascular tissue engineering using bioprinting. Biomaterials 2009;30(30):5910-7.
33. Gentile C, Fleming PA, Mironov V, Argraves KM, Argraves WS, Drake CJ. VEGF-mediated fusion in the generation of uniluminal vascular spheroids. Dev Dyn 2008;237(10):2918-25.
34. Jakab K, Norotte C, Damon B, Marga F, Neagu A, Besch-Williford CL, Kachurin A, Church KH, Park H, Mironov V and others. Tissue engineering by self-assembly of cells printed into topologically defined structures. Tissue Eng Part A 2008;14(3):413-21.
35. Ahlfors JE, Billiar KL. Biomechanical and biochemical characteristics of a human fibroblast-produced and remodeled matrix. Biomaterials 2007;28(13):2183-91.
36. Seliktar D, Black RA, Vito RP, Nerem RM. Dynamic mechanical conditioning of collagen-gel blood vessel constructs induces remodeling in vitro. Ann Biomed Eng 2000;28(4):351-62.
37. Rowe SL, Stegemann JP. Interpenetrating collagen-fibrin composite matrices with varying protein contents and ratios. Biomacromolecules 2006;7(11):2942-8.
38. Gwyther TA, Hu JZ, Christakis AG, Skorinko JK, Shaw SM, Billiar KL, Rolle MW. Engineered vascular tissue fabricated from aggregated smooth muscle cells. Cells Tissues Organs 2011;194(1):13-24.

Chapter 2: Background

Cardiovascular disease is the leading cause of death in the United States. Therefore, much research is being done to better understand the mechanisms by which vascular disease progresses, to improve disease detection, and to discover new treatments to help patients with such diseases. This chapter discusses current work in this field and how it pertains to this thesis.

2.1 Clinical need for vascular grafts

In a healthy adult, the three layers of the vessel wall work together and generate functioning blood vessels which contract and relax to maintain proper blood pressure and flow throughout the body. However, 16 million Americans have some form of cardiovascular disease where their blood vessels do not behave normally.[1] No matter the specific event to trigger disease onset, the vascular structure changes as the disease progresses.[2] For example, in patients with atherosclerosis, lipid- and cholesterol-rich plaques build up on the vascular walls, slowly occluding the vessel and generating a less compliant, stiffer extracellular matrix (ECM) which ultimately alters blood flow.[3-5] In patients with intimal hyperplasia, smooth muscle cells (SMCs) directly below the internal elastic lamina begin to proliferate abnormally, leading to a thickening of the intima and stenosis or occlusion of the vessel.[2] In patients with blood clots, injury to the endothelial lining of the blood vessel reveals a "sticky" thrombogenic surface onto which platelets adhere, leading to formation of a clot.[6] In large vessels, this blood clot, or thrombus, can impede blood flow, whereas it can completely block the flow in smaller vessels.[3,7] In each of these diseases, the end result is the same: a severe decrease in blood flow due to vessel occlusion.

When a vascular disease has progressed to the point where blood flow is severely impeded or completely blocked, an intervention is needed. Percutaneous coronary interventions (PCI, also known as angioplasty) combined with stenting are generally the first course of treatment.[1] Each year, there are over one million PCI procedures performed and 560,000 of those combine PCI with stents.[1] However, some patients do not respond well to this treatment and have increased intimal thickening which can lead to blockage again after surgery.[8-10] In cases such as this, open heart surgery is a last resort. To perform these operations, a surgeon uses a donor vessel to bypass around the blockage to restore blood flow downstream. While any

vessel is susceptible to disease, certain vessels, such as those exposed to high flow rates and high pressures, as well as branched vessels, are more likely to become diseased.[11] One example of a vessel prone to disease is the coronary arteries. Each year, hundreds of thousands of patients undergo coronary artery bypass surgery in the United States.[12] The most common approach to bypassing blockages in the coronary arteries is to utilize an autologous blood vessel as a donor vascular graft. Common blood vessels used as donor grafts are the internal mammary arteries, the radial arteries, or the saphenous veins.[13,14] However, approximately one third of these patients do not have suitable autologous donor vessels due to the extent of vascular disease or previous harvest. In such patients, surgeons must look to alternatives such as allografts (transplants from another human vessel) or xenografts (transplants from another species).[15,16] Yet, these alternatives are associated with the need for life-long immunosuppressive drugs and/or low patency; which often requires follow up surgeries.[16,17] Recently, tissue engineering has emerged as a promising new approach to generating vascular graft alternatives.[18,19] Several different methods for engineering tissues have been explored, including seeding cells on natural polymer scaffolds,[20-24] synthetic polymer scaffolds,[25,26] decellularized tissue,[27] or creating tissues from cells and cell-derived ECM.[18,28-33]

Each of these approaches is associated with advantages and disadvantages. For example, synthetic polymer scaffolds are an appealing approach because their mechanical properties and degradation parameters are easily modified with material choice and manufacturing processes. Further, these materials are consistent from batch to batch. However, these materials are not normally found in the body, and they can elicit unwanted inflammatory responses from the cells because their degradation byproducts.[34] Natural polymers, such as collagen or fibrin, are able to be rapidly fabricated. Through injection of these polymers with cells, various shapes can be formed quickly. Further, these proteins are found naturally in the body so the cells are able to interact with them. While some recent studies have shown that strong vascular grafts can be generated and successfully implanted using this approach, the fabrication of these vessels takes long culture periods, extensive mechanical conditioning and media supplementation.[35-37]

Decellularized tissues are another alternative to engineering vascular grafts. The cells are removed from native vessels and used as a scaffold on which to repopulate with autologous cells. With this approach, the scaffold contains native proteins; however, some of the native structure is washed away with the harsh detergents required for decellularization.[38] More recently this decellularization approach has been utilized in combination with other tissue engineering approaches.[39] For example vascular grafts generated from human SMCs seeded onto PGA scaffolds which were cultured for 8 weeks then decellularized with

detergents prior to implantation in a rat model.[40] Finally, another approach has been to generate vascular grafts completely from cells and the matrix they produce.[29,41] While this approach is appealing because the resulting vessels are composed only of cells and their ECM (no exogenous material), the current methods require very long culture times or specialized equipment to manufacture.[18,41,42]

No matter the approach used, all vascular grafts aim to mimic the structural and functional properties of native vasculature.

2.2 Vascular structure and function

The cardiovascular system is one of the most important organ systems in the body because it delivers blood containing nutrients to all other tissues. The vasculature is a network of tubes which carries oxygenated blood away from the heart and lungs (through arteries) and carries oxygen-deficient blood back to the heart and lungs (through veins) for re-oxygenation. Blood leaves the heart through a large muscular artery called the aorta after which it splits into smaller arteries, then arterioles, and continues to branch into smaller vessels, which eventually become single cell capillaries. At this point the surrounding tissues have depleted the blood of all nutrients and it begins to flow back to the heart through a series of successively larger veins. Both the arteries and veins vary in size and structural characteristics with successive branching throughout the body, but consist of the same three main layers, the tunica adventitia, the tunica media, and the tunica intima. The composition and abundance of the individual components that make up the layers vary among different vessels according to size and type. Figure 2.1 shows a schematic to demonstrate this concept (modified from Burton *et al.* [43]).
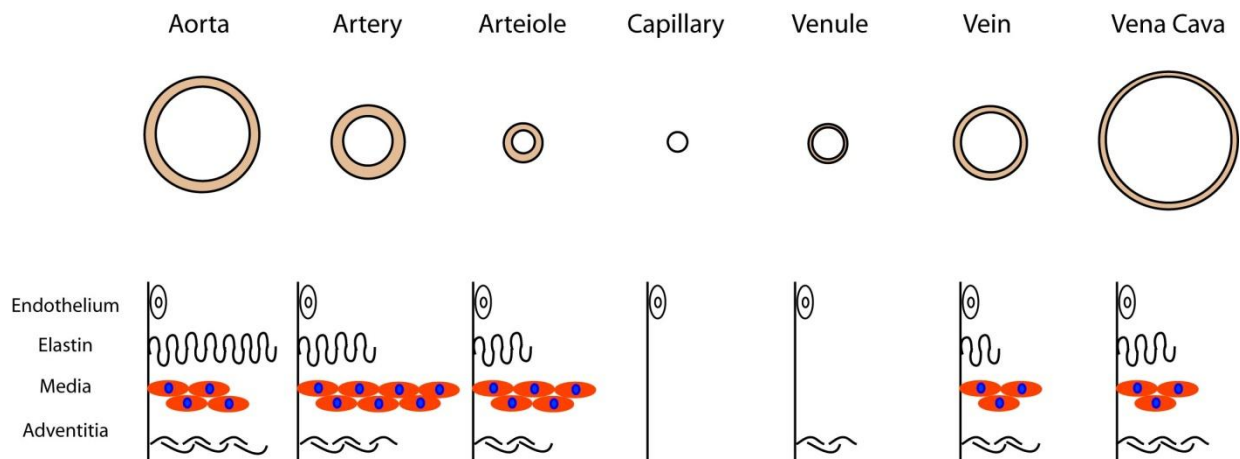
Figure 2.1 – Composition of blood vessels. This schematic shows the major components of the blood vessels throughout the circulatory system. Vessels that have different functions contain different quantities of these primary components. (Modified from [43])

2.2.1 Tunica Adventitia

The tunica adventitia is the outermost layer of connective tissue around the blood vessel and is composed primarily of fibroblasts, collagen, and elastin.[44,45] This layer provides structure, anchors the vessels to nearby tissues, and is partly responsible for vascular tensile strength and stiffness.[46] In large arteries, this layer contains a vasa vasorum, which is a capillary network that supplies nutrients to the muscular wall of the vessel itself.[47] While mainly responsible for the structure of the vessel, this layer has also been implicated in cell trafficking into and out of the vascular wall, growth and repair of the vessel, as well as mediating communication between other vascular cells and their surrounding tissues.[48-50]

2.2.2 Tunica Media

The tunica media is the central layer of the blood vessel, which is located between the tunica adventitia and the tunica intima. The media consists of layers of smooth muscle cells (Figure 2.2A, green fluorescent cells) separated by elastic lamellae (Figure 2.2B, black stain).[51] In general, arteries have a much thicker medial layer than veins due to the higher blood pressures in the arterial system.[43] Large muscular arteries (such as the aorta or the coronary arteries) contain more layers of smooth muscle cells and elastic fibers than smaller arteries because these vessels must withstand the highest pressures.[43,52] In addition to providing structure to the vessel, the medial layer is responsible for the compliance and the contraction performed by the blood vessels.[53] The layers of elastin found throughout the medial wall directly contribute to the compliance and elasticity of the vessel, allowing it to stretch with each increase in pressure then recoil back to its initial shape and size.[51] The smooth muscle cells in the media are

responsible for the contraction and relaxation of the vessel to maintain proper blood flow throughout the body.[54]
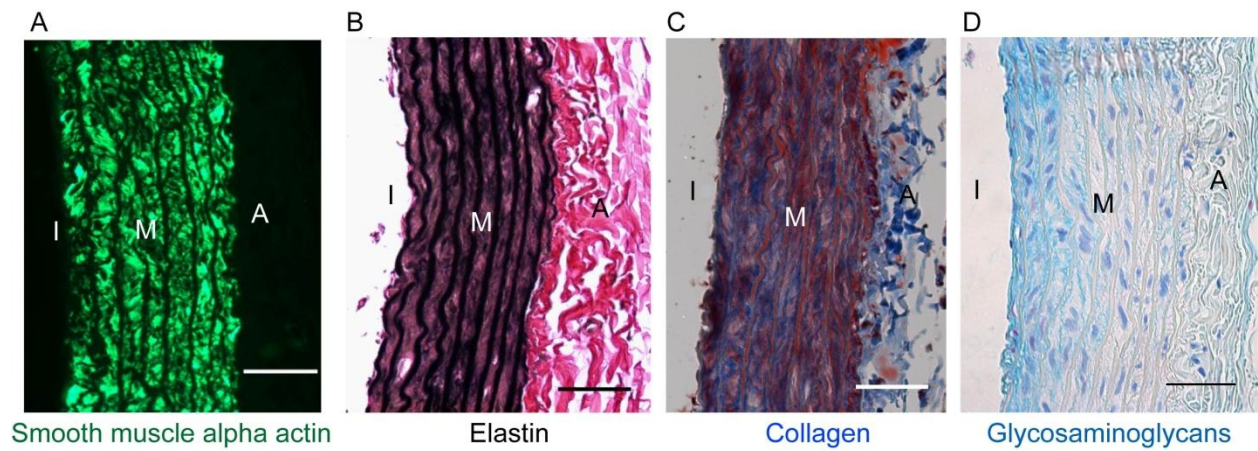
Figure 2.2 – Structure of the medial layer of a blood vessel. Rat aorta stained with various smooth muscle cell or extracellular matrix stains. (A) An image to show smooth muscle cells (green = marker for smooth muscle, smooth muscle alpha actin), (B) Verhoeff van Gieson staining to show elastic fibers (black stain) within the media layer, (C) Masson's Trichrome to show collagen (blue) and muscle (red), and (D) Alcian Blue to show glycosaminoglycans (blue). Letters indicate the location of the three vascular layers; I=intima, M=media, A=adventitia. Scale=50μm.

2.2.3 Tunica Intima

The innermost layer of the vessel, the tunica intima, is composed of a monolayer of endothelial cells (ECs) adhered to a basement membrane. The basement membrane is a thin layer of ECM rich in laminin and fibronectin, which is deposited by both the endothelial cells and the smooth muscle cells.[55,56] The ECs are polarized in that they are anchored to the membrane on one side and exposed directly to blood flow on the other side.[57] ECs have antithrombogenic properties which inhibit platelet adhesion and clot formation.[58] Because ECs are exposed to blood flow, they are very sensitive to changes in shear stress. In response to changes in shear stress ECs can release factors which regulate the contraction and relaxation of smooth muscle cells to help maintain constant blood flow.[59]

2.3 Vascular tissue engineering

From the first published report of blood vessel tissue engineering in the late 1980s,[20] engineers have looked to native blood vessel *structure* and *function* as a model for vascular graft synthesis. An ideal vessel needs to be strong enough to withstand arterial pressures while maintaining compliance. It also needs to be physiologically responsive to vasodilatory and contractile stimulants. And finally, it needs an

antithrombogenic surface to resist platelet adhesion. While achievement of strength, compliance, vasoactivity, and antithrombogenicity requires a harmonious interaction of all three vascular layers, tissue engineers most often focus on recapitulating the medial layer due to its more significant contribution to vascular mechanical strength and vasoregulatory function than other layers.[60,61] Further, the addition of an intimal layer in vascular grafts has been a lower priority because grafts without endothelial cells combined with immunosuppressive drugs remain patent during *in vivo* studies.[39] Therefore, most engineered vascular tissues consist of a media mimetic.

2.3.1 Challenges in engineering the vascular tunica media

For an engineered vascular *media* to truly mimic native tissue, it needs to have 1) a high fractional content of contractile smooth muscle cells and 2) sufficient tensile strength to withstand arterial pressure while maintaining adequate compliance to address pressure fluctuations and sustain normal blood flow. To address these criteria, vascular grafts need high cell densities (similar to native tissues) of functionally contractile SMCs combined with an ECM rich in collagen and elastic fibers. The abundance of collagen within the tissue will aid in providing strength while the elastic fibers will contribute to overall tissue compliance. To date, few engineered vascular grafts have sufficiently achieved these criteria.

2.3.2 Approaches to vascular tissue engineering (scaffold-based vs. cell-derived)

Among the challenges in building a physiologically functional vascular construct are low cell density,[25,62] low compliance,[63] and low contractility.[25] These limitations remain, in part, due to the use of scaffolds as the structural framework of many grafts. Scaffolds can dominate graft mechanical properties and limit initial cell-seeding densities.[25,62] Additionally, rapid scaffold degradation prior to the synthesis of sufficiently strong structural ECM can jeopardize graft structural integrity (Figure 2.3A,C).[53]

Cell-derived tissues are an attractive alternative because they address some of the scaffold-based limitations.[31,42,64,65] Given that such tissues are created entirely from cells and the matrix they produce, they inherently have much higher cell densities which lead to vessels with higher fractional content of cells.[66] Cell-derived tissues are also able to attain substantial mechanical strength without the need for exogenous scaffolds and have even been shown to be stronger than cells in natural polymer scaffolds.[66,67] In traditional scaffold-based approaches, cells need to proliferate to populate the scaffold, degrade and remodel the scaffold so that they can migrate throughout, and build up their own ECM (Figure 2.3A). However, cell-derived tissue does not need to go through those first two steps of proliferating and degrading the scaffold. Instead, the cells can begin to generate their own ECM immediately (Figure

2.3B). This can allow cell-derived tissue to generate a strong matrix faster than scaffold-based approaches. Cell-derived tissues have higher mechanical strength,[66,67] greater amount of total protein,[66] and greater amount of collagen than tissues generated from cells in biopolymer gels.[66] As such, cell-derived tissues attained burst pressures (3400 mmHg) which exceed that of the human saphenous vein (1600 mmHg).[65]

The culture environment plays an important role in the final characteristics of vascular tissue. Controlling the mechanical and chemical cues that cells are exposed to will enhance their ability to produce ECM and ultimately affect cell-derived tissue material properties. For example, mechanical conditioning, or cyclic distension, of vascular grafts has been shown to increase tissue strength and burst pressures to levels sufficient for implantation without failure due to bursting.[37] Additionally, researchers have capitalized on the use of media supplementation with or without mechanical stimulation to increase type I collagen content within vascular tissues, resulting in grafts with mechanical properties similar to that of native vein.[29,37,65] Adding these environmental cues to the culture of cell-derived engineered grafts can enhance ECM production and increase the material strength more rapidly (Figure 2.3D), leading to overall shorter production times.
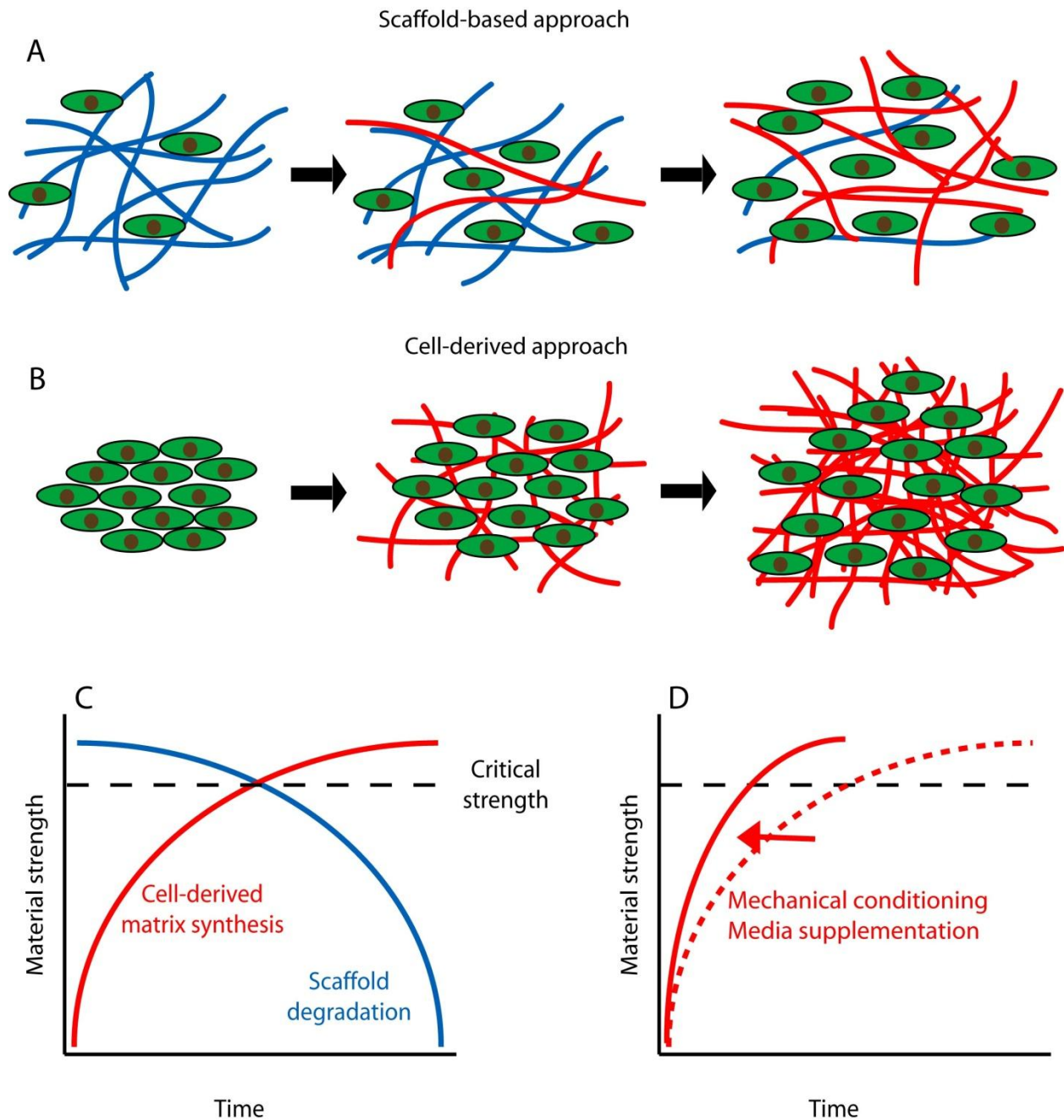
Figure 2.3 – Material properties depend on matrix synthesis. In scaffold-based engineering approaches (A), cells proliferate to populate the scaffold, degrade the existing matrix (blue) so they can migrate throughout, and begin to synthesize their own extracellular matrix (red).   The cell-derived approach starts with a higher cell density (B) which allows the cells to begin to generate their own extracellular matrix (red) more rapidly. A representative graph illustrates the need for cells to generate their own extracellular matrix prior to degradation of the scaffold or their strength will drop below critical levels (C).   With the alteration of culture conditions (to include media supplementation or mechanical conditioning) the rate at which ECM is produced can be increased (D).

2.3.3 Limitations of cell-based approaches

Although cell-derived tissues offer an attractive engineering approach because they inherently have increased cell densities and no exogenous material, they are also associated with limitations. Some reasons that cell-derived approaches are not widely used are the large quantity of cells required to fabricate tissue and the long culture times required to develop the tissues.

Another challenge limiting the utility of cell-derived tissue is the lack of methods available to easily fabricate 3D tissue without the use of scaffolds. To date, the current approaches include "cell-sheet engineering",[18,28,29] "bioprinting",[42,68-70] and the aggregation and fusion of cells-based spheroids.[31,71] Cell-sheet engineering, more recently referred to as tissue engineering by self-assembly (TESA),[72,73] has become an established approach to generating cell-derived tissue. This technique involves growing cells on tissue culture plastic until they from multiple cell layers and synthesize sufficient ECM so that they are robust enough for removal from their culture dishes as intact sheets. In addition to vascular tissue engineering, this approach has other applications such as engineering cornea,[74] peridontal reconstruction,[75] skin substitutes,[76] skeletal muscle,[77] adipose tissue,[78] and connective tissue.[78] For vascular engineering, fibroblast-derived sheets are wrapped around a central mandrel into a tube-shape.[18,29,41] These wrapped layers are then allowed to fuse together in culture before endothelialization and implantation. The resulting tissues have been met with clinical success,[18] however, there are limitations to this method. The cell sheets take approximately 6-8 weeks before they are removed from the flasks. Then the layers fuse together for 12 additional weeks to mature. The entire process thus requires 3 months production time. Further, there is manual manipulation required to wrap the sheets into tubes, which may lead to difficulties in replicating this method.

Another approach to scaffold-free tissue engineering is the formation (and fusion) of cell spheres.[31] With this approach, individual cell suspensions are pipetted into droplets which are inverted to create "hanging-drops". The cells then aggregate by gravity in the base of the drop to form a sphere. These spheres have been used as a platform to study cell-derived vascular tissue contraction.[71,79] For example, SMC spheroid micro-tissues cultured in the presence of vascular endothelial cell growth factor (VEGF) were found to express high levels of SMA and MHC and even demonstrate contraction in response to potassium chloride, although the force of this contraction was not measured directly due to the spherical geometry of the tissues.[71] This method of generating cell-derived tissue spheres is not conducive to quantitative assessment of tissue mechanics due to its geometry and size. More recently, these spheres have been used for tissue engineering applications where they are fused together to form tubes.[31] However, there is a lot of manual manipulation required to transfer the quantity of spheres needed to fuse into tissue tubes.

In an effort to make cell spheres easier to manipulate, another technique known as "bio-printing" has been established. With this method, a specialized printer is loaded with "bio-ink" or cell aggregates, and the bio-ink is literally printed onto a surface to generate the tissue structure of interest.[42,68-70] The "ink" can be in the form of small cell spheres, or cell-aggregated rods generated from fused spheres.[42,69] Similar to the cell aggregate approaches, the small sub-units are not conducive to mechanical or functional analysis. Most labs do not have access to a "bio-printer" and therefore cannot readily use this method.

As such, a need exists for a method to *easily* assemble cells into 3D cell-derived tissues. Further, due to the large quantity of cells and the long culture times required for cell-derived vascular tissue fabrication, evaluating and optimizing culture conditions for vascular tissue growth on tubular constructs would be an expensive, reagent-, and time- consuming endeavor. Therefore, there is a need for a *straight-forward* method to *rapidly* generate 3D tissue with fewer cells, which can be used to "screen" the effects of culture conditions on the mechanics, structure, and function of vascular tissue.

2.4 Goal of this thesis

To address this need, this thesis describes the development of a new method to generate 3D cell-derived tissue rings from aggregated smooth muscle cells and cell-derived ECM. The ring shape was chosen because of its precedent in vascular biomechanics and contraction studies.[65,80] Ring segments are often removed from vessels to analyze mechanical properties or contractile properties of vascular tissue.[25,65] These engineered ring-shaped structures are ideal for testing the effects of culture parameters on the overall tissue composition, biomechanics, and contractile properties. Further, to demonstrate direct translation of the tissue rings to vascular tissue tubes, we show tissue rings can be fused together to form tube-shaped constructs.

Overall, engineered vascular tissue offers a valuable alternative to current blood vessel graft materials, but may also serve as an *in vitro* model system to evaluate culture conditions which promote optimal vascular tissue growth. The current tissue engineering systems available are limited by their lack of appropriate cell densities, mechanical strength, or contractility. We believe that by fabricating vascular tissue entirely from cells and cell-derived ECM, we will be able to better recapitulate native tissue by increasing cell densities and ECM production leading to increased contractility and strength. The following chapters discuss the system we have developed to generate cell-derived vascular tissue rings, and its potential utility and impact on the field of vascular engineering.

2.5 References

1.   Roger VL, Go AS, Lloyd-Jones DM, Adams RJ, Berry JD, Brown TM, Carnethon MR, Dai S, de Simone G, Ford ES and others. Heart disease and stroke statistics--2011 update: a report from the American Heart Association. Circulation 2011;123(4):e18-e209.
2.   Yutani C, Imakita M, Ishibashi-Ueda H, Tsukamoto Y, Nishida N, Ikeda Y. Coronary atherosclerosis and interventions: pathological sequences and restenosis. Pathol Int 1999;49(4):273-90.
3.   Conti CR. Finding the vulnerable plaque. Clin Cardiol 2010;33(6):320-1.
4.   Shah VK, Shalia KK, Mashru MR, Soneji SL, Abraham A, Kudalkar KV, Vasvani JB, Sanghavi ST. Role of matrix metalloproteinases in coronary artery disease. Indian Heart J 2009;61(1):44-50.
5.   Akyildiz AC, Speelman L, van Brummelen H, Gutiérrez MA, Virmani R, van der Lugt A, van der Steen AF, Wentzel JJ, Gijsen FJ. Effects of intima stiffness and plaque morphology on peak cap stress. Biomed Eng Online 2011;10:25.
6.   Shah PK. Inflammation and plaque vulnerability. Cardiovasc Drugs Ther 2009;23(1):31-40.
7.   Conti CR. Vascular events responsible for thrombotic occlusion of a blood vessel. Clin Cardiol 1993;16(11):761-2.
8.   Timmins LH, Miller MW, Clubb FJ, Moore JE. Increased artery wall stress post-stenting leads to greater intimal thickening. Lab Invest 2011;91(6):955-67.
9.   Chung IM, Gold HK, Schwartz SM, Ikari Y, Reidy MA, Wight TN. Enhanced extracellular matrix accumulation in restenosis of coronary arteries after stent deployment. J Am Coll Cardiol 2002;40(12):2072-81.
10.   Farb A, Kolodgie FD, Hwang JY, Burke AP, Tefera K, Weber DK, Wight TN, Virmani R. Extracellular matrix changes in stented human coronary arteries. Circulation 2004;110(8):940-7.
11.   Hariton I, deBotton G, Gasser TC, Holzapfel GA. Stress-modulated collagen fiber remodeling in a human carotid bifurcation. J Theor Biol 2007;248(3):460-70.
12.   Roger VL, Go AS, Lloyd-Jones DM, Adams RJ, Berry JD, Brown TM, Carnethon MR, Dai S, de Simone G, Ford ES and others. Heart Disease and Stroke Statistics--2011 Update: A Report From the American Heart Association. Circulation 2010.
13.   Buxton B, Tatoulis J, Fuller J. Arterial conduits update. Heart Lung Circ 2005;14 Suppl 2:S14-7.
14.   Tatoulis J, Buxton BF, Fuller JA. The radial artery in reoperative coronary bypass surgery:. J Card Surg 2004;19(4):296-302.
15.   Sebesta P, Stádler P, Sedivý P, Bartík K. The seven-year' secondary patency of a fresh arterial allograft in the femorocrural position in a heart transplant recipient. Ann Vasc Surg 2010;24(7):953.e7-953.e10.
16.   Englberger L, Noti J, Immer FF, Stalder M, Eckstein FS, Carrel TP. The Shelhigh No-React bovine internal mammary artery: a questionable alternative conduit in coronary bypass surgery? Eur J Cardiothorac Surg 2008;33(2):222-4.
17.   Augelli NV, Lupinetti FM, el Khatib H, Sanofsky SJ, Rossi NP. Allograft vein patency in a canine model. Additive effects of cryopreservation and cyclosporine. Transplantation 1991;52(3):466-70.
18.   L'Heureux N, McAllister TN, de la Fuente LM. Tissue-engineered blood vessel for adult arterial revascularization. N Engl J Med 2007;357(14):1451-3.
19.   Shin'oka T, Imai Y, Ikada Y. Transplantation of a tissue-engineered pulmonary artery. N Engl J Med 2001;344(7):532-3.
20.   Weinberg CB, Bell E. A blood vessel model constructed from collagen and cultured vascular cells. Science 1986;231(4736):397-400.
21.   Isenberg BC, Tranquillo RT. Long-term cyclic distention enhances the mechanical properties of collagen-based media-equivalents. Ann Biomed Eng 2003;31(8):937-49.
22.   Long JL, Tranquillo RT. Elastic fiber production in cardiovascular tissue-equivalents. Matrix Biol 2003;22(4):339-50.
23.   Ross JJ, Tranquillo RT. ECM gene expression correlates with in vitro tissue growth and development in fibrin gel remodeled by neonatal smooth muscle cells. Matrix Biol 2003;22(6):477-90.
24.   Seliktar D, Black RA, Vito RP, Nerem RM. Dynamic mechanical conditioning of collagen-gel blood vessel constructs induces remodeling in vitro. Ann Biomed Eng 2000;28(4):351-62.

25.   Niklason LE, Gao J, Abbott WM, Hirschi KK, Houser S, Marini R, Langer R. Functional arteries grown in vitro. Science 1999;284(5413):489-93.

26.   Hibino N, Shin'oka T, Matsumura G, Ikada Y, Kurosawa H. The tissue-engineered vascular graft using bone marrow without culture. J Thorac Cardiovasc Surg 2005;129(5):1064-70.

27.   Borschel GH, Huang YC, Calve S, Arruda EM, Lynch JB, Dow DE, Kuzon WM, Dennis RG, Brown DL. Tissue engineering of recellularized small-diameter vascular grafts. Tissue Eng 2005;11(5-6):778-86.

28.   Gauvin R, Ahsan T, Larouche D, Lévesque P, Dubé J, Auger FA, Nerem RM, Germain L. A novel single-step self-assembly approach for the fabrication of tissue-engineered vascular constructs. Tissue Eng Part A 2010;16(5):1737-47.

29.   L'Heureux N, Pâquet S, Labbé R, Germain L, Auger FA. A completely biological tissue-engineered human blood vessel. FASEB J 1998;12(1):47-56.

30.   L'Heureux N, Stoclet JC, Auger FA, Lagaud GJ, Germain L, Andriantsitohaina R. A human tissue-engineered vascular media: a new model for pharmacological studies of contractile responses. FASEB J 2001;15(2):515-24.

31.   Kelm JM, Lorber V, Snedeker JG, Schmidt D, Broggini-Tenzer A, Weisstanner M, Odermatt B, Mol A, Zünd G, Hoerstrup SP. A novel concept for scaffold-free vessel tissue engineering: self-assembly of microtissue building blocks. J Biotechnol 2010;148(1):46-55.

32.   Campbell JH, Efendy JL, Campbell GR. Novel vascular graft grown within recipient's own peritoneal cavity. Circ Res 1999;85(12):1173-8.

33.   Chue WL, Campbell GR, Caplice N, Muhammed A, Berry CL, Thomas AC, Bennett MB, Campbell JH. Dog peritoneal and pleural cavities as bioreactors to grow autologous vascular grafts. J Vasc Surg 2004;39(4):859-67.

34.   Hedberg EL, Kroese-Deutman HC, Shih CK, Crowther RS, Carney DH, Mikos AG, Jansen JA. In vivo degradation of porous poly(propylene fumarate)/poly(DL-lactic-co-glycolic acid) composite scaffolds. Biomaterials 2005;26(22):4616-23.

35.   Liu JY, Swartz DD, Peng HF, Gugino SF, Russell JA, Andreadis ST. Functional tissue-engineered blood vessels from bone marrow progenitor cells. Cardiovasc Res 2007;75(3):618-28.

36.   Liu JY, Peng HF, Andreadis ST. Contractile smooth muscle cells derived from hair-follicle stem cells. Cardiovasc Res 2008;79(1):24-33.

37.   Syedain ZH, Meier LA, Bjork JW, Lee A, Tranquillo RT. Implantable arterial grafts from human fibroblasts and fibrin using a multi-graft pulsed flow-stretch bioreactor with noninvasive strength monitoring. Biomaterials 2011;32(3):714-22.

38.   Schaner PJ, Martin ND, Tulenko TN, Shapiro IM, Tarola NA, Leichter RF, Carabasi RA, Dimuzio PJ. Decellularized vein as a potential scaffold for vascular tissue engineering. J Vasc Surg 2004;40(1):146-53.

39.   Quint C, Kondo Y, Manson RJ, Lawson JH, Dardik A, Niklason LE. Decellularized tissue-engineered blood vessel as an arterial conduit. Proc Natl Acad Sci U S A 2011;108(22):9214-9.

40.   Quint C, Arief M, Muto A, Dardik A, Niklason LE. Allogeneic human tissue-engineered blood vessel. J Vasc Surg 2011.

41.   L'Heureux N, Dusserre N, Konig G, Victor B, Keire P, Wight TN, Chronos NA, Kyles AE, Gregory CR, Hoyt G and others. Human tissue-engineered blood vessels for adult arterial revascularization. Nat Med 2006;12(3):361-5.

42.   Norotte C, Marga FS, Niklason LE, Forgacs G. Scaffold-free vascular tissue engineering using bioprinting. Biomaterials 2009;30(30):5910-7.

43.   Burton AC. Relation of structure to function of the tissues of the wall of blood vessels. Physiol Rev 1954;34(4):619-42.

44.   Di Wang H, Rätsep MT, Chapman A, Boyd R. Adventitial fibroblasts in vascular structure and function: the role of oxidative stress and beyond. Can J Physiol Pharmacol 2010;88(3):177-86.

45.   Ottani V, Raspanti M, Ruggeri A. Collagen structure and functional implications. Micron 2001;32(3):251-60.

46.   Et-Taouil K, Schiavi P, Lévy BI, Plante GE. Sodium intake, large artery stiffness, and proteoglycans in the spontaneously hypertensive rat. Hypertension 2001;38(5):1172-6.

47.   Clarke JA. An x-ray microscopic study of the postnatal development of the vasa vasorum in the human aorta. J Anat 1965;99(Pt 4):877-89.

48.   Gutterman DD. Adventitia-dependent influences on vascular function. Am J Physiol 1999;277(4 Pt 2):H1265-72.

49.   Sartore S, Chiavegato A, Faggin E, Franch R, Puato M, Ausoni S, Pauletto P. Contribution of adventitial fibroblasts to neointima formation and vascular remodeling: from innocent bystander to active participant. Circ Res 2001;89(12):1111-21.

50.   Haurani MJ, Pagano PJ. Adventitial fibroblast reactive oxygen species as autacrine and paracrine mediators of remodeling: bellwether for vascular disease? Cardiovasc Res 2007;75(4):679-89.

51.   Farand P, Garon A, Plante GE. Structure of large arteries: orientation of elastin in rabbit aortic internal elastic lamina and in the elastic lamellae of aortic media. Microvasc Res 2007;73(2):95-9.

52.   Koeppen B, Stanton B. Physiology: Mosby, Elsevier, Inc.; 2008.

53.   Opitz F, Schenke-Layland K, Cohnert TU, Starcher B, Halbhuber KJ, Martin DP, Stock UA. Tissue engineering of aortic tissue: dire consequence of suboptimal elastic fiber synthesis in vivo. Cardiovasc Res 2004;63(4):719-30.

54.   Steedman WM. Micro-electrode studies on mammalian vascular muscle. J Physiol 1966;186(2):382-400.

55.   Candiello J, Balasubramani M, Schreiber EM, Cole GJ, Mayer U, Halfter W, Lin H. Biomechanical properties of native basement membranes. FEBS J 2007;274(11):2897-908.

56.   Candiello J, Cole GJ, Halfter W. Age-dependent changes in the structure, composition and biophysical properties of a human basement membrane. Matrix Biol 2010;29(5):402-10.

57.   Lombardi T, Montesano R, Orci L. Polarized plasma membrane domains in cultured endothelial cells. Exp Cell Res 1985;161(1):242-6.

58.   Yang Z, Wang JM, Wang LC, Chen L, Tu C, Luo CF, Tang AL, Wang SM, Tao J. In vitro shear stress modulates antithrombogenic potentials of human endothelial progenitor cells. J Thromb Thrombolysis 2007;23(2):121-7.

59.   Burghoff S, Schrader J. Secretome of human endothelial cells under shear stress. J Proteome Res 2011;10(3):1160-9.

60.   Schutte SC, Chen Z, Brockbank KG, Nerem RM. Tissue engineering of a collagen-based vascular media: Demonstration of functionality. Organogenesis 2010;6(4):204-11.

61.   Grassl ED, Oegema TR, Tranquillo RT. A fibrin-based arterial media equivalent. J Biomed Mater Res A 2003;66(3):550-61.

62.   Ziegler T, Nerem RM. Tissue engineering a blood vessel: regulation of vascular biology by mechanical stresses. J Cell Biochem 1994;56(2):204-9.

63.   de Valence S, Tille JC, Mugnai D, Mrowczynski W, Gurny R, Möller M, Walpoth BH. Long term performance of polycaprolactone vascular grafts in a rat abdominal aorta replacement model. Biomaterials 2012;33(1):38-47.

64.   Jakab K, Norotte C, Damon B, Marga F, Neagu A, Besch-Williford CL, Kachurin A, Church KH, Park H, Mironov V and others. Tissue engineering by self-assembly of cells printed into topologically defined structures. Tissue Eng Part A 2008;14(3):413-21.

65.   Konig G, McAllister TN, Dusserre N, Garrido SA, Iyican C, Marini A, Fiorillo A, Avila H, Wystrychowski W, Zagalski K and others. Mechanical properties of completely autologous human tissue engineered blood vessels compared to human saphenous vein and mammary artery. Biomaterials 2009;30(8):1542-50.

66.   Ahlfors JE, Billiar KL. Biomechanical and biochemical characteristics of a human fibroblast-produced and remodeled matrix. Biomaterials 2007;28(13):2183-91.

67.   Adebayo O, Gwyther T, Hu J, Billiar K, Rolle M. Vascular smooth muscle cell derived tissue rings exhibit greater tensile strength than smooth muscle cells in fibrin or collagen gels. in submission.

68.   Jakab K, Neagu A, Mironov V, Forgacs G. Organ printing: fiction or science. Biorheology 2004;41(3-4):371-5.

69.   Mironov V, Visconti RP, Kasyanov V, Forgacs G, Drake CJ, Markwald RR. Organ printing: tissue spheroids as building blocks. Biomaterials 2009;30(12):2164-74.

70.   Visconti RP, Kasyanov V, Gentile C, Zhang J, Markwald RR, Mironov V. Towards organ printing: engineering an intra-organ branched vascular tree. Expert Opin Biol Ther 2010;10(3):409-20.

71.   Gentile C, Fleming PA, Mironov V, Argraves KM, Argraves WS, Drake CJ. VEGF-mediated fusion in the generation of uniluminal vascular spheroids. Dev Dyn 2008;237(10):2918-25.

72.   Peck M, Gebhart D, Dusserre N, McAllister TN, L'heureux N. The Evolution of Vascular Tissue Engineering and Current State of the Art. Cells Tissues Organs 2011.

73.   Wystrychowski W, Cierpka L, Zagalski K, Garrido S, Dusserre N, Radochonski S, McAllister TN, L'heureux N. Case study: first implantation of a frozen, devitalized tissue-engineered vascular graft for urgent hemodialysis access. J Vasc Access 2011;12(1):67-70.

74.   Proulx S, d'Arc Uwamaliya J, Carrier P, Deschambeault A, Audet C, Giasson CJ, Guérin SL, Auger FA, Germain L. Reconstruction of a human cornea by the self-assembly approach of tissue engineering using the three native cell types. Mol Vis 2010;16:2192-201.
75.   Iwata T, Yamato M, Tsuchioka H, Takagi R, Mukobata S, Washio K, Okano T, Ishikawa I. Periodontal regeneration with multi-layered periodontal ligament-derived cell sheets in a canine model. Biomaterials 2009;30(14):2716-23.
76.   Jean J, Bernard G, Duque-Fernandez A, Auger FA, Pouliot R. Effects of serum-free culture at the air-liquid interface in a human tissue-engineered skin substitute. Tissue Eng Part A 2011;17(7-8):877-88.
77.   Kino-Oka M, Ngo TX, Nagamori E, Takezawa Y, Miyake Y, Sawa Y, Saito A, Shimizu T, Okano T, Taya M. Evaluation of vertical cell fluidity in a multilayered sheet of skeletal myoblasts. J Biosci Bioeng 2011.
78.   Labbé B, Marceau-Fortier G, Fradette J. Cell sheet technology for tissue engineering: the self-assembly approach using adipose-derived stromal cells. Methods Mol Biol 2011;702:429-41.
79.   Fleming PA, Argraves WS, Gentile C, Neagu A, Forgacs G, Drake CJ. Fusion of uniluminal vascular spheroids: a model for assembly of blood vessels. Dev Dyn 2010;239(2):398-406.
80.   Gonzales RJ, Carter RW, Kanagy NL. Laboratory demonstration of vascular smooth muscle function using rat aortic ring segments. Adv Physiol Educ 2000;24(1):13-21.

Chapter 3: Engineered vascular tissue fabricated from aggregated smooth muscle cells

(Gwyther, T.A., Hu, J.Z., Christakis A.G., Skorinko J.K., Shaw S.M., Billiar K.L., Rolle M.W. Cells Tissue Organs, 194(1):13-24, 2011, reprinted with permission, Appendix A)

3.1 Introduction

Over the past three decades, tissue engineering has emerged as a promising approach to create blood vessel substitutes for clinical transplantation, as well as model systems to study vascular tissue function *in vitro*. To date, the majority of strategies for tissue engineered blood vessel (TEBV) synthesis have involved seeding cells within scaffolds made from synthetic [1-5] or natural polymers.[6-11] Alternatively, "scaffold-free" tissue engineering approaches have been explored in which TEBV are fabricated entirely from self-assembled cells and cell-derived extracellular matrix (ECM), such as rolling cultured cell sheets [12,13], organ printing [14,15] or assembly and fusion of clustered cells.[16] Autologous vascular grafts produced by the cell sheet-based engineering method exhibit comparable tensile strength to human saphenous veins [17] although graft fabrication and maturation requires 2-3 months.[18] However, vascular grafts created with this method have already shown clinical promise as arteriovenous fistulas.[19]

Despite the promise and increasing number of reports using cell-based approaches to tissue engineering, few studies to date have examined the mechanical strength or other functional properties of engineered tissue constructs created entirely from cells and cell-derived ECM. Safe and successful *in vivo* application of TEBV made entirely from cells will depend on achieving adequate strength and mechanical stability. The aim of this study was therefore to develop a simple system to generate strong 3-D tissue constructs from aggregated cells within an experimentally useful time frame (1-2 weeks) in a format that is conducive to mechanical and physiological testing. To achieve this aim, we chose to create ring-shaped constructs due to their simple geometry and the precedent for using vascular tissue rings for mechanical and physiological analysis of blood vessel function. We predict that this model system will enable systematic assessment of the roles of cell source and culture parameters on cell-derived tissue structure and function.

To create ring-shaped tissue constructs, rat aortic smooth muscle cells (SMCs) were seeded into custom round-bottomed, annular wells cast in agarose, with post sizes of 2, 4, or 6 mm (to produce rings with 2, 4 or 6 mm inner diameters). Tissue rings were cultured for 8 or 14 days prior to thickness measurements and analysis of handling and mechanical properties. Uniaxial tensile testing was performed to measure ultimate tensile strength, stiffness and failure strain, and tissue structure and ECM composition were examined by histology. Finally, we assessed the feasibility of using tissue rings as subunits to generate larger, tube-shaped constructs.

3.2 Materials and Methods

3.2.1 Custom cell culture well fabrication

A custom polycarbonate mold was created by machining annular wells with inner post diameters of 2, 4, and 6 mm (Small Parts, Inc., Miramar, FL). The wells were machined with round bottoms to facilitate cell settling and self-aggregation to form rings. Polydimethylsiloxane (PDMS; Sylgard 184, Dow Corning, Midland, MI) was mixed at a 10:1 ratio (w/w) of base to curing agent, degassed for 2 hours, and poured onto the polycarbonate mold. After curing at 60°C for 4 hours, the PDMS was peeled from the mold and used as a template. Two percent agarose (w/v; Lonza, Rockland, ME) was dissolved in Dulbecco's Modified Eagle Medium (DMEM; Mediatech, Herndon, VA), autoclaved, and poured onto the PDMS template to form the wells for cell seeding. Individual agarose wells were cut away from the PDMS template and placed into 6-well plates. The agarose wells were incubated in DMEM supplemented with 10% fetal bovine serum (FBS; PAA, Ontario, Canada) and 1% penicillin/streptomycin (Mediatech) and equilibrated in an incubator for 1 hour prior to cell seeding at 37°C and 5% CO_2. A schematic of this process is shown in Figure 3.1.
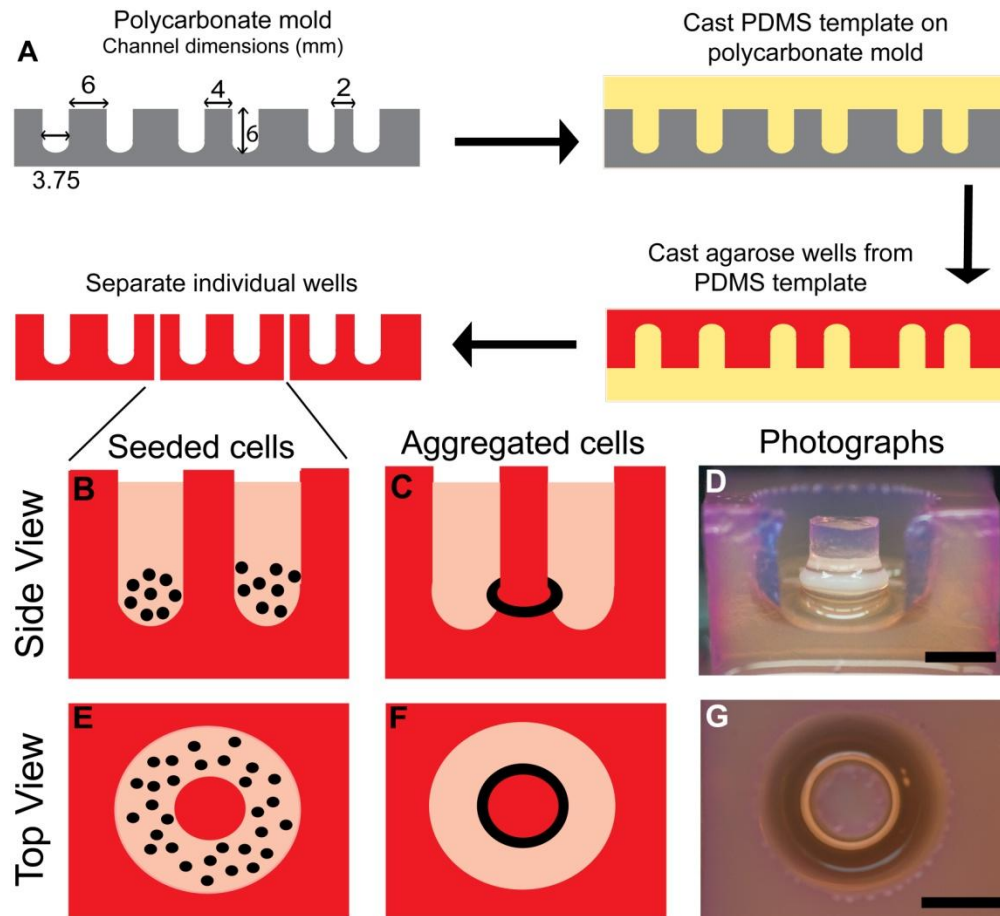
Figure 3.1 – Tissue ring production process. Schematic of tissue ring mold formation (A). PDMS was poured into a polycarbonate mold which then served as a template for casting 2% agarose wells. The agarose was separated into individual wells prior to cell seeding and culture. A cell suspension was then pipetted into agarose wells as shown schematically in (B) and (E) from the side and top, respectively (black dots represent individual cells). The cells were allowed to aggregate undisturbed for 48 hours, which resulted in aggregation, contraction and tissue ring formation (C) and (F); black bands represent aggregated cells contracted around the post. Photographs of the side view (D) and the top view (G) of a 4 mm ID tissue ring in an agarose well after 8 days in culture. Scale bars = 4 mm.

3.2.2 Smooth muscle cell culture and seeding

Rat aortic SMCs (WKY 3M-22; a cell line derived from smooth muscle cells isolated from 3 month old adult male Wistar-Kyoto rat aortas by enzymatic digestion;[20,21] generously provided by Dr. Thomas Wight) were cultured in DMEM (Mediatech) supplemented with 10% FBS (PAA) and 1% penicillin/streptomycin (Mediatech). At 90% confluence, SMCs were trypsinized and re-suspended in culture medium. The number of SMCs seeded into each well was scaled to the size of the channel (0.66, 1.3 and 2.0 x 10^6 cells per well seeded into 2, 4 and 6 mm inner diameter wells, respectively). Plates were

left undisturbed in the incubator for the first 48 hours after seeding, after which the culture medium was changed every 48 hours for the duration of the 8 or 14 day culture period. Four batches of 2, 4 and 6 mm rings were produced for mechanical testing studies (two batches harvested at 8 days and 2 batches harvested at 14 days) as described below. An additional two batches (one at each time point) of 4 mm rings were created for histological evaluation of tissue rings not subjected to mechanical testing (n=3 rings per time point).

3.2.3 Tissue ring thickness measurements

On the final day of each study, the tissue rings were removed from the agarose wells and transferred to 60 mm Petri dishes filled with phosphate buffered saline (PBS) at room temperature. The rings were centered under a machine vision system (DVT Model 630; DVT Corporation, Atlanta, GA) and thickness measurements were acquired in three separate positions along the circumference of the ring using edge detection software (Framework 2.4.6, DVT). Three measurements were averaged to yield a mean thickness value for each sample.

3.2.4 Mechanical testing

Mechanical properties of tissue rings were measured using a uniaxial testing machine (ElectroPuls E1000; Instron, Norwood, MA). The tissue rings were mounted between two small stainless steel pins (referred to as "grips") and submerged in PBS. One grip was connected to an electromagnetic actuator and the other to a 1 N ($\pm$ 1 mN) load cell. Force (F) and displacement (Δl) were recorded continuously throughout the test at a frequency of 10 Hz. The measured thickness value described above was used to calculate the initial cross-sectional area, A, for each ring sample assuming a circular cross-section. A tare load of 5 mN was applied to the mounted ring and the gauge length (l_g) was recorded. The rings were then preconditioned (to eliminate plastic deformation) for 8 cycles from the initial (tare) load to 50 kPa engineering stress (F/A) and then pulled to failure at a rate of 10 mm/min.

Engineering stress and grip-to-grip strain ($\Delta l/l_g$) data were analyzed using MATLAB (The MathWorks, Inc., Natick, MA) to obtain the ultimate tensile strength (UTS), failure strain, maximum tangent modulus (MTM, the maximum slope of the stress-strain curve) and toughness (area under the curve). The MTM is the maximum slope of the linear region of the curve and was used in these studies because it approximates the failure properties of the material to allow sample to sample comparisons, and compare our results to tissue constructs analyzed in other published studies in the Discussion section. The force at failure and the functional stiffness of the rings were also calculated as structural mechanical properties.

The force at failure was recorded from the raw force data as a measure of the overall tissue strength. The product of the structural stiffness (k, the maximum slope of the force-displacement curve; $F/\Delta l$) and the gauge length, l_g, was calculated as a measure of the functional stiffness of the rings. This calculation was performed to normalize structural stiffness (k) to the initial length of the sample in order to allow a fair comparison between samples with different inner diameters ($l_g \sim \frac{1}{2}\pi d_i$). This metric, $k \cdot l_g$, can simply be obtained by multiplying the MTM of each sample by its initial cross-sectional area i.e., $(F/A)/(\Delta l/l_g) \cdot A = (F/\Delta l) \cdot l_g = k \cdot l_g$.

3.2.5 Histology

Tissue rings were fixed in 10% neutral buffered formalin and embedded in paraffin. Five micrometer sections were cut and adhered to Superfrost Plus slides (VWR, West Chester, PA). The sections were stained with hematoxylin and eosin (H&E; reagents from Richard Allan Scientific, Kalamazoo, MI), Movat's pentachrome (reagents from Sigma, St. Louis, MO), Alcian Blue (American MasterTech Scientific, Inc., Lodi, CA), and Fast Green/Picrosirius Red (reagents from Sigma; 0.1% each of Fast Green FCF and Direct Red 80 in Picric Acid) and images were acquired on an upright microscope (Leica DMLB2) equipped with a digital camera (Leica DFC 480). Polarized light images of samples stained with Picrosirius Red alone were acquired with an inverted microscope (Olympus, IX81) with a digital camera (Olympus, Q-Color 5). A linear polarizer was placed between the light source and the specimen, while the analyzer was installed in the light path between the specimen and the camera. The analyzer was rotated until maximum light diminishment was obtained prior to image acquisition from tissue samples. Under polarized light, small collagen I fibers and collagen III fibers appear green, whereas larger collagen I fibers appear yellow [22].

To visualize nuclei, deparaffinized, rehydrated histological sections were stained with Hoechst 33342 dye (10μg/ml; Invitrogen, Eugene, OR) for 3 minutes, rinsed with PBS and coverslipped with aqueous mounting medium (Prolong Gold, Invitrogen).

3.2.6 Tissue ring fusion for cell-derived tube fabrication

Cell-derived rings were created with 2 mm inner diameters and 500,000 cells per ring using the process described above. The rings were cultured for seven days in agarose molds and then transferred onto 1.9 mm OD silicone tubes (SMI, Saginaw, MI). The rings were pushed into tight contact, the silicone was clamped into custom polycarbonate holders, and the rings were cultured horizontally for an additional seven days. After a total of 14 days in culture (seven days as individual rings in agarose wells, seven days

grouped on silicone tubes) the aggregated tube-shaped samples were removed from the mandrels, fixed, and processed for histology.

3.2.7 Statistics

Samples from four different batches of rings (two for each time point) were analyzed to obtain sample sizes of 5-11 tissue rings per group for mechanical testing (8 day groups included n = 6, 8 and 5 tissue ring samples of 2, 4 or 6 mm inner diameter respectively; 14 day groups included n = 6, 9, and 11 samples per 2, 4 or 6 mm tissue ring group). The data are reported as mean ± SEM for the tissue ring thickness values (3 measurements were obtained per ring sample) and as mean ± SD for mechanical properties. A two-way ANOVA was used to analyze the effects of culture duration and ring inner diameter on tissue ring thickness and mechanical properties. SigmaPlot software (Version 11.0 Systat Software, Inc.) was used to perform the ANOVA with Holm-Sidak post hoc analysis to identify significant differences ($p < 0.05$) between parameter values.

3.3 Results

3.3.1 Cells aggregated and formed tissue rings after seeding into agarose wells

Representative photographs of tissue rings derived from aggregated SMCs are shown in Figure 3.1. Within 48 hours after seeding into agarose wells (the earliest time point examined), SMCs spontaneously aggregated to form rings that contracted around the center posts of non-adhesive, round-bottomed agarose wells. This aggregation was consistently observed for all rings generated, regardless of inner (post) diameter.

3.3.2 Tissue ring thickness increased with culture time

Tissue ring thickness increased significantly with culture duration for rings of all sizes, from an average of 0.76 mm at 8 days to 0.94 mm at 14 days (19%, 33%, and 22% increase between 8 and 14 days for 2, 4, and 6 mm rings, respectively; Figure 3.2). At each time point examined, there were no statistically significant differences in thickness between rings of different inner diameters (Figure 3.2).
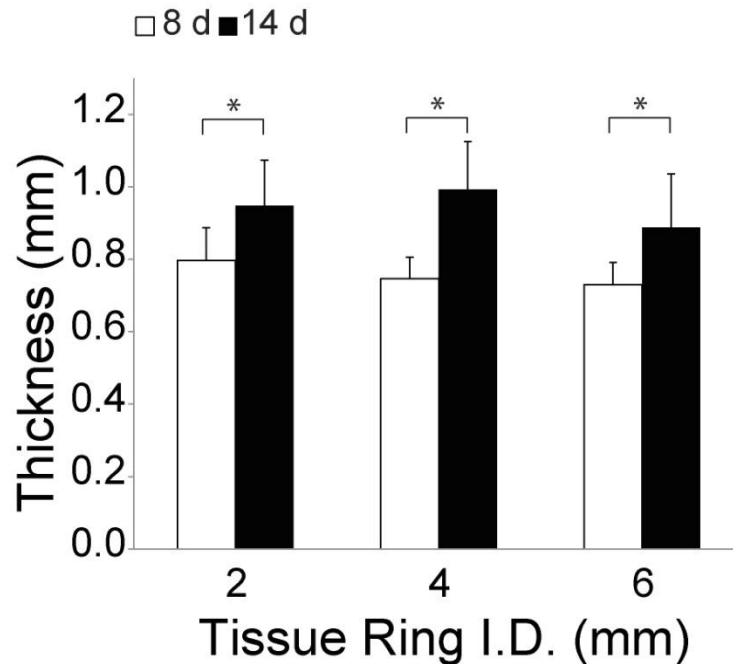
Figure 3.2 – Tissue ring thickness increased with culture time. Three thickness measurements were obtained for each ring sample (values are expressed as mean ± S.E.M., *p<0.05; n = 5-11 per group) cultured for 8 days (white bars) or 14 days (black bars).

3.3.3 Tissue rings were mechanically robust after only 8 days of culture

Stress-strain plots were generated from each of the tissue rings tested and used to calculate mechanical properties of tissue rings (a representative plot is shown in Figure 3.3). Eight days after cell seeding, larger tissue rings exhibited greater ultimate tensile strength values (UTS) than smaller rings (169±45 kPa, 339±131 kPa, and 503±76 kPa for 2, 4 and 6 mm rings, respectively; p<0.05 for all comparisons, Figure 3.4A). Compared to 8 days of culture, the UTS was lower after 14 days (97±30 kPa, 201±63 kPa, and 302±42 kPa, a decrease of 43% (n.s.), 41% (p<0.05), and 40% (p<0.05) for 2, 4 and 6 mm rings, respectively, Figure 3.4A). Tissue ring stiffness (MTM) was similarly greatest in the largest rings after 8 days in culture (0.81±0.28 MPa, 1.21±0.46 MPa, and 1.98±0.4 MPa, respectively, for 2, 4 and 6 mm rings; Figure 3.4B). Similar to the UTS, the MTM values increased with post size by 33% and 59% for 4 and 6 mm rings compared to the 2 mm rings (p<0.05 for all comparisons between ring diameters, Figure 3.4B). Further, the MTM decreased as a function of time in culture to 0.50±0.09 MPa, 0.71±0.20 MPa, and 1.08±0.14 MPa for 2, 4 and 6 mm rings at 14 days (a decrease of 39% (n.s.), 41% (p<0.05), and 45%

(p<0.05) for 2, 4 and 6 mm rings, respectively, Figure 3.4B). The toughness, or the ability of the tissue to absorb energy before rupture, decreased with culture time and increased with ring diameter in similar proportion to the changes in UTS (Figure 3.4C).
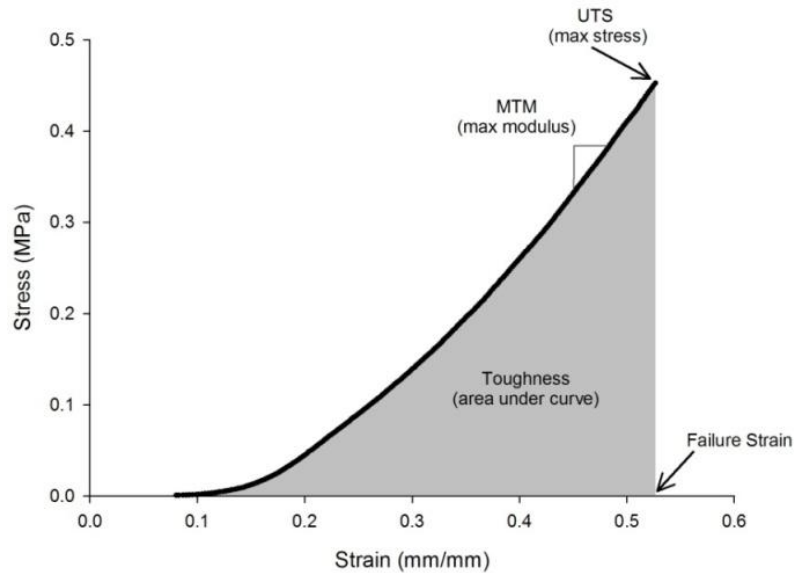
Figure 3.3 – Representative stress-strain data. A sample stress-strain curve obtained from a 4 mm tissue ring cultured for 8 days is shown with definitions of ultimate tensile strength (UTS), maximum tensile modulus (MTM), failure strain and toughness.

The structural properties also varied as a function of ring size. More force was required for failure of large rings (6 mm) than small rings (2 mm) at both time points (Figure 3.4D), and statistically significant increases in the functional stiffness metric ($k \cdot l_g$) were observed with increasing ring size (Figure 3.4E). However, despite the observed changes in intrinsic properties (UTS and MTM) with culture duration, the structural properties were not significantly different at 8 and 14 days. Further, the failure strain averaged 0.46 mm/mm for all samples with no statistical differences between sample groups of different size or culture duration (Figure 3.4F). Combined, these results indicated that the rings became thicker at 14 days but their structural properties did not change significantly between 8 and 14 days in culture.
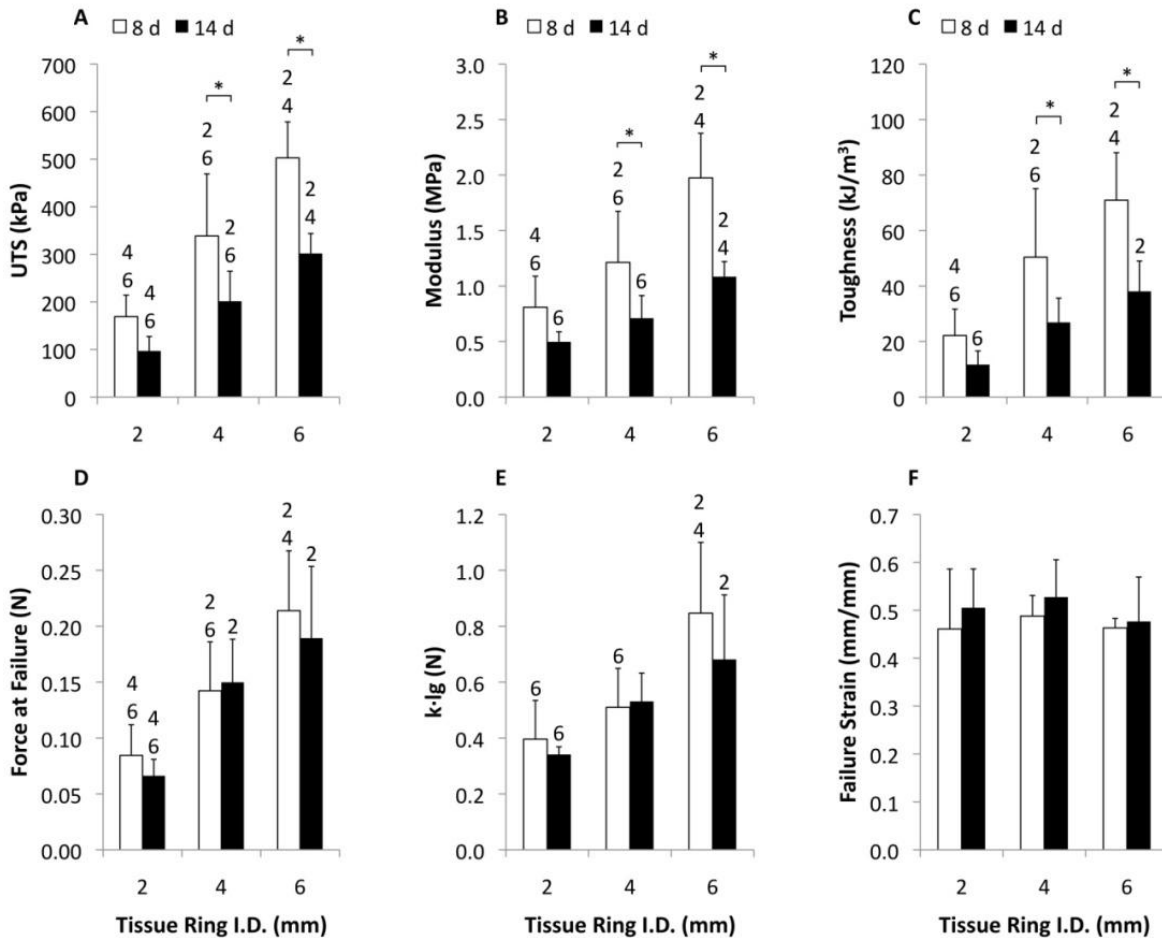
Figure 3.4 – Mechanical properties of cell-derived vascular tissue rings. Uniaxial tensile test results as a function of tissue ring inner diameter: (A) ultimate tensile strength (UTS), (B) modulus (maximum tangent modulus; MTM), (C) toughness, (D) force at failure, (E) $k*l_g$ (functional stiffness), and (F) failure strain. All values are reported as mean ± S.D.; n = 5-11 per group. The asterisks indicate statistical differences between sample groups cultured for different times (p<0.05). Numbers above the bars refer to the inner diameters of the sample groups cultured for the same time for which values are statistically different (p<0.05).

3.3.4 Structure and cellular morphology of tissue rings

Representative micrographs of untested 4 mm rings are shown in Figure 3.5. In tissue rings cultured for 8 or 14 days, cell density appeared highest along the edges of the rings (in direct contact with cell culture medium; Figure 3.5B, E), whereas the number of cells per area appeared to decrease at the centers of the rings (Figure 3.5C, F). In many regions along the circumference of the tissue rings, cells along both the inner and outer edges of the rings contained circumferentially aligned cells (Figure 3.5B, E) whereas cells at the centers of the tissue rings did not appear aligned (Figure 3.5C, F). Additionally, the cells at the

center of the thickest rings (cultured for 14 days) contained fragmented nuclei, which may indicate tissue necrosis (14 day samples; Figure 3.5F).
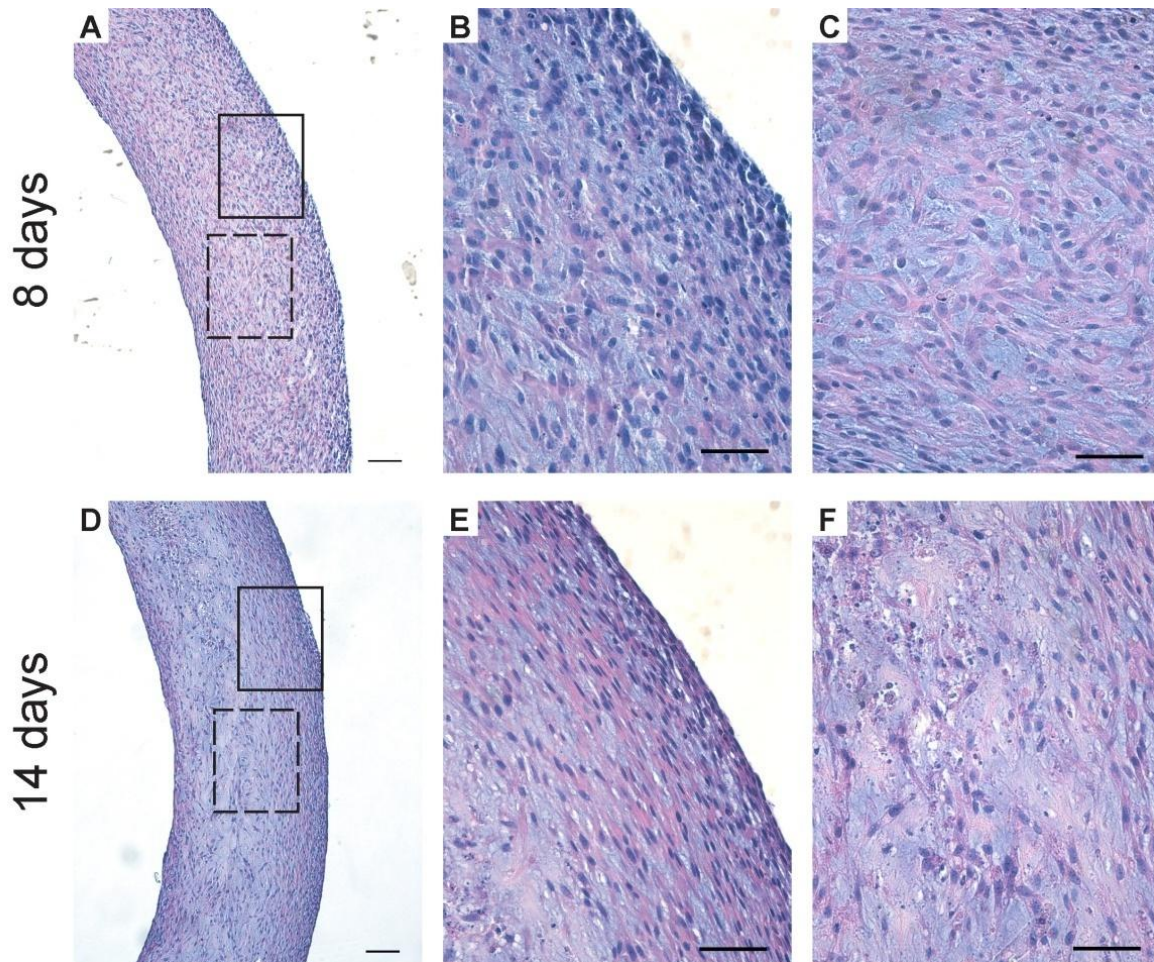
Figure 3.5 – Tissue ring morphology. Representative photomicrographs of 4-mm inner diameter tissue rings cultured for 8 (A-C) and 14 days (D-F). Low magnification views of the rings stained with H&E (A, D; scale bars= 100μm) show the overall morphology of the rings. The boxes indicate the regions of interest magnified in B, E (solid boxes) and C, F (dashed boxes). Scale bars = 50 μm (B, C, E, F).

To more closely examine the composition of the tissue rings, histochemical stains were utilized to assess the composition of the tissue ring ECM (Figure 3.6). Movat's pentachrome and Alcian Blue staining showed that the predominant ECM components in the tissue rings after 8 or 14 days in culture are glycosaminoglycans (GAGs; indicated by the blue stain, Figure 3.6A, B, E, F). Collagen deposition was also detected and appeared to increase in quantity with culture time (red stain; Figure 3.6C, G). Examination of samples stained with Picrosirius Red by polarized light microscopy revealed that collagen quantity, circumferential alignment, and fiber size (Figure 3.6D, H) increased with culture duration.
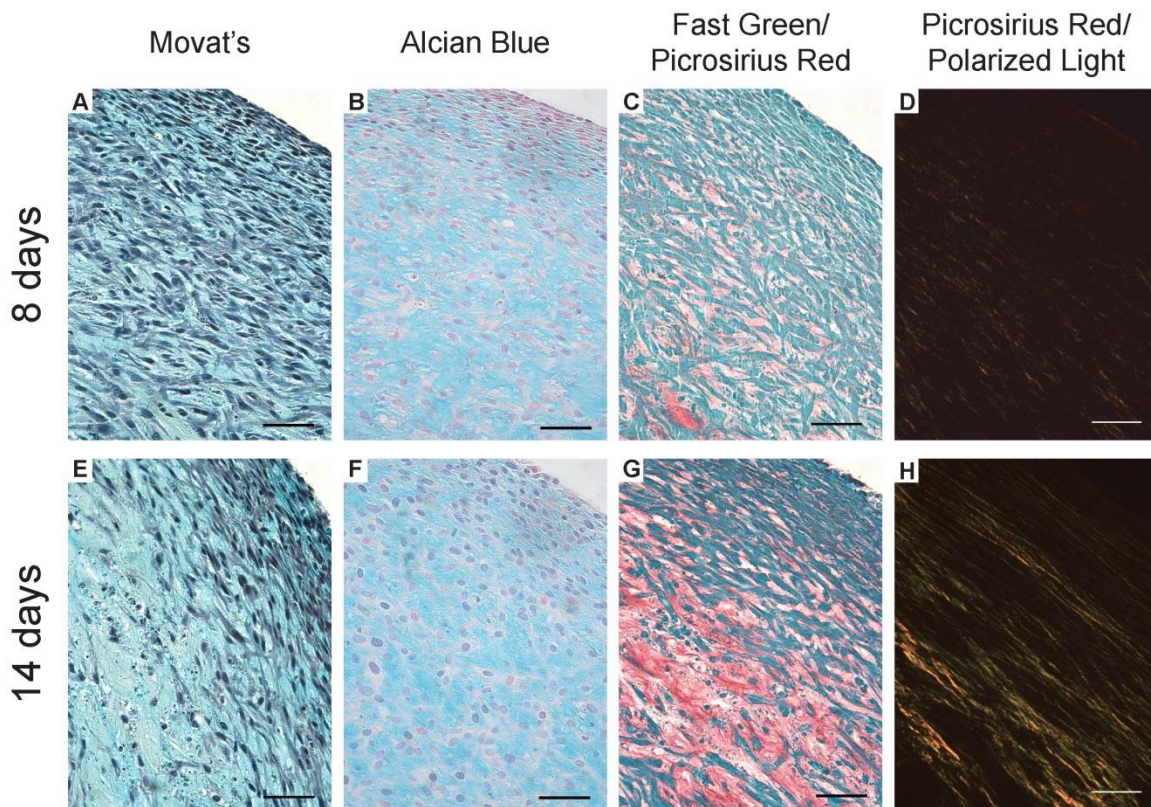
Figure 3.6 – Histochemical assessment of tissue ring ECM composition. Movat's pentachrome (A, E) and Alcian Blue (B, F) staining indicated an abundance of sulfated glycosaminoglycans (blue) at 8 and 14 days of culture. Fast Green/Picrosirius Red staining (C, G) demonstrated the presence of collagen (red) at 8 days and 14 days. Picrosirius Red staining alone observed under polarized light highlights yellow bands of collagen fibers (D, H). Scale bars = 50 μm.

3.3.5 Translation of rings to tubes

To assess the feasibility of using tissue rings as building blocks to create tissue tubes, 2 mm rings cultured for 7 days were removed from agarose wells, transferred to silicone tube mandrels (Figure 3.7A) and

cultured in close contact (Figure 3.7B). Similar to 8 and 14 day rings tested in mechanical studies, 7 day rings were easy to handle and transfer. Individual rings become less distinct after 7 days in culture (Figure 3.7C), at which time cohesive tube constructs were successfully harvested from the silicone mandrels (Figure 3.7D). Tissue tubes remained intact during subsequent handling and processing for histological analysis. The original ring margins were still clearly visible by histology after 7 days of ring fusion (Figure 3.8A) with evidence of tissue reorganization and closure of "gaps" between rings. Upon closer examination of the fusion junctions, the cells along the outer edge of the tube appear to form a healthy, contiguous cell layer (Figure 3.8B, C) whereas there are some fragmented nuclei at the centers of the tissue and along the central region of the fusion junction (Figure 3.8D, E). The nuclei on the inner edge (adjacent to the silicone mandrel, Figure 3.8F, G) also appear to form a contiguous layer that spans adjacent rings.
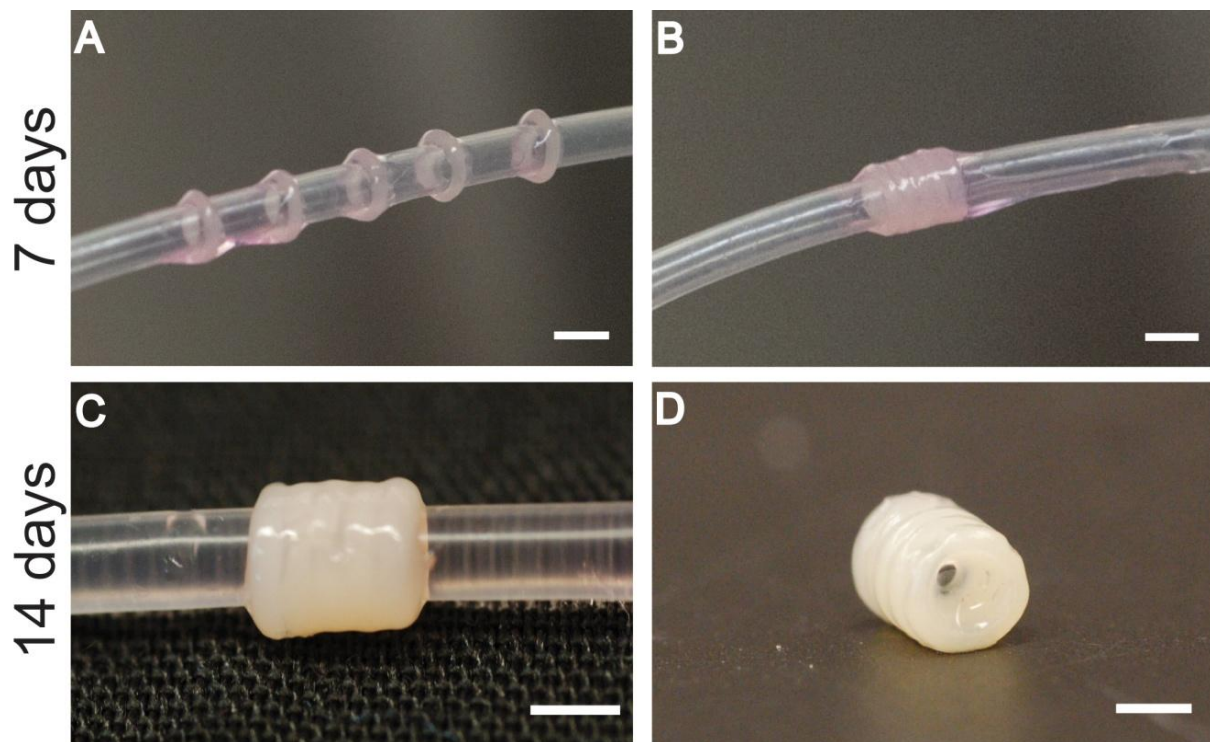
Figure 3.7 – Tissue ring fusion to form a tube. Tissue rings were cultured for 7 days before transfer onto a 1.9 mm OD silicone mandrel (A) where they are placed in close contact (B). The tubes were then cultured for 7 days (C) before removal of the silicone mandrel to harvest the tissue tube (D). Scale bars = 2 mm
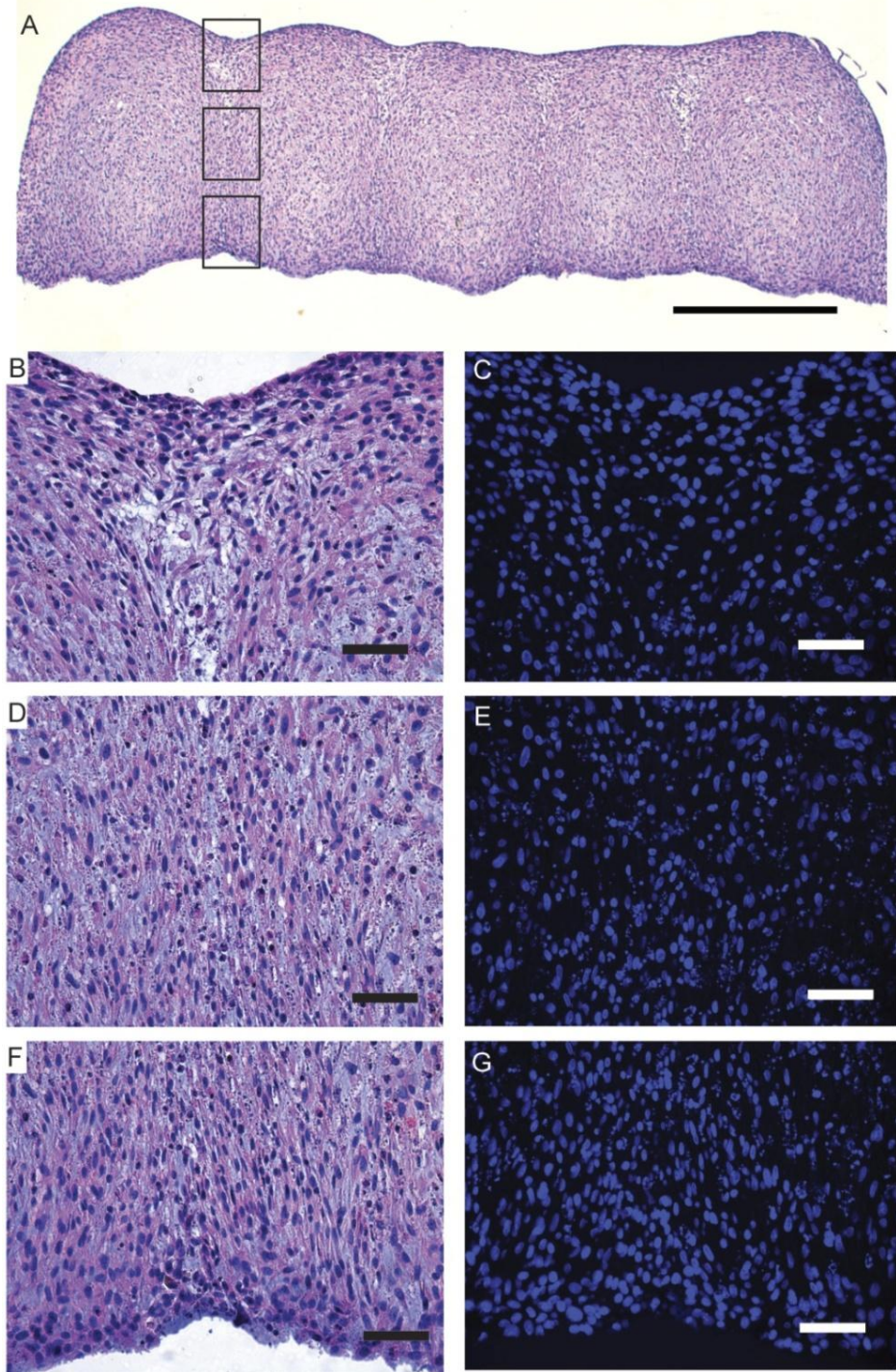
Figure 3.8 – Tissue tube morphology. Representative photomicrographs of tissue tubes cultured for a total of 14 days (7 days as rings, 7 days on silicone mandrels). The tube appears completely fused, although ring margins are visible by H&E staining (A; scale bar = 0.5 mm). Higher magnification views of the junction between the first two rings are highlighted in three parts corresponding to the boxes in panel A; the outer junction (B, C), the middle junction (D, E), and the inner junction closest to the silicone tube (F, G) stained with H&E (B, D, F) and Hoechst nuclear dye (C, E, G). Scale bars for B-G = 50 µm.

3.4 Discussion

We have developed and validated a method for fabricating ring-shaped tissue constructs entirely from aggregated smooth muscle cells that are strong enough to withstand handling and mechanical testing within 8 days of cell seeding. To our knowledge, this is the first study to report biomechanical evaluation of tissue constructs generated in a one-step process from aggregated cells and cell-derived ECM in static culture in this time frame. Our results demonstrate that facilitated cell aggregation can be used to create strong 3-D tissue constructs within the diameter range of clinically useful vascular grafts (2 – 6 mm). Although the focus of the current study was to characterize the strength and structure of ring-shaped constructs as a function of ring size and culture duration, however, we believe that this system will be useful for screening the effects of cell source and culture conditions on material properties of cell-derived tissues. Finally, we have provided evidence that these ring constructs can be used as building blocks to generate cell-derived tissue tubes, suggesting that information gained from functional ring studies may be directly translated to the design and construction of tubular structures such as vascular grafts.

Overall, cell-derived tissue rings were stronger than ring segments from engineered vascular tissue equivalents cultured for similar time periods. For example, the average UTS (100–500 kPa) far exceeded that reported for engineered tissues made with smooth muscle cells cultured statically within collagen (16 kPa at 8 days[11]) and collagen/fibrin mixtures (28 kPa at 7 days[23]). Without growth factor supplementation, the strength of our rings at 8 days approached that reported for SMC-populated fibrin gels cultured for 3 weeks with TGF-β1 and insulin (476 kPa[6]). The MTM (0.5-2 MPa) of the cell-derived tissue rings also compared favorably to other engineered tissue rings (0.07-5.35 MPa[11,24]) and tissue ring toughness values (12-71 kJ/m^3) were also high relative to what has been observed for collagen gel-based model vessels (0.5 kJ/m^{3,24}). However, all of these values are low compared to native arteries (e.g., porcine carotid artery UTS ~ 6.6 MPa[25]). In future studies, optimization of culture conditions to increase ECM synthesis and tissue strength may be performed, such as treatment with soluble factors (e.g. sodium ascorbate,[26] TGF-β1,[27] and insulin[27]) or mechanical conditioning[3,28] to further strengthen cell-derived tissue rings.

Previous studies in which the strength and composition of planar cell-derived tissues were compared to constructs comprised of an equal number of cells seeded within fibrin or collagen gels demonstrated that cell-derived constructs exhibit greater tensile strength and ECM synthesis [26]. Similarly, robust synthesis of ECM, comprised primarily of glycosaminoglycans and collagen, may be the basis for the observed strength and stiffness of the cell-derived tissue rings. Quantitative biochemical analysis of ECM composition, organization and cross-linking will be performed in future studies to evaluate the molecular basis of tissue ring structure and material properties.

Ring size had a significant effect on tissue mechanical properties, with lower force at failure, UTS, and MTM recorded for the smallest (2 mm rings) at all time points. Ring wall thickness was consistent across samples of different dimensions (cultured for the same duration; Figure 3.2), therefore the length-to-cross-sectional-area ratio of the constructs at the initial gauge length differed as a function of ring ID. We attempted to account for the effects of ring ID by defining and reporting the functional stiffness (data shown in Figure 3.4E). As stated in the Methods section, this calculation was performed to normalize samples with different inner diameters ($l_g \sim \frac{1}{2}\pi d_i$). As a result of the high thickness to ID ratio in smaller (2 mm) compared to larger (6 mm) rings, there may be greater bending stiffness associated with the smaller rings, therefore a greater load would be applied to the smaller rings to straighten them prior to pre-cycling. Consequently, the smaller rings may be subjected to higher stresses prior to the pull-to-failure test, which could result in lower recorded UTS and force at failure values in the 2 mm rings. However, regardless of the lower strength and modulus compared to larger rings, the 2 mm rings in this study were mechanically robust compared to those reported in other studies of engineered vascular tissue, as detailed above, and tissue ring fusion studies demonstrated that 2 mm rings cultured for 7 days were strong enough to withstand transfer and manipulation on silicone tubes. Histologically, the tissue rings were indistinguishable on the basis of size at a given time point (data not shown), and thickness and failure strain values were not statistically different.

Tissue ring wall thicknesses were greater (up to 0.94 mm after 14 days in culture) than those reported for other cell-derived tissue constructs. This may be partially explained by the high density of cell seeding used to form rings and greater proliferation rate of the rat cell line used in this study compared to primary human cells. By comparison, cell-derived tissue sheets generated from human dermal fibroblasts seeded at 10,000 cells/cm^2 and cultured for 6 weeks were 43 µm thick (more than 20-fold thinner), which increased by 5 µm per week thereafter (up to 15 weeks [18]). Thicker constructs (125-395 µm) were created from human dermal fibroblasts within 3 weeks by seeding at a higher density (2 million cells seeded in a 4.5 cm^2 well) and cultured in chemically-defined medium [26]. In our tissues, high thicknesses may have contributed to necrosis observed at the tissue centers. This necrosis may have contributed to a reduction in structural integrity due to a loss of cells, which may partially explain the observed decrease in UTS despite an increase in ring thickness between days 8 and 14. The polarized light microscopy data suggested that collagen synthesis and remodeling increased in the tissue rings between days 8 and 14, although this did not coincide with an increase in tissue strength or stiffness. Interestingly, preliminary studies suggest that culturing tissue rings in culture medium supplemented with sodium ascorbate and amino caproic acid, conditions that have been shown to increase collagen synthesis and cross-linking, also improved tissue ring strength and stiffness (data not shown). It may be possible to optimize culture

conditions (by decreasing or eliminating serum, adding growth factors or mechanical stimulation, as described above) to make tissue rings stronger without increasing thickness.

Given the large number of cells needed to generate four batches of tissue rings in three different sizes to establish the basic parameters (e.g., initial cell seeding number per well, culture duration, mechanical testing protocol, etc.) for creating and analyzing cell-derived tissue rings, we chose to use the WKY 3M-22 rat smooth muscle cell line for the experiments reported in this study. However, we recently applied the same techniques to successfully assemble primary human coronary artery SMCs into cell-derived tissue rings, which were then cultured for 14 days. Despite their slower doubling time, in preliminary experiments the human SMC rings exhibited greater mechanical strength than the rat SMCs reported here (data not shown), thereby demonstrating that this cell aggregation system can be applied to create tissue rings from primary cells. Ongoing studies are focused on histological and biochemical analysis of the human SMC tissue constructs.

An important difference between the tissue ring constructs and vascular ring segments from native arteries is the lack of an endothelium or adventitia. Like most in vitro reports of TEBV construction, our study focused on a single cell type, smooth muscle cells, to mimic the vascular media. Recent studies have shown that cell sheet-based vascular grafts comprised of both smooth muscle cells and fibroblasts exhibit greater ECM synthesis and higher burst pressures compared to constructs made from smooth muscle cells alone [13]. Furthermore, microtissue aggregation studies have shown that endothelial cells can co-aggregate with fibroblasts to form spheroids [16,29,30]. It may therefore be possible to add fibroblasts and endothelial cells to smooth muscle cells to increase strength and more closely mimic blood vessel structure and function in cell-derived tissue rings.

Upon successful fabrication and handling of cell-based ring constructs, it became evident that cell-derived tissue rings could be used as building blocks to form tissue tubes. Here we report proof-of-concept that tissue rings cultured in close proximity fuse to form a cohesive tissue tube within 14 days (7 days for ring fabrication and 7 days for fusion). Culturing the tubes for an extended period may result in further fusion and elimination of ring boundaries. A recent study by Livoti and Morgan showed that toroid microtissues (600 µm inner diameter) self-assembled from H35 hepatocytes cultured for 48 hours could be stacked and cultured, with fusion of adjacent toroids within 72 hours [31]. The ease with which 2 mm smooth muscle cell rings could be handled after 7 days in our study suggests that it may be possible to harvest our rings even earlier to accelerate the process of graft fabrication. Finally, histological evaluation demonstrated that individual rings had fused to form a contiguous tissue mass within 7 days. However, burst pressure

analysis will be a critical benchmark to determine the feasibility of transplanting vascular grafts created with this method.

In conclusion, we have shown that tissue constructs that are suitable for manipulation and functional testing can be created from aggregated smooth muscle cells within a few days. Although these rings are not as strong as ring segments of native blood vessels or tissue engineered blood vessels generated from cultured cell sheets for 2-3 months, their strength compares favorably to other engineered tissue constructs reported to date. Given the short time frame and simplicity of this system (which relies on commercially available materials and methods), it may enable systematic assessment of a variety of parameters on tissue structure and function (e.g., cell source, culture medium composition, dynamic culture regimens). The ring-shaped geometry of these constructs is useful for mechanical testing, and based on the ease with which they could be mounted onto wire grips, may also be used in a myograph system to measure tissue responses to pharmacologic agents. This system has potential as a new 3-D in vitro model of vascular tissue function, and a versatile tool to advance development of cell-derived vascular grafts.

3.5 References

1.   Hashi CK, Zhu Y, Yang GY, Young WL, Hsiao BS, Wang K, Chu B, Li S. Antithrombogenic property of bone marrow mesenchymal stem cells in nanofibrous vascular grafts. Proc Natl Acad Sci U S A 2007;104(29):11915-20.
2.   Nieponice A, Soletti L, Guan J, Deasy BM, Huard J, Wagner WR, Vorp DA. Development of a tissue-engineered vascular graft combining a biodegradable scaffold, muscle-derived stem cells and a rotational vacuum seeding technique. Biomaterials 2008;29(7):825-33.
3.   Niklason LE, Gao J, Abbott WM, Hirschi KK, Houser S, Marini R, Langer R. Functional arteries grown in vitro. Science 1999;284(5413):489-93.
4.   Opitz F, Schenke-Layland K, Cohnert TU, Starcher B, Halbhuber KJ, Martin DP, Stock UA. Tissue engineering of aortic tissue: dire consequence of suboptimal elastic fiber synthesis in vivo. Cardiovasc Res 2004;63(4):719-30.
5.   Shinoka T, Shum-Tim D, Ma P, Tanel R, Isogai N, Langer R, Vacanti J, Mayer JJ. Creation of viable pulmonary artery autografts through tissue engineering. J Thorac Cardiovasc Surg 1998;115(3):536-45; discussion 545-6.
6.   Grassl ED, Oegema TR, Tranquillo RT. A fibrin-based arterial media equivalent. J Biomed Mater Res A 2003;66(3):550-61.
7.   Stegemann JP, Kaszuba SN, Rowe SL. Review: advances in vascular tissue engineering using protein-based biomaterials. Tissue Eng 2007;13(11):2601-13.
8.   Swartz DD, Russell JA, Andreadis ST. Engineering of fibrin-based functional and implantable small-diameter blood vessels. Am J Physiol Heart Circ Physiol 2005;288(3):H1451-60.
9.   Weinberg CB, Bell E. A blood vessel model constructed from collagen and cultured vascular cells. Science 1986;231(4736):397-400.
10. Zavan B, Vindigni V, Lepidi S, Iacopetti I, Avruscio G, Abatangelo G, Cortivo R. Neoarteries grown in vivo using a tissue-engineered hyaluronan-based scaffold. Faseb J 2008;22(8):2853-61.
11. Seliktar D, Black RA, Vito RP, Nerem RM. Dynamic mechanical conditioning of collagen-gel blood vessel constructs induces remodeling in vitro. Annals of Biomedical Engineering 2000;28(4):351-362.

12.   L'Heureux N, Paquet S, Labbe R, Germain L, Auger FA. A completely biological tissue-engineered human blood vessel. Faseb J 1998;12(1):47-56.
13.   Gauvin R, Ahsan T, Larouche D, Lévesque P, Dubé J, Auger F, Nerem R, Germain L. A novel single-step self-assembly approach for the fabrication of tissue-engineered vascular constructs. Tissue Eng Part A 2010;16(5):1737-47.
14.   Mironov V, Visconti R, Kasyanov V, Forgacs G, Drake C, Markwald R. Organ printing: tissue spheroids as building blocks. Biomaterials 2009;30(12):2164-74.
15.   Norotte C, Marga F, Niklason L, Forgacs G. Scaffold-free vascular tissue engineering using bioprinting. Biomaterials 2009;30(30):5910-7.
16.   Kelm J, Lorber V, Snedeker J, Schmidt D, Broggini-Tenzer A, Weisstanner M, Odermatt B, Mol A, Zünd G, Hoerstrup S. A novel concept for scaffold-free vessel tissue engineering: Self-assembly of microtissue building blocks. J Biotechnol 2010.
17.   Konig G, McAllister T, Dusserre N, Garrido S, Iyican C, Marini A, Fiorillo A, Avila H, Wystrychowski W, Zagalski K and others. Mechanical properties of completely autologous human tissue engineered blood vessels compared to human saphenous vein and mammary artery. Biomaterials 2009;30(8):1542-50.
18.   L'Heureux N, Dusserre N, Konig G, Victor B, Keire P, Wight TN, Chronos NA, Kyles AE, Gregory CR, Hoyt G and others. Human tissue-engineered blood vessels for adult arterial revascularization. Nat Med 2006;12(3):361-5.
19.   McAllister T, Maruszewski M, Garrido S, Wystrychowski W, Dusserre N, Marini A, Zagalski K, Fiorillo A, Avila H, Manglano X and others. Effectiveness of haemodialysis access with an autologous tissue-engineered vascular graft: a multicentre cohort study. Lancet 2009;373(9673):1440-6.
20.   Lemire J, Covin C, White S, Giachelli C, Schwartz S. Characterization of cloned aortic smooth muscle cells from young rats. Am J Pathol 1994;144(5):1068-81.
21.   Lemire J, Potter-Perigo S, Hall K, Wight T, Schwartz S. Distinct rat aortic smooth muscle cells differ in versican/PG-M expression. Arterioscler Thromb Vasc Biol 1996;16(6):821-9.
22.   Whittaker P, Kloner RA, Boughner DR, Pickering JG. Quantitative Assessment of Myocardial Collagen with Picrosirius Red Staining and Circularly Polarized Light %J Basic Research in Cardiology. 1994;89:397-410.
23.   Rowe SL, Stegemann JP. Interpenetrating collagen-fibrin composite matrices with varying protein contents and ratios. Biomacromolecules 2006;7(11):2942-8.
24.   Gildner CD, Lerner AL, Hocking DC. Fibronectin matrix polymerization increases tensile strength of model tissue. Am J Physiol Heart Circ Physiol 2004;287(1):H46-53.
25.   Dahl SL, Rhim C, Song YC, Niklason LE. Mechanical properties and compositions of tissue engineered and native arteries. Ann Biomed Eng 2007;35(3):348-55.
26.   Ahlfors JE, Billiar KL. Biomechanical and biochemical characteristics of a human fibroblast-produced and remodeled matrix. Biomaterials 2007;28(13):2183-91.
27.   Long JL, Tranquillo RT. Elastic fiber production in cardiovascular tissue-equivalents. Matrix Biol 2003;22(4):339-50.
28.   Isenberg BC, Tranquillo RT. Long-term cyclic distention enhances the mechanical properties of collagen-based media-equivalents. Ann Biomed Eng 2003;31(8):937-49.
29.   Napolitano AP, Chai P, Dean DM, Morgan JR. Dynamics of the self-assembly of complex cellular aggregates on micromolded nonadhesive hydrogels. Tissue Engineering 2007;13(8):2087-2094.
30.   Napolitano AP, Dean DM, Man AJ, Youssef J, Ho DN, Rago AP, Lech MP, Morgan JR. Scaffold-free three-dimensional cell culture utilizing micromolded nonadhesive hydrogels. Biotechniques 2007;43(4):494-+.
31.   Livoti C, Morgan J. Self-assembly and tissue fusion of toroid-shaped minimal building units. Tissue Eng Part A 2010;16(6):2051-61.

Chapter 4: Fabrication of cell-derived vascular tissue tubes using a modular tissue engineering approach

4.1 Introduction

In previous studies, we demonstrated that cell-aggregated tissue rings can be generated in as little as 8 days and are strong enough for handling and subsequent uniaxial tensile testing.[1] We showed that these rings are easy to create, and when pressed end to end and cultured for up to 7 days, they fuse to form tissue tubes. Although cohesive tubes were observed (indicated by their ability to remain intact throughout handling), ring margins remained visible by histology which suggested that tissue fusion was incomplete.

In an effort to improve ring fusion, we explored self-assembled cell ring culture parameters that could be manipulated in order to enhance the cell rings' ability to fuse together. Published studies have suggested that "less mature" cell aggregates fuse together more rapidly than "more mature" tissues.[2] For example, fusion of small cell spheroid aggregates (~100-300 μm in diameter) into rods occurred within 24 hours when spheroids were cultured for only one day prior to fusion, whereas spheroids cultured for seven days exhibited minimal fusion at the 24 hour time point.[2] One of the motivations for the current study was to explore this concept toward the goal of enhancing tissue ring fusion, decreasing the required culture duration, and ultimately building a more cohesive cell-derived vascular tissue construct from self-assembled cell ring building blocks. Therefore, the first goal of the current work was to investigate the effect of ring culture duration on fusion of the tissue rings into tubes. To do this, we cultured tissue rings for 1, 3, 5, or 7 days prior to fusion, and measured how quickly the rings remodeled to form tubes.[1] We hypothesized that decreasing the ring culture duration prior to stacking would decrease the length of time required to generate tissue tubes, and enhance cell ring fusion.

Additionally, we explored another unique attribute of this modular system, which is the ability to spatially control cell placement within the tubes and generate complex chimeric tissue structures. Many vascular diseases (including aneurysm and plaque formation) affect certain regions of blood vessels with greater frequency. Within these regions, the SMC phenotype and ECM may be altered by either synthesis of unwanted molecules such as lipids and collagen, or degradation of the existing matrix molecules such as

elastin.[3,4] Using the modular stacking approach enabled by the ring system, we hypothesized that (in principle) we can introduce and retain spatially distinct regions within the tissue tubes, derived from different cellular origins along the tube length.

Finally, atherosclerosis and intimal thickening has been shown to occur more frequently at branching points within vessels.[5,6] However, these regions remain largely unstudied due to the complexity in their structure and the difficulty involved in fabricating and modeling living branched tissues *in vitro*. The generation of branched structures has proven especially challenging to model with cell-derived approaches because of the difficulty in getting cells to self-assemble into complex geometries. Recent studies have demonstrated that bio-printing can be used to generate branched vessel networks,[7,8] but this requires custom, specialized equipment not readily available to all researchers. Due to the modular characteristics of our ring-based system, one of the goals of this study was to build structures with complicated geometries by assembling the ring subunits into different shapes, such as "Y"-shaped tubes. These branched vessels have potential applications as implantable vascular networks or as *in vitro* models to study disease progression at vessel bifurcations.

In the present study, we describe a method for generating fully biological small-diameter vascular tissue constructs completely from cells and the matrix they produce in a short amount of time (8 - 14 days). We show that fusion of self-assembled cell ring building blocks is enhanced by decreasing their initial culture length, and that we can capitalize on the "modular" aspects of the system by controlling spatial location and building complex "Y"-shaped tubes.

4.2 Methods

4.2.1 Cell culture

Rat aortic SMCs (WKY 3M-22; a cell line derived from SMCs isolated from 3-month-old adult male Wistar-Kyoto rat aortas by enzymatic digestion,[9,10] generously provided by Dr. Thomas Wight, referred to as rat SMCs) were cultured in Dulbecco's modified Eagle medium (DMEM, Mediatech) supplemented with 10% FBS (PAA) and 1% penicillin/streptomycin (Mediatech). All cells were passaged at 90% confluence prior to tissue ring formation.

4.2.2 Tissue ring fabrication

Cell-derived tissue rings were formed as described in Gwyther et al.[1,11] Briefly, polycarbonate molds were custom machined with round-bottomed annular wells with inner post diameters of 2 mm. Polydimethylsiloxane (PDMS) was then poured over the mold to form a negative template. Two percent agarose dissolved in DMEM was autoclaved and poured onto the PDMS template to form the seeding wells. The wells were cut apart and placed in each well of a 12 well plate. Media was added around the outside of the well to equilibrate. To each well, 100 µL of cell suspension was added (at a concentration of 5×10^6 cells/ml). Wells were left undisturbed for one day to allow the cells to settle and aggregate. After one day, medium was exchanged, and complete medium exchange was performed every two days for the duration of culture.

4.2.3 Tissue tube fusion

Tissue rings were removed from their agarose molds after 1, 3, 5, or 7 days in culture. The rings were then transferred onto silicone tubing mandrels (SMI, Saginaw, MI – O.D. 1.9 mm). In initial studies, the silicone mandrel was made by gluing the tip of a 20G needle (Becton Dickinson, NJ) into the end of the tube using sterile silicone adhesive ((Silastic, Dow Corning, MI). We found that a pointed tip, rather than a blunt end, made it easier to transfer the rings onto the silicone mandrels. In subsequent studies, we found that cutting the silicone tubes at an angle to create beveled ends resulted in a sufficiently narrow point to facilitate ring mounting more simply and consistently.[11] Regardless of the silicone tube mounting method, the rings were placed in contact with one another by pushing the stacked rings back and forth as a group, and the silicone mandrels were secured into custom polycarbonate holders. All tubes were then allowed to fuse for 7 additional days (referred to as "fusion culture"). All sample groups were labeled according to the number of days in ring culture, followed by the number of days the rings were in fusion culture (ex. group 3-7 means the sample was cultured for 3 days as rings followed by 7 days in fusion culture, see Figure 4.1).
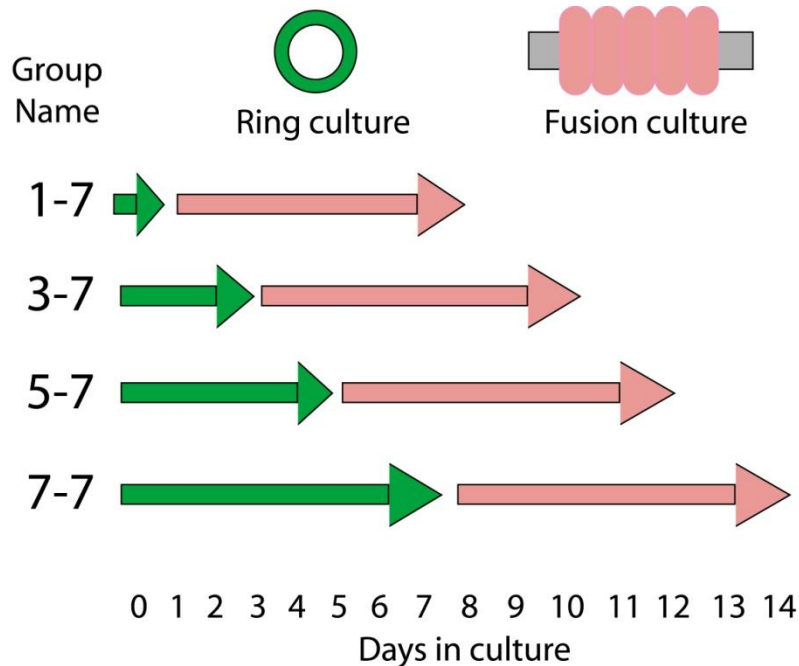
Figure 4.1 – Schematic indicating tissue tube culture groups. Rings were cultured for 1, 3, 5, or 7 days ("ring culture"), followed by an additional 7 days in fusion culture for all groups. Groups are named as: days in ring culture – days in fusion culture (ex. Group 1-7 = 1 day in ring culture followed by 7 days in fusion culture).

4.2.4 Tube fusion on porous mandrels

In a follow up study, the same procedure was used with a different mandrel material. The mandrel material used was an electrospun blended co-polymer of 7% polyurethane (PU) and 3% polyethylene terephthalate (PET); electrospun onto a 1mm-thick cylindrical mandrel (final O.D. ~2mm), generously donated by BioSurfaces, Inc. Twelve rings were harvested at one day and stacked onto an electrospun blended co-polymer mandrel cut with a beveled end. The tubes were clamped into custom polycarbonate tube holding devices and cultured for 7 days.[11]

4.2.5 Fusion angle measurements

To measure the rate of fusion between tissue rings, three rings were placed in contact on silicone mandrels. A Leica upright microscope (model DMLB2) with a digital camera (Leica DFC 480) was used to take low magnification (5X) phase contrast images each day for one week. Image J software (NIH) was used to measure the angle between rings (described as fusion angle),[12] the thickness of the tube, and the length of the tube (measurements indicated in Figure 4.3). All four angle measurements were averaged together to yield a fusion angle measurement for each tube sample per time point. Similarly, two thickness measurements were averaged to yield a mean thickness value for each tube per time point, and two length measurements were averaged to yield a single mean length value per tube per time point.

4.2.6 Burst pressure testing

Tissue tubes were harvested after a total of 8 days in culture (1 day in ring culture, followed by 7 days in fusion culture). The tubes were removed from the silicone mandrel and mounted onto 22 gauge blunt end needles (Small Parts). These needles were secured into a custom burst pressure device.[13] The tissue tube was then filled with saline at a constant rate of 0.5 ml/min and the pressure inside the tube was monitored by a pressure transducer (PX26-100, Omega) and displayed on a panel meter (PX300-15GV, Omega). The peak pressure at failure was recorded as the burst pressure.

4.2.7 Histology and immunohistochemistry

Tissue samples were fixed in 10% neutral buffered formalin, processed, and embedded in paraffin. Five micron sections were cut and adhered to positively charged slides (Superfrost Plus, VWR). The slides were then stained with H&E (Newcomers Supply), Fast Green/Picrosirius Red (0.1% each of Fast Green and Direct Red 80 in picric acid, Sigma), and Alcian Blue (Newcomers Supply). For immunohistochemical analysis of the tissues, the slides were deparaffinized and rehydrated prior to heat-induced epitope retrieval (heated in pressure cooker for 5 minutes in Tris/EDTA buffer, pH 9.0) and blocking in serum for 1 hour. The slides were then exposed to a primary antibody against proliferating cell nuclear antigen (PCNA, Abcam, 1:3000 dilution) for 1 hour. This was followed by green fluorescent labeling with secondary antibodies conjugated to AlexaFluor 488 (Invitrogen, 1:400 dilution). All slides were counterstained with Hoechst (Invitrogen) and mounted with Prolong Gold (Invitrogen). Images were acquired using an upright microscope (Leica DMLB2) with a digital camera (Leica DFC 480).

For quantification of the relative nuclear density throughout the thickness of the tubes, 40x magnification images were acquired of Hoechst-stained samples, at the outer and inner edges of the fused tube samples. Eight images were taken from each tube, four on the outer edge and four along the inner edge. These images were then binarized in ImageJ software (NIH), and the percent area occupied by nuclei was calculated. There were 28-40 images analyzed and averaged for each the inner and outer edges.

The images were taken as close to the edge of the tube as possible. In some samples there were small gaps of non-tissue area (example in the top edge of Figure 4.6B). These areas were not accounted for in the analysis. These results were averaged together to yield a nuclear density for the outer and the inner edges as a mean ± SD of percent nuclei coverage.

For quantification of the PCNA-positive region, fluorescent images were taken in the green channel (PCNA staining) and the blue channel (Hoechst counterstain). The images were merged together in Image J software. The depth of the PCNA-positive region was measured as well as the overall thickness of the tissue tube. Measurements were taken for each side of the tube (two measurements per tube) and averaged together. The data is represented as both the average depth of PCNA-positive cells per experimental group ± S.D. and also normalized to the percent thickness of the PCNA-positive region (i.e. depth of PCNA-positive region divided by the total thickness) ± S.D.

4.2.8 Cell tracking

Rat SMCs were pre-labeled with Vybrant® CFDA SE (Invitrogen) prior to ring formation to track the distribution of cells in the fused rings. Vybrant was added to a plate of rat SMCs at a concentration of 10 μM for 15 minutes (dye was added 45 minutes prior to rat SMC trypsinization and seeding to form rings). One day after ring formation, the rings were removed from the agarose molds and transferred onto silicone mandrels such that one unlabeled ring contacted one Vybrant-labeled ring. Two samples were generated per experiment and this experiment was performed twice. The rings were then allowed to culture for an additional 1 or 3 days before both phase and fluorescent images were acquired with a Leica DMLB2 equipped with a digital camera (Leica DFC 480).

4.2.9 Generation of branched vessels

To generate branched vessels, custom Y-shaped mandrels were made from three pieces of silicone tubing (Specialty Manufacturing, Inc., Saginaw, MI). The base portion was 4 mm OD (beveled on one end), and the two branches were 2 mm OD (beveled on both ends). One beveled end of each 2 mm OD piece of silicone tubing was placed facing each other and inserted into the flat end of the 4 mm OD tube. The branched mandrel was then cleaned and autoclaved before use. To create the branched vessels, four-eight 2 mm rings were transferred onto each of the small branches of the mandrel. Four-eight 4 mm rings were then transferred onto the 4 mm OD branch of the y-shaped mandrel. All rings were moved in contact with one another and allowed to fuse in culture for 7 days prior to removal of the silicone tubing mandrels. Low magnification images of the branched tubes were obtained with a Leica EZ4D stereomicroscope. A schematic of the branched tube generation process is shown in Figure 4.2 below.
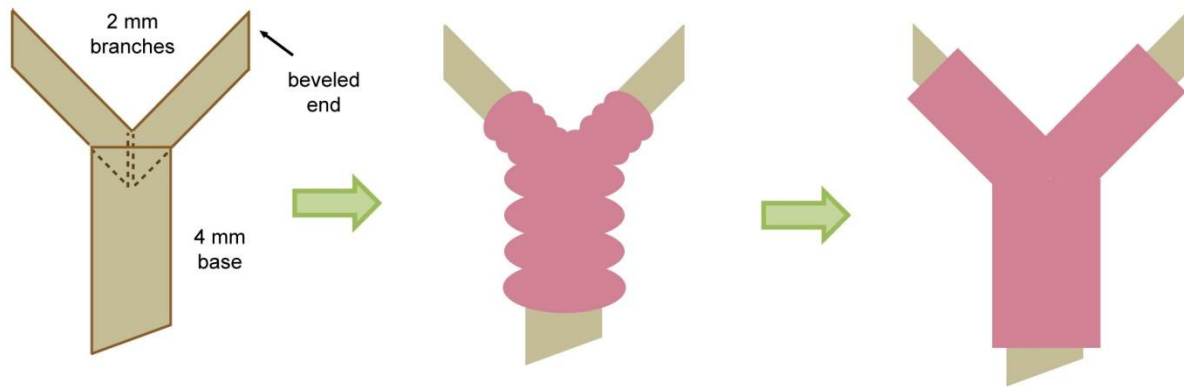
Figure 4.2 – Schematic of branched vessel generation by self-assembled cell ring fusion. The Y-shaped silicone mandrel was generated from two 2 mm OD tubes placed in the end of one 4mm OD tube. One-day-old rings of corresponding sizes were placed on the three branches of the mandrel, stacked together, and allowed to culture for 7 days for ring fusion and branched tissue tube formation.

4.2.10 Statistics

For fusion studies, samples from two different experiments were pooled and analyzed to obtain sample sizes of seven to ten tissue tubes per group (3-7 group included seven tubes, 5-7 group included seven tubes, and 7-7 group included ten tubes). In the follow-up study comparing 1-7 tubes to 3-7 tubes, four tubes of each type were measured and analyzed. Data is reported as mean ± SEM for the fusion angle studies. A two-way ANOVA with Holm-Sidak post hoc analysis was used to analyze differences in fusion parameters as a function of experimental group (3-7, 5-7, or 7-7, n=7-10) and day in culture. A two-way ANOVA was also used to analyze the differences in the relative percent nuclei coverage as a function of tissue tube wall position and experimental group (3-7, 5-7, and 7-7, n=7-10). Finally, a one-way ANOVA was used to evaluate significant differences in PCNA staining as a function of experimental group (3-7, 5-7, and 7-7, n=7-10). SigmaPlot software (version 11.0, Systat Software Inc., Chicago, IL) was used to perform the ANOVA with Holm-Sidak post hoc analysis to identify significant differences (p<0.05) between parameter values.

4.3 Results

4.3.1 Increased rate of fusion with decreased ring culture duration

The goal of the first part of this study was to determine the effect of tissue ring culture duration on ring fusion kinetics. To do this, rings were removed from culture after 3, 5, or 7 days, transferred to silicone mandrel supports, and cultured in close contact for 7 days to allow fusion and tube formation. Fusion was measured as the angle between adjacent rings. All tissue rings were easily removed from their agarose

wells at every time point and for transfer onto the silicone mandrels. The fusion angle increased each day of culture for each group (3-7, 5-7, and 7-7, Figure 4.3A). The fusion angle of the 7-7 group was statistically lower than either the 3-7 or 5-7 groups until day 7 of fusion culture (p<0.05). The 3-7 group and the 5-7 group were not statistically different from each other at any time point during the study.

Throughout this experiment, the thickness and the length of the tubes were also monitored (Figure 4.3B, C). The thickness of each tube increased with time; with the 7-7 group exhibiting the greatest average thickness of the three groups. The starting thickness of rings cultured for 7 days were thicker than rings cultured for 3 days, consistent with our previous observation that thickness of the tissue rings increases with culture time.[1] The length of the tubes remained fairly constant throughout culture; however, tissue tubes in the 7-7 group were statistically longer than the tissue tubes in the 3-7 and 5-7 sample groups at all time points (this may have been due to the greater initial thickness of the 7 day rings).
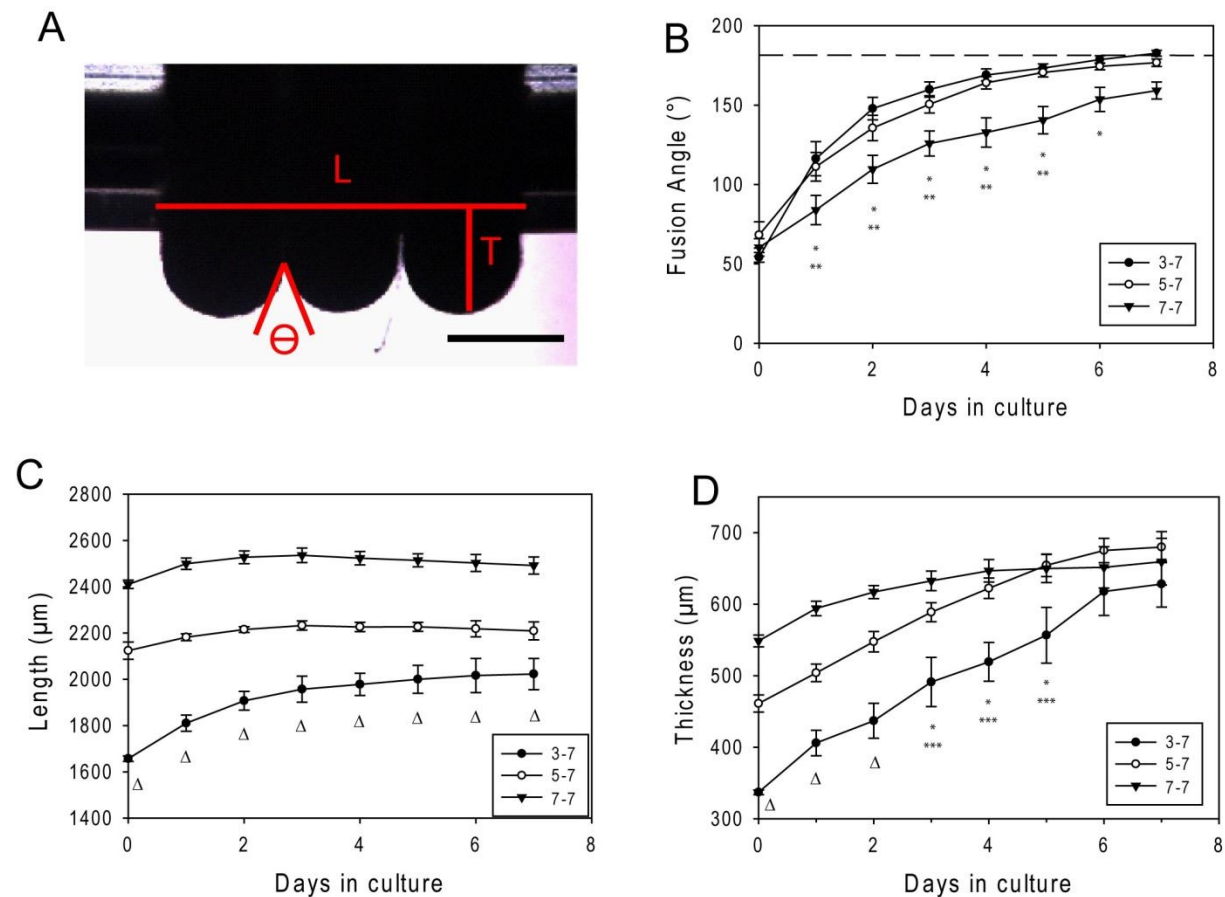
Figure 4.3 – Measurement of tissue tube fusion as a function of culture duration. Three rings were removed at 3, 5, or 7 days in culture and placed in contact on a silicone tube (A). The angle between rings (ϴ), length (L), and thickness (T) were obtained for each sample for each day of culture. The image (A) shows 7-day-old rings stacked onto a silicone tube. Scale bar=0.5mm. Graphs of fusion angle (B), length (C), and thickness (D) are reported as a

function of time in culture. All values are reported as mean ± SEM, n=7-10 tube samples per group. * indicates statistical differences between 3-7 and 7-7 groups and ** between 5-7 and 7-7 groups, Δ indicates statistical significance between all groups.

4.3.2 Structure and morphology of fused tissue tubes

To further investigate the ability of self-assembled cell rings to fuse into seamless tissue tubes, histology was performed. Representative photomicrographs of the fused tissue tubes are shown in Figure 4.4. Hematoxylin and eosin (H&E) staining indicated that all groups showed evidence of fusion between cell rings; however, the individual ring margins remained visible in all samples. Each of the tissues contained a high cell density throughout. To more closely examine the structure and composition of the tubes, additional histochemical stains were performed. All fused tube samples stained positively for glycosaminoglycans, visible by the blue color in Alcian Blue staining (Figure 4.5A, D, G). Further, Fast Green/ Picrosirius Red staining showed some noticeable collagen deposition within the tissues (red stain in Figure 4.5B, E, H). The collagen appeared to be primarily located within the centers of the original rings (and less prominent at the border regions between rings), and closer to the silicone mandrel than to the outside of the tissue (Figure 4.5B, E, H).
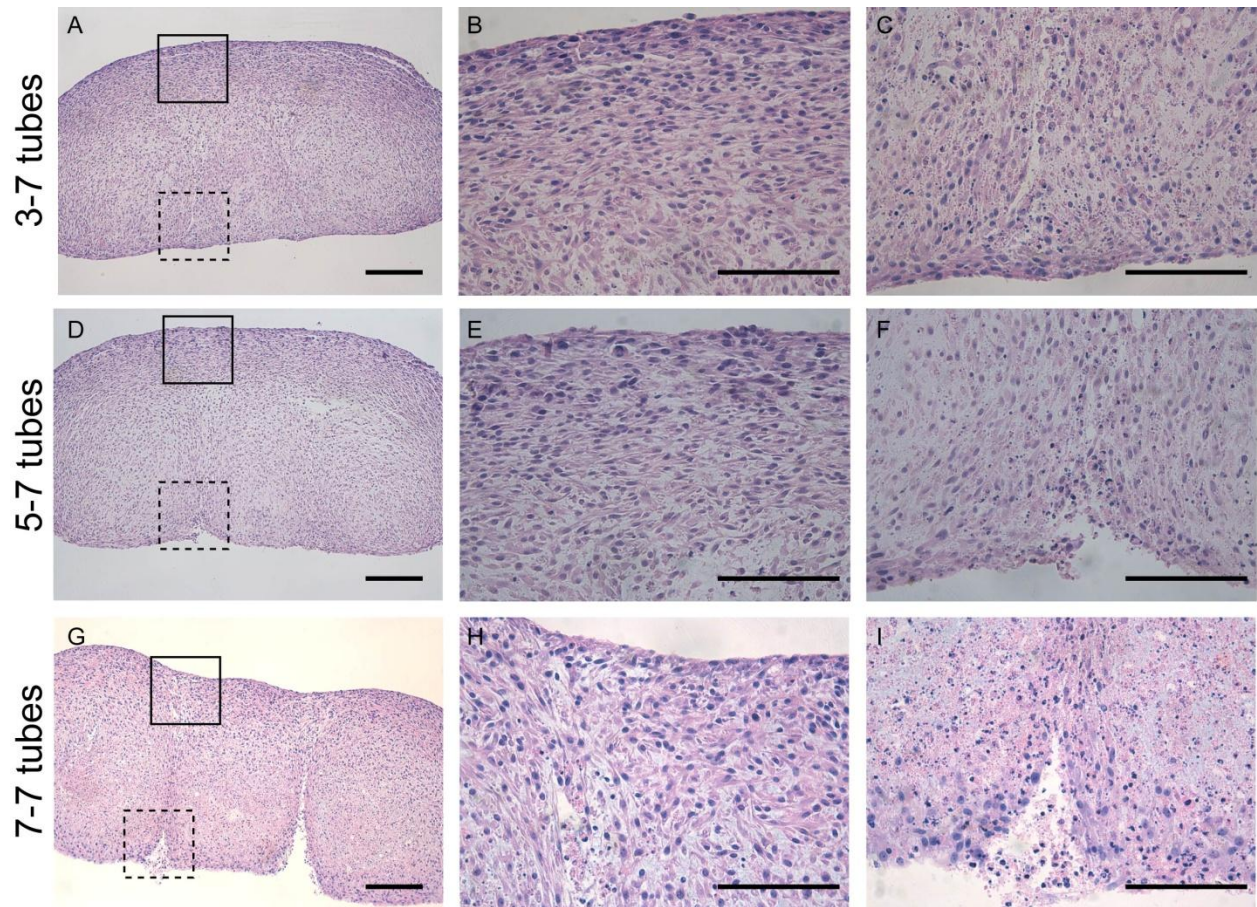
Figure 4.4 – Representative tissue tube morphology of 3-7, 5-7, and 7-7 tubes. Low magnification longitudinal cross-sectional views of H&E-stained tissue tubes show fusion of three tissue rings after 7 days in fusion culture (A, D, G). All tubes are oriented such that the bottom edge of the tissue tube wall was adjacent to the silicone mandrel, and the top edge was directly in contact with the culture medium. Higher magnification views show one fusion point at the outer surfaces (B, E, H) and the inner surfaces (C, F, I) of the tissue tubes. The solid boxes correspond to regions magnified in B, E, and H, whereas the dotted boxes correspond to regions magnified in C, F, and I. Images are representative of n=7-10 samples per group. Scale bars = 250 μm (A, D, G) and 100 μm (B, C, E, F, H, I)
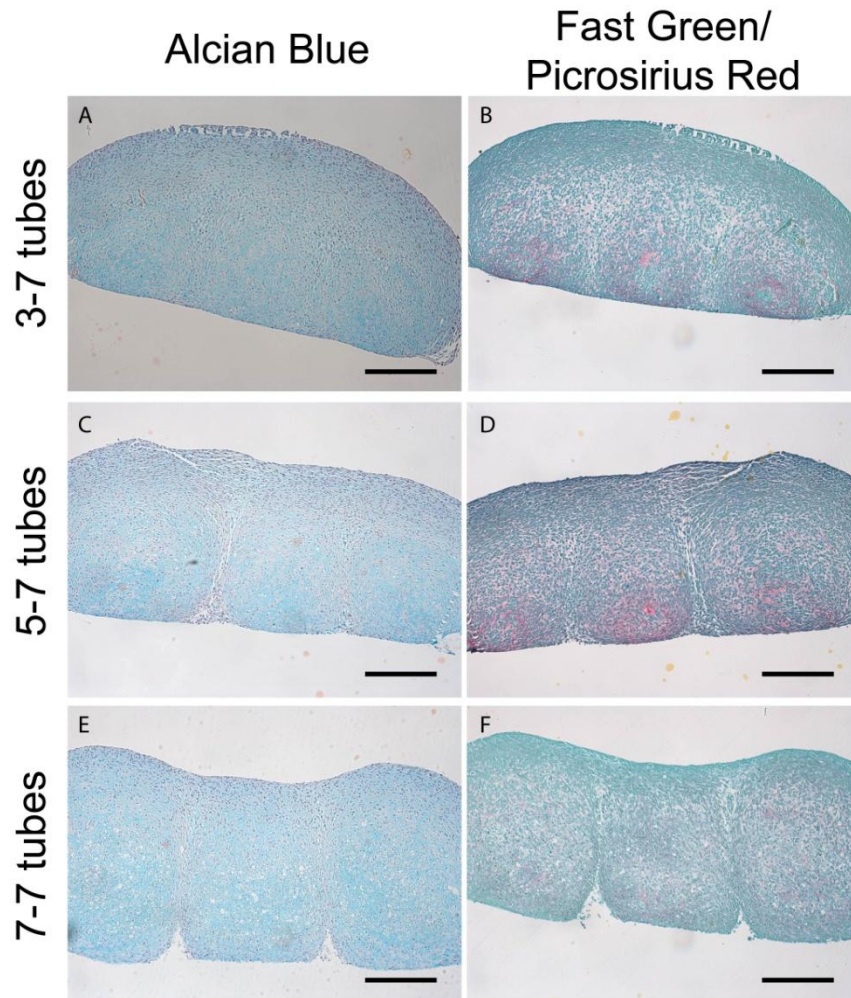
Figure 4.5 – Histochemical assessment of fused tissue tube extracellular matrix. Representative photomicrographs of 3-7, 5-7, and 7-7 tubes. Sections stained with Alcian Blue (A, C, E, blue=glycosaminoglycans) and Fast Green/Picrosirius Red (B, D, F, red=collagen). All tubes are oriented such that the bottom edge is adjacent to the silicone mandrel and the top edge is directly in contact with the culture medium. For all groups n= 7-10 samples, Scale bars = 250 μm

4.3.3 Proliferating cells located along the outer edge of fused tubes

Although there was a high cell density throughout the tissue tube, there appeared to be an increase in the number of cells per area along the outer edge and also at the ring borders where the individual rings have fused together. To quantify this, images of Hoechst-stained slides were acquired from four different locations along the inner (adjacent to the silicone tube) and outer edges of each tube sample. We then calculated the percent nuclei coverage (amount of Hoechst signal) per image area in the different regions. The results suggest that there is an increase in Hoechst signal along the outer edge of the tubes compared to the inner edge (Figure 4.6A), suggesting that more cells are located along the outer edges of the tubes.

Additionally, the nuclei appeared rounded and intact along the outer edge, compared to the inner edge where the nuclei appeared fragmented (Figure 4.6B and C).
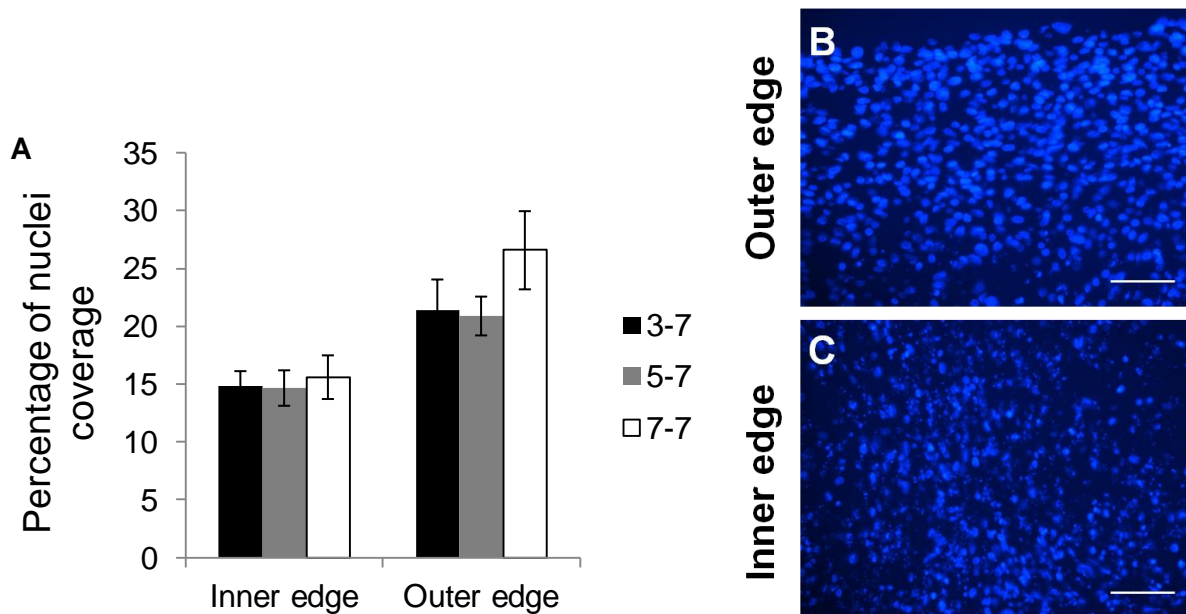
Figure 4.6 – Quantification of relative Hoechst signal per image area. Relative Hoechst signal was compared in regions along the inner and outer edge of the tubes. Percent area coverage of nuclei in images acquired from along the inner edge and along the outer edge in 3-7, 5-7, and 7-7 tubes, A. (data represented as mean±S.D., n=7-10, four measurements per sample) Representative images are shown in B and C of Hoechst-stained cells at the outer edge and the inner edge of a 7-7 tube. Scale = 50μm.

To further investigate whether the outer layers of the tubes contained proliferating cells, we stained the samples with PCNA. The staining showed that the outer edges and ends of the tissue tubes where the cells were in direct contact with the media contained PCNA-positive cells in all tubes (Figure 4.7 B, C, and D). To compare the groups, the distance from the outer edge of the tissue tube wall to the "deepest" PCNA-positive cells was measured. These values are displayed in Figure 4.7A. To normalize these tissue "depths", we divided by the total wall thickness of the tissue tube (Figure 4.7B). This provided a comparison of the thickness of the proliferative band of cells between the groups. There were no statistical differences found between experimental groups when analyzed either as PCNA-positive depth (Figure 4.7A) or when normalized to thickness (Figure 4.7B). The proliferating cells occupied between 10-15% of the total thickness of the tissue tubes in all groups (Figure 4.7B)
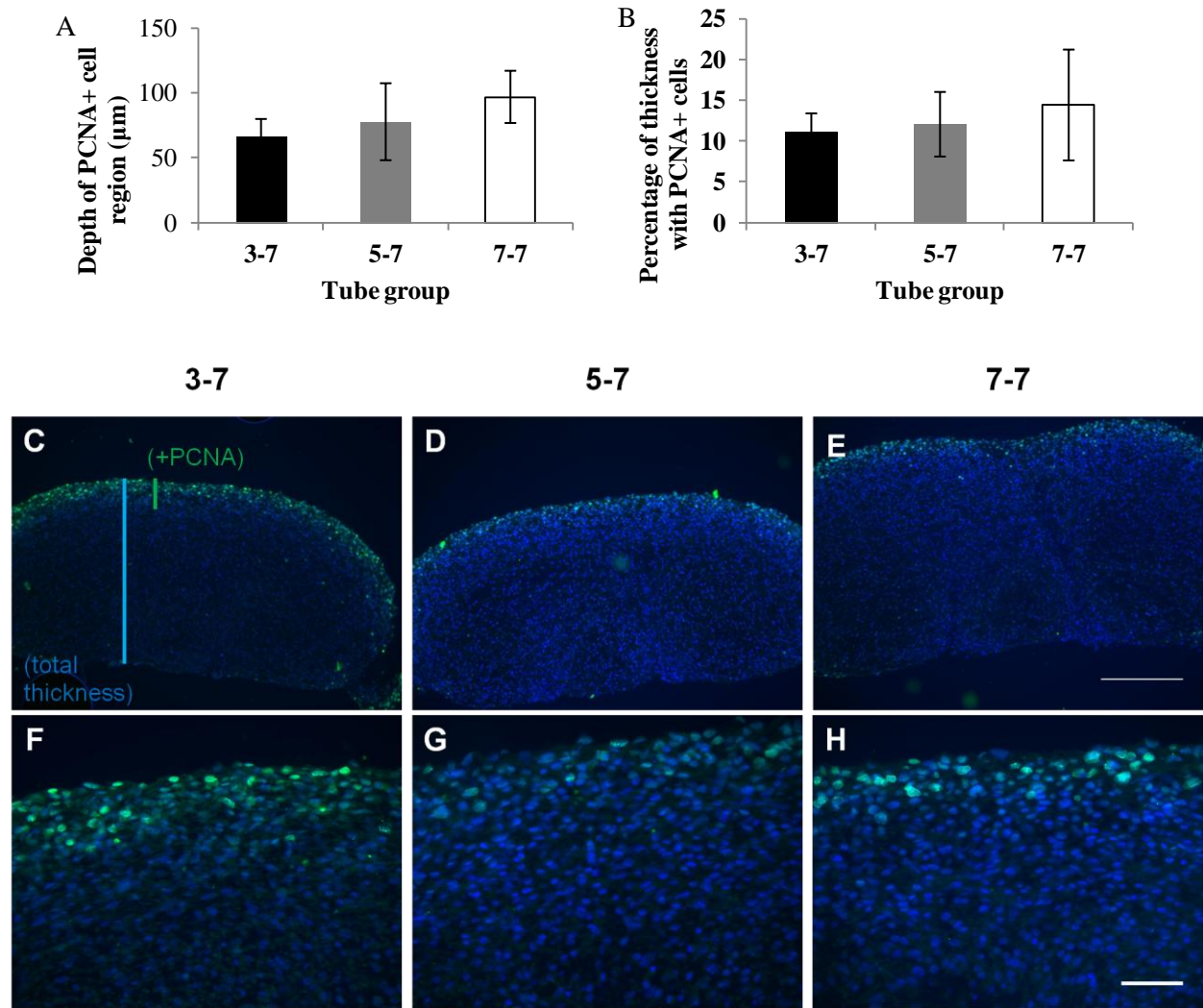
Figure 4.7 – PCNA-positive cell region displayed as a depth and a percentage of tube thickness. The distance of PCNA-positive cellular region expressed as a depth (A) and also normalized to tube thickness (B). No statistical differences were observed (n=7-10, mean±SD). Sample images are shown in B-H of a 3-7, 5-7, and 7-7 tube. Example measurements are shown in B with the green line indicating the thickness of the PCNA-positive cells and the blue indicating the tube thickness. Scale= 0.5mm. Higher magnification images of the PCNA-positive region are shown in F, G, and H. Scale = 50 μm.

4.3.4 Tissue tubes form in as little as 8 days

Based on the observation that the 3 day-old rings showed improved fusion compared to 5 or 7 day-old rings, we aimed to see if we could remove rings from culture as early as one day after cell seeding. Rings harvested after only one day after cell seeding were sufficiently robust for removal from the agarose wells, and could be transferred onto silicone mandrels. Fusion angle data showed that there were no statistical differences in the rate at which the 1-7 tubes fused compared to the 3-7 tubes (Figure 4.8A). However, H&E-stained sections showed that 1-day-old rings fused into near seamless tubes after 7 days

in fusion culture. Whereas the ring margins were still visible in the 3-7 tubes, they are barely distinguishable in the 1-7 tubes (Figure 4.8B).
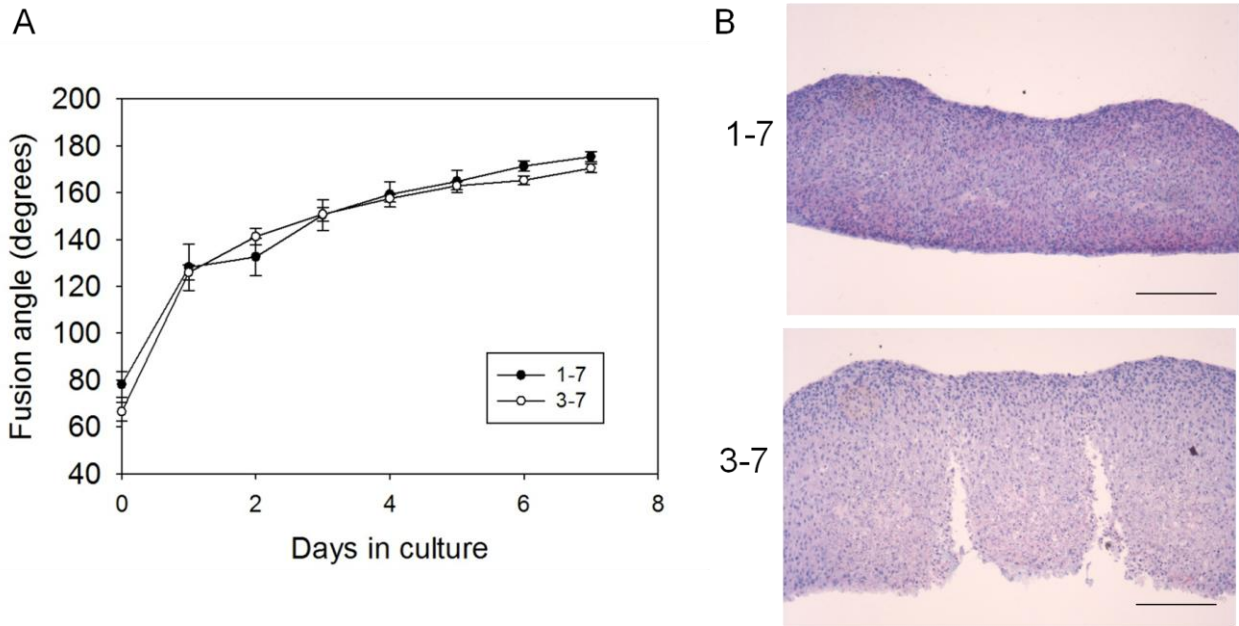
Figure 4.8 – Fusion angle measurements in 1-7 and 3-7 tubes. Graph of fusion angle measurements as a function of the number of days in culture (A). Data is represented as mean ± SEM, n=3, no statistically significant differences were found between groups. Representative photomicrographs of 1-7 and 3-7 tubes stained with H&E (B). Scale = 0.5mm

4.3.5 Smooth muscle cells retain their spatial position within rings with fusion

Based on our observations of tissue ring fusion, we were interested in determining whether cell position was retained within fused tubes. This would indicate the feasibility of creating tubes with distinct tissue regions along the tube length. To test this hypothesis, one-day-old tissue rings were created from green fluorescent, pre-labeled cells (as described in Methods section) and cultured in contact with one-day-old tissue rings formed from unlabeled cells. These rings were allowed to fuse, and monitored by microscopy over time. Fluorescent imaging of the stacked rings after one day of fusion culture (1-1 indicates one day old rings after one day in fusion culture) showed a strong green fluorescence signal in the ring that was formed from pre-labeled cells and no signal from the unlabeled ring. The margin between the rings became blurred, indicating some possible mixing of the cells at the junction. Although the fluorescent signal was not as bright overall, the pattern was retained in the fused rings even after 3 days of fusion culture (Figure 4.9).
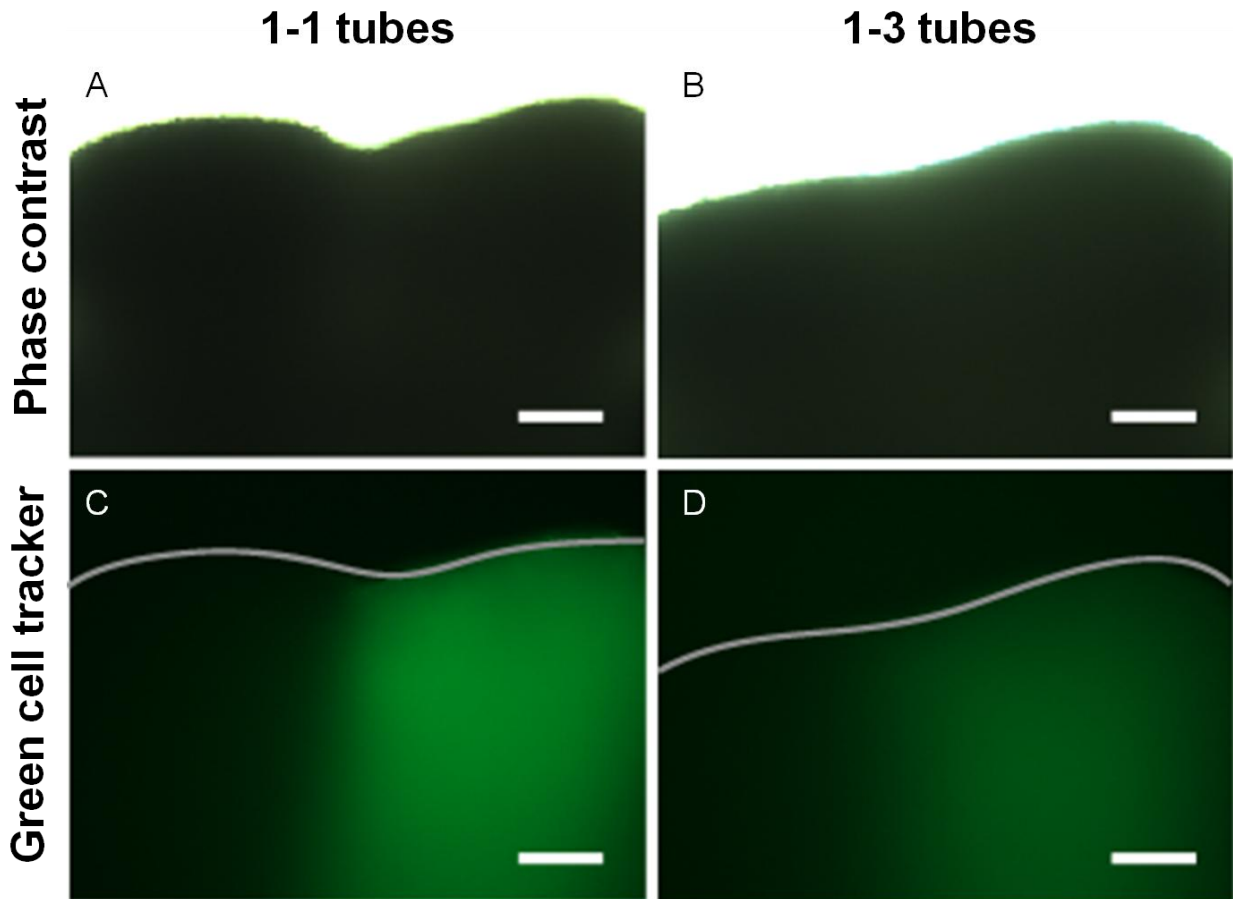
Figure 4.9 – Spatial retention of cell position throughout ring fusion.   Photomicrographs of fusion between unlabeled and fluorescently pre-labeled tissue rings. Phase contrast (A) and fluorescent (C) images of a 1-1 tissue tube. Images of a different 1-3 tissue tube acquired by phase contrast (B) and fluorescence (D). Cell-aggregated rings pre-labeled with a green cell labeling dye (Vybrant CFDA green fluorescent dye) are on the right adjacent to unlabeled rings on the left in each image. Scale = 100µm.

4.3.6 Assessment of fused tissue tube strength

To test whether ring fusion resulted in strong tissue tubes, we conducted burst pressure testing of fused tissue tubes. Our previous fused tubes consisted of three tissue rings, however, tubes must be at least approximately 5-7mm in length for mounting on the burst pressure testing device. Therefore, twelve, one-day-old rings were stacked on silicone mandrels and cultured as tubes for 7 days (n=5 tissue tubes). These tubes were then removed from the mandrels, mounted onto blunt end needles, and pressurized with saline until failure (Figure 4.10A). Only one out of three samples was successfully tested to failure, which reached a maximum pressure of 48 mmHg. Complete tests could not be performed on the other samples due to difficulties with tube mounting and attachment. The mode of tube failure for the successful test was via longitudinal splitting rather than tearing or separation between rings (Figure 4.10D).
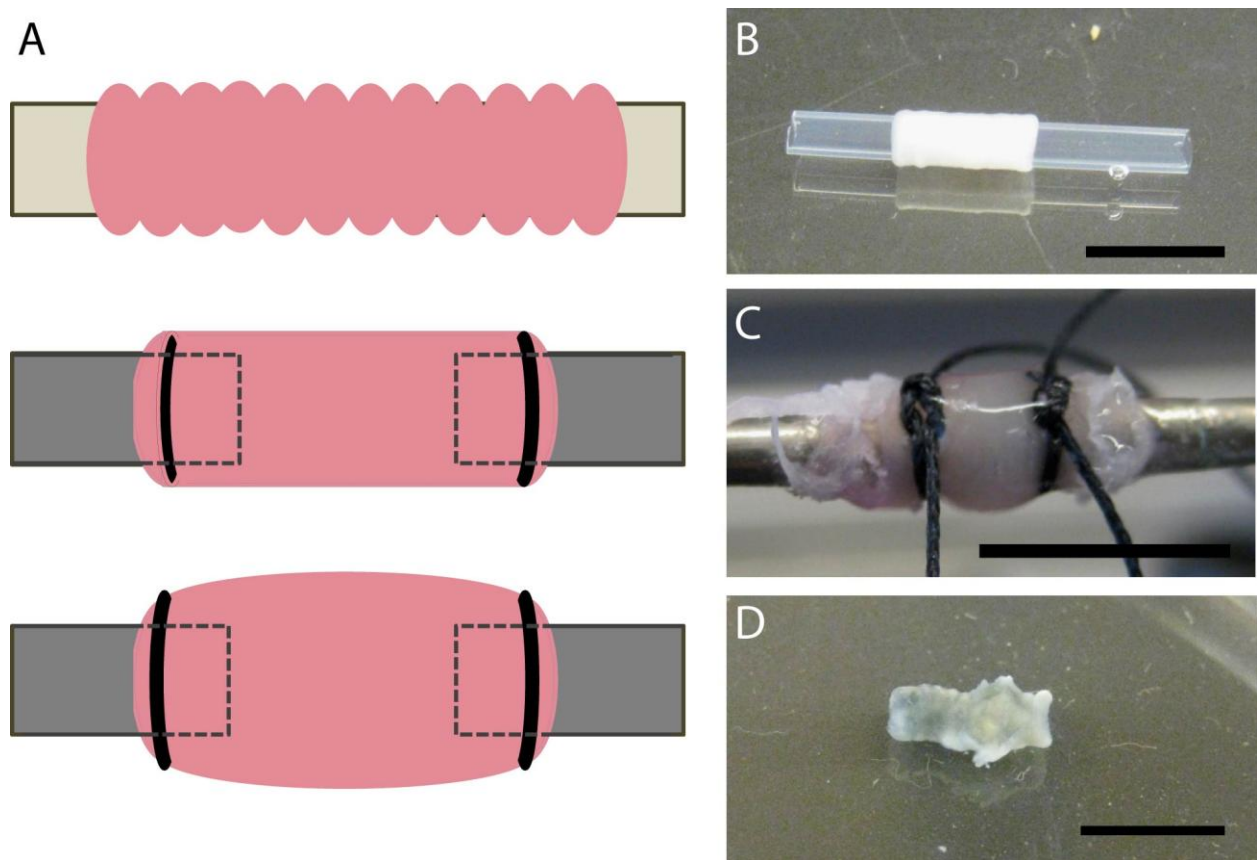
Figure 4.10 – Burst pressure testing process. (A) Twelve one-day old rings were stacked together, allowed to fuse for 7 days, and pressurized with saline until failure. Photos of a twelve ring 1-7 tube on silicone mandrel (B), a 1-7 tube mounted on blunt needles for burst pressure testing (C), and a burst-tested tube that failed longitudinally down the length (D). Scale = 1cm.

4.3.7 Histology of the tissue tube and new alternative to mandrel material

Histology was performed on all tested (n=3) and untested (n=2) 1-7 tissue tube samples to evaluate tissue morphology. Hematoxylin and eosin staining indicated that complete fusion of the tubes was achieved; however, the long tubes appeared to have an altered morphology in the area adjacent to the silicone mandrel (Figure 4.11). The tissue appeared less stable and pulled apart during the cutting and staining in histology. The nuclei of the cells appeared rounded and smaller than the nuclei in the outer region. This observation was in contrast to the short (3 stacked rings) 1-7 tubes grown for the fusion angle studies (section 4.3.4) in which the tubes appeared fully fused, healthy and viable throughout the tissue (1-7 tube from Figure 4.8B). The necrosis observed along the inner edge adjacent to the silicone mandrel in the tubes may have been a result of the increase in tube length from three rings to 12 rings. We wanted to determine if we could increase the overall tissue health if we replaced the silicone mandrel with a porous mandrel through which media diffusion would occur.
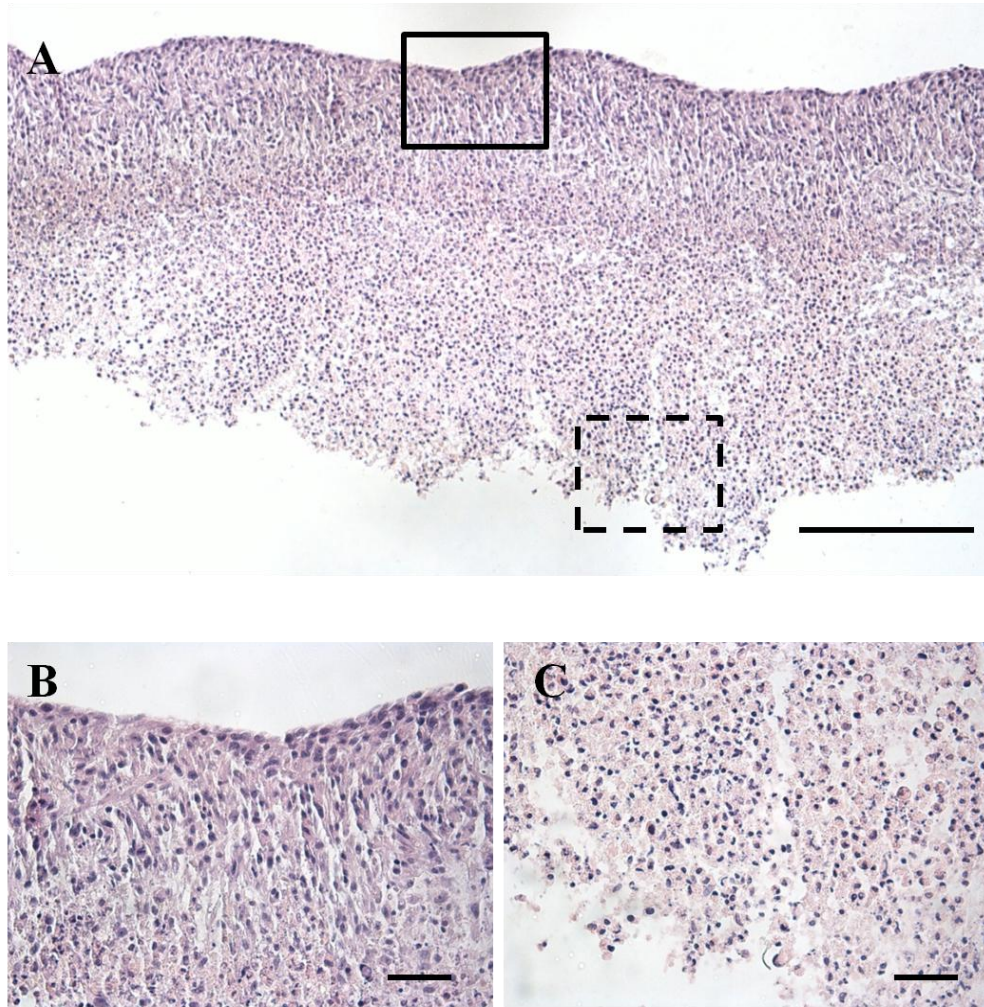
Figure 4.11 – Tissue morphology of 12-ring long, 1-7 tissue tube. Hematoxylin and Eosin staining showed tissue tube structure of a long, 12-ring tube (A). A change in morphology was observed along the inner edge adjacent to the silicone tube (bottom of the image) of a long 1-7 tube. A low magnification image is shown in A to visualize a longer portion of the tube (scale=0.5mm). Higher magnification images are shown in the regions marked by the solid box (B) and the dashed box (C) along the outer and inner edges. Scale = 250 µm (A) and 50µm (B,C).

In an effort to reduce the observed cell necrosis, we elected to use a porous mandrel (in contrast to the solid silicone tubing mandrel) that may be permeable to culture medium on the luminal side of the tube. We obtained a porous electrospun co-polymer tube (generously provided by BioSurfaces, Inc.) which was used as a mandrel material in these studies. To do this, 1.5cm lengths of the electrospun tube were cut with beveled ends. Rings were transferred onto the electrospun tube mandrel similarly to transfer onto the silicone tubes (described in Methods 4.2.3). For this proof-of-concept study, three tubes (twelve rings each) were created by ring fusion on the porous mandrels. We had planned to remove these tubes from the porous mandrel; however it became evident that the tubes could not be removed as easily without ripping the tissues. One of the tube samples was removed successfully from the porous mandrel after 7

days in fusion culture, but one tube ripped during removal, which suggested that the tissue tubes may be more strongly adhered to the porous polymer mandrel than they were to the silicone tube mandrels. The third tube was processed on the porous mandrel. Histological evaluation revealed evidence of cellular infiltration into the porous polymer mandrel (Figure 4.12). In addition, it appeared that tubes cultured on porous polymer mandrels were fully fused and lacked necrosis (indicated by rounded nuclei). This new porous mandrel material may be an alternative to silicone, allowing us to generate longer, viable tubes. (Figure 4.12)
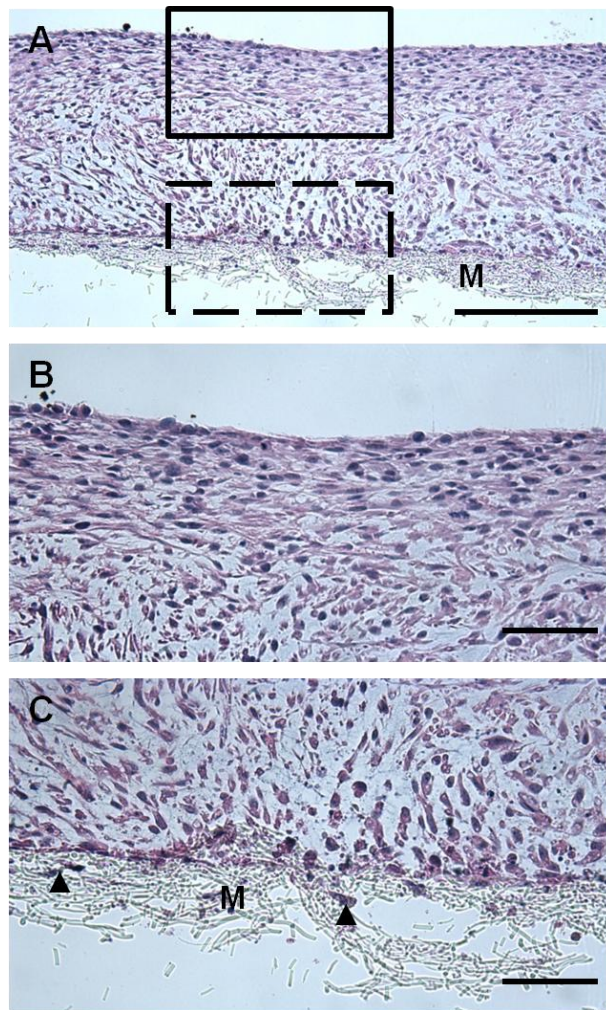
Figure 4.12 – Tissue tubes on a porous mandrel. Hematoxylin and eosin staining of fused tissue rings on a porous mandrel. Low magnification image is shown in (A) to visualize a longer portion of the tube. Higher magnification images are shown in the regions marked by the solid box (B) and the dashed box (C), corresponding to the outer and inner tube regions, respectively. The porous polymer mandrel is marked by (M) and the arrows (▲) indicate infiltrating cells. Scale=250 µm (A) and 50 µm (B,C)

4.3.8 Generation of branched tube structures

To test the feasibility of using the fused ring method to generate branched tube structures, we created "Y-shaped" silicone mandrels as described in the Methods section. We then transferred one-day-old cell rings of the corresponding size onto the mandrels. Phase contrast images showed evidence that the 1-day-old tissue rings fused into a branched structure (Figure 4.13). The rings located at the bends in the "Y" fused with one another, which appeared to create seamless junctions of the edges of the three branches. However, on the opposite face of the construct, the bifurcation point did not fully fuse, and we observed a triangular hole at the center of the junction. This data suggests that fusing rings into branched tubes is possible and that we may utilize different sized rings to model variations in vessel diameter at branching junctions.
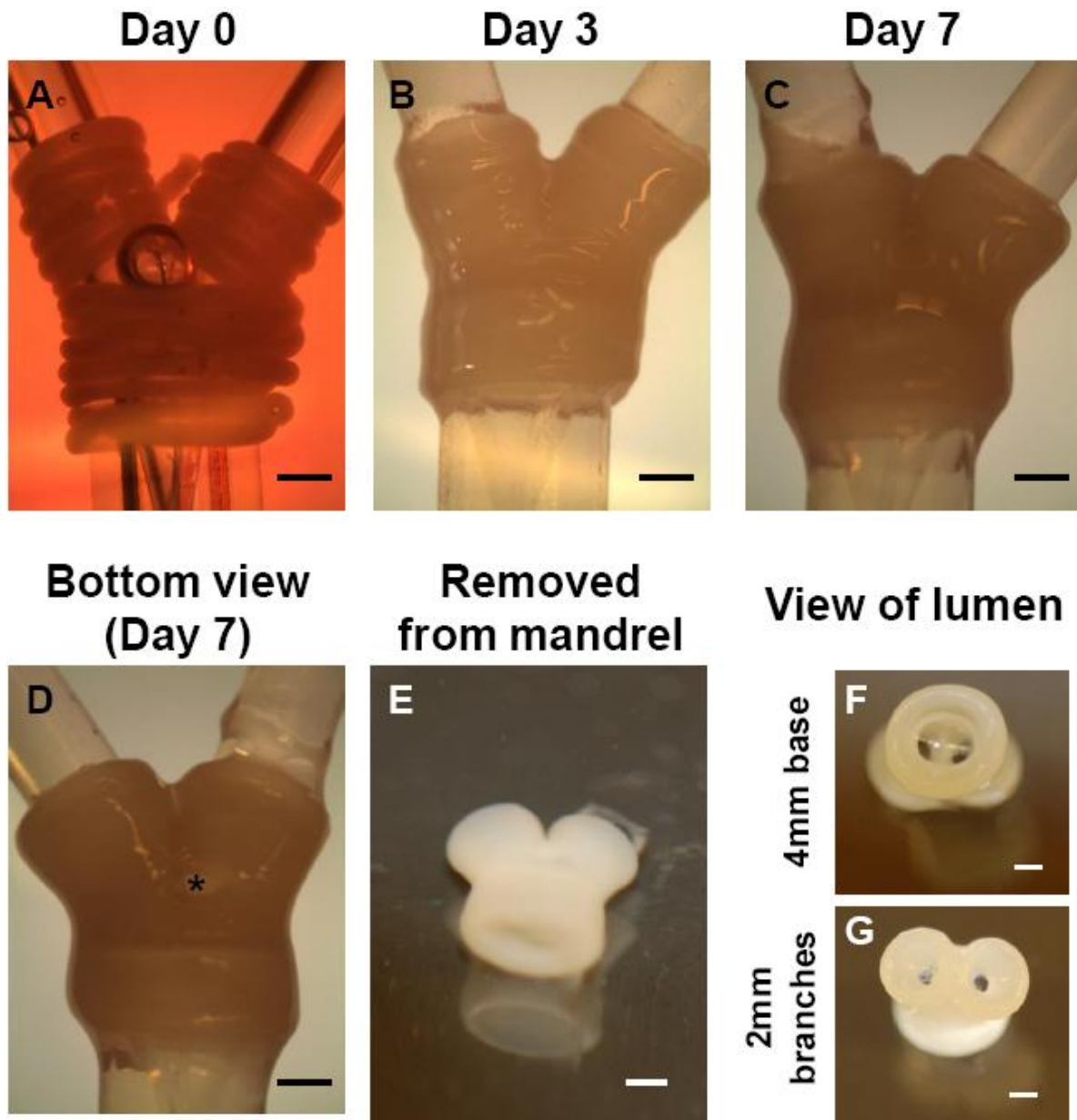
Figure 4.13 – Branched tube fusion. Brightfield microscope images of the branched tube fusion process, one-day-old rings stacked onto the silicone "Y-shaped" mandrel (A). The base of the mandrel is made from 4 mm rings and the branches of the vessel are made from 2 mm rings. Rings fused together to form a branched tube after 3 days in culture (B), or 7 days in culture (C). The bottom side of the branch had a small hole at the junction, indicated by the asterisk (D). The tube was removed from the mandrel (E) and the lumen remained intact (F,G). Scale = 1mm

4.4 Discussion

Here we describe the development of a method to rapidly generate vascular tissue tubes entirely from cells and the ECM they produce. In this study, we investigated how the "pre-culture" duration of the self-

assembled cell rings can be manipulated, resulting in the generation of seamless cell-derived tissue tubes in as little as 8 days of culture. We previously described how these rings can be used to evaluate the structural, morphological, and mechanical properties of cell-derived tissue.[1] Here, we further expand on this idea to show that the same tissue rings can fuse to form tissue tubes. As described previously, we can use the tissue rings as a platform to systematically evaluate culture parameters which lead to optimal tissue growth. We can then generate tissue tubes by fusing rings cultured with these different parameters. For example, one such culture parameter is ring size. In our previously studies we showed that we can culture SMC rings that are 2, 4, or 6 mm in diameter.[1] In this study, we were then able to fuse the different sized rings together and form branched vessels. Therefore, this method of generating tubes from aggregated cell rings holds advantages over alternative methods in that information obtained from ring studies can then *directly* apply to generation of tissue tubes made from fused self-assembled SMC rings.

In the first part of this study we examined the effect of tissue ring culture duration on ring fusion into tissue tubes. In our studies, fusion is defined as a combination of an increase in fusion angle (angle between adjacent rings) and seamless integration where ring margins are undetectable upon histological analysis. We found that rings cultured for less time prior to fusion (one, three or five days old) fused more rapidly and more completely into tissue tubes than rings cultured for longer durations prior to fusion (seven days old), which is consistent with other reported studies.[2,14,15] For example, Rago *et al*. showed that fibroblast spheroids removed from culture after one day fused together more rapidly than spheroids cultured for 7 days prior to fusion.[2] A different study showed that aggregated cell spheroids composed of co-cultured fibroblasts and endothelial cells harvested after 5 days demonstrated only moderate levels of fusion when cultured statically for an additional 14 days.[14] By comparison, spheres composed of fibroblasts alone cultured for only one day prior to fusion appeared to fuse together after only 3 days of fusion culture.[15] These fusion studies were carried out using different cell types (fibroblasts, SMCs, ECs, etc.) which may also impact the tissue's ability to fuse. However, the results of these studies are consistent with our findings; namely that self-assembled tissues cultured for shorter durations have the ability to remodel into larger tissue constructs with seamless fusion more rapidly and completely than cell-derived tissues cultured for longer durations prior to fusion.

When characterizing the fusion of our tissue tubes, we monitored length, thickness, and fusion angle of the constructs. The experiments described in this paper were controlled in length by the number of rings per tube, but due to the differences in thickness of the starting tissue rings (350 μm for 3-day-old rings vs. 550 μm for 7-day-old rings), resulted in tubes of different starting lengths and thicknesses. Interestingly, we did not observe a change in tube length with fusion of ring-based subunits, unlike the fusion of

spheroids into rods reported by others.[2,16] This may be due to differences in the size scale or geometry of the building block tissues (relatively large rings, compared to smaller spheroids). For example, in one study, fusion of large and small fibroblast microspheroids (300 μm vs. 100 μm) was compared. Small spheroids fused more completely within 7 days compared to the large spheres, although the differences were not statistically significant.[2]

To measure the degree of tissue fusion, we monitored the angle between tissue rings as a function of time, using a method described previously.[12] Other studies in which tissue fusion was analyzed have used different methods of assessing the extent of fusion. For example, the extent of fusion with fibroblast microspheres was not measured by the angle between spheres, but was measured by the length of the tissue rod resulting from fused spheroids positioned within an oblong trough.[2] The authors observed that rod length did not change over time with the fusion of large spheres, compared to fusion of small spheres. However, the representative photos of the fibroblast spheroids suggest that the fusion between the aggregates may be enhanced in the smaller spheroids compared to the larger spheroids, based on the observed fusion angle between spheroids from the images in the study. This could indicate that larger tissue subunits may remain discrete entities for longer periods of time (consistent with our observations of slower fusion times compared to other published reports).[2,12] In our studies, we fused SMC tissue rings which were approximately 350-550 μm in thickness, which are much larger than in other published reports. Therefore, generating thinner rings in future studies may also ultimately enhance tissue fusion.

In addition to the size of the subunit tissues used in our study, the geometry of these tissues may also play a role in their rate of fusion. Spheres, the most common building block shape used to date, are the lowest energy state of a tissue and most cell types will spontaneously re-orient into spheroids,[17] unless given some external stimulus to maintain an alternative structure. Generally, such stimuli are mechanical cues such as a physical barrier[12,16,18,19] (agarose post or silicone mandrel in our case) or dynamic culture[14] (such as fluid flow through a lumen). Remodeling occurs in such tissues by thinning in directions of tension to compensate for forces placed on them.[18] This process of cell-mediated tension occurs as the cells are self-assembling and contracting to form tissue.

Tissue fusion and cellular self-assembly may be partially driven by mechanisms of cellular adhesion. Various cell-adhesion molecules including connexins and cadherins have been implicated in the self-assembly process as well as in cell mediated tension.[20-22] While all cells that have adhesion molecules seem to aggregate, cell types without cadherin molecules (such as L cells) do not aggregate well.[20] Further, it has been observed that the more adhesion molecules cells have, the faster they aggregate into

tissues.[21] This suggests that the presence of adhesion molecules on the cell surface is a major factor dictating their ability to aggregate and assemble into tissues. Another interesting behavior to note is that the longer the tissue has been cultured within a mold (such as agarose ring molds), the slower it contracts to close the lumen upon removal, which may be due to an increase in ECM deposition within the tissue.[18] The rate and extent of lumen closure differs by tissue geometry and cell type, but occurs with predictable kinetics.[23] Cell types that rapidly self-assemble into tissues also rapidly contract to close their lumens, suggesting that some cell types have an increased ability to remodel tissue.[18,21]

Successful tissue engineering relies on cells to synthesize and remodel ECM to generate tissue structure. Recently it has been shown that 3D tissue culture leads to enhanced extracellular matrix (ECM) production compared to 2D culture.[14] For example, gene expression of ECM molecules (collagens I, III and tropoelastin) and ECM binding integrins ($\alpha 1$, $\beta 1$, and $\beta 3$) was up-regulated in smooth muscle cells cultured in 3D collagen and fibrin gels compared to on 2D gel films.[24] Further, in applying these findings to cell-based, "scaffold-less" tissue engineering, Kelm *et al*. found that ECM related genes (such as collagens, fibronectins, laminins, MMPs, etc.) were significantly upregulated in 3D fibroblast spheroids compared with fibroblasts cultured on 2D tissue culture plastic.[14] Future work on this project should focus on whether ECM content increases in the self-assembled rings with time and if that plays a role in lowering their ability to fuse together into tissue tubes.

While scaffold-less tissue engineering is an appealing approach to creating living tissue equivalents, one challenge is the length of time it takes for cells to synthesize, accumulate and organize ECM in culture. For example, we have observed increased amounts of collagen deposition in aggregated cell rings cultured for 14 days compared to 8 days.[1]   Other studies have found similar results. For example, Hajdu *et al* [25] examined the fusion of spheroids grown with or without "maturogenic" treatments (TGF-$\beta 1$ and seratonin), toward the goal of developing a system to screen optimal methods for accelerated tissue remodeling and maturation.[25] Two spheroids were placed in contact and monitored to determine which spheroid "enveloped" the other. The spheroid that was enveloped by the other was the more "cohesive" or "mature" tissue. In their study, the treatment of cardiac valve interstitial cells with either TGF-$\beta 1$ or serotonin led to increased collagen deposition, and ultimately to a more cohesive tissue.[25] This suggests that tissues with increased ECM (such as collagen) are generally more cohesive and more difficult to remodel. We have found that tissue rings cultured for longer durations (7 days) fuse together less completely than rings harvested at earlier time points (1, 3, or 5 days). We hypothesize that one reason "older" rings do not fuse as readily is due to an increase in ECM production, leading to more cohesive tissues. To confirm that the decrease in fusion ability may in part be due to an increase in ECM

production, further analysis of tissue ECM needs to be conducted. In all, this suggests that the observed changes in the fusion kinetics may be partially due to changes in the ECM composition and that the more ECM the tissues produce, the less likely they are to fuse.

Ultimately, the desired goal would be to create a tissue tube rich in ECM components such as collagen and elastin. While too much ECM deposition prior to ring fusion may be detrimental, after fusion of the ring sub-units it will be important to increase the rate of ECM synthesis to obtain tissue tubes strong enough for implantation. ECM synthesis can take weeks;[26,27] however, synthesis and deposition in culture can be manipulated by supplementing the cell culture environment with various factors. The tubes in this study were cultured in a basic growth medium (10% serum) without any additional supplementation. While the presence of serum allowed the cells to proliferate, we did not include factors known to enhance synthesis of collagen or other ECM molecules. In future studies, we may need to add factors such as ascorbic acid, TGF-β1, EGF, or insulin-transferrin-selenium, which are implicated in increasing ECM deposition and tissue strength.[26,28-30] For example, fibroblasts cultured in chemically-defined medium with epidermal growth factor (EGF) supplementation exhibited increased strength, thickness, total protein, and total collagen compared to fibroblasts grown in medium with serum.[28,29]

Building tissue tubes with a modular approach as described in this chapter has benefits in that we could potentially spatially control cell location along the tissue tube length leading to a vessel with distinct tissue regions. Further, by using different cell types or genetically-modified cells for ring self-assembly, we could feasibly generate vessels with regions of cells that are compositionally different from adjacent regions (such as elastin-deficient regions as would be found in aneurysm or lipid-rich regions as would be found in plaque formation). As a first step toward developing such models, we found that at relatively short time points (1 and 3 days of fusion culture) the cells from one ring retain their spatial position, a finding consistent with what others have observed.[12,15,31,32] The ring margins became blurred after one or three days of fusion, suggesting there may be some amount of migration between the rings. To further assess this, studies should be carried out with double labeling of adjacent rings (e.g., one green and one red) to see how much migration occurs between rings. For example, fused tissues generated from a single cell type (rat hepatocytes)[12] or from multiple cell types (human SMCs and fibroblasts)[15] have been observed to remain segregated. However, some studies suggest that the degree of cell separation or cell sorting is dependent on the cell types used. In this study we only used one cell type, SMCs, to generate self-assembled tissue and for our tissue fusion studies. However, different cell types have different surface adhesion proteins and different cytoskeletal tension which both contribute to their ability to self-sort.[2,21,33,34] This could become critical in future studies when examining the tissue self-assembly

properties of rings fabricated from multiple cell types or tubes generated from rings of different cell types. In all, our preliminary data suggest that we may be able to retain spatial retention of cells within rings, and that cell ring fusion may be achieved by a combination of local migration and proliferation.

Further, while vascular disease often occurs at the site of branched vessels,[5,6] due to the complexity involved in building these branches, such vascular junctions remain largely unstudied. Recently, bioprinting has been used to show proof-of-concept of generating branched vessel networks.[8,15,31] In our study, we showed that our modular ring system can be used to generate branched tube structures. We demonstrate versatility in this model system by using different sized rings to generate different branches of the vessels. Four millimeter rings were used to build the trunk of the vessels whereas 2 millimeter rings were used to fuse into the two branches. The rings are able to fuse at the junction of the branches. This gives rise to another useful *in vitro* modeling tool.

In conclusion, we have shown that self-assembled rings generated from SMCs alone can be fused together to form tissue tubes. We found that the earlier rings are removed from culture, the more completely they fuse into contiguous tubes. Finally, we demonstrated that even after fusion occurred, the cells remained within the original ring tissues, thereby demonstrating spatial retention of cells, potentially allowing us to generate tubes with different regional properties. Ultimately, one of the advantages of this method over other existing methods to generate vascular grafts is the direct translation of cell-derived rings to tissue tubes. We can screen the effects of culture parameters to determine the optimal combination of conditions that promotes vascular tissue growth, then use those parameters to generate vascular tissue tubes by fusing rings.

4.5 References

1. Gwyther TA, Hu JZ, Christakis AG, Skorinko JK, Shaw SM, Billiar KL, Rolle MW. Engineered vascular tissue fabricated from aggregated smooth muscle cells. Cells Tissues Organs 2011;194(1):13-24.
2. Rago AP, Dean DM, Morgan JR. Controlling cell position in complex heterotypic 3D microtissues by tissue fusion. Biotechnol Bioeng 2009;102(4):1231-41.
3. Homme JL, Aubry MC, Edwards WD, Bagniewski SM, Shane Pankratz V, Kral CA, Tazelaar HD. Surgical pathology of the ascending aorta: a clinicopathologic study of 513 cases. Am J Surg Pathol 2006;30(9):1159-68.
4. Nesi G, Anichini C, Tozzini S, Boddi V, Calamai G, Gori F. Pathology of the thoracic aorta: a morphologic review of 338 surgical specimens over a 7-year period. Cardiovasc Pathol 2009;18(3):134-9.
5. De Syo D, Franjić BD, Lovricević I, Vukelić M, Palenkić H. Carotid bifurcation position and branching angle in patients with atherosclerotic carotid disease. Coll Antropol 2005;29(2):627-32.
6. Kleinstreuer C, Hyun S, Buchanan JR, Longest PW, Archie JP, Truskey GA. Hemodynamic parameters and early intimal thickening in branching blood vessels. Crit Rev Biomed Eng 2001;29(1):1-64.

7.   Jakab K, Norotte C, Damon B, Marga F, Neagu A, Besch-Williford CL, Kachurin A, Church KH, Park H, Mironov V and others. Tissue engineering by self-assembly of cells printed into topologically defined structures. Tissue Eng Part A 2008;14(3):413-21.
8.   Visconti RP, Kasyanov V, Gentile C, Zhang J, Markwald RR, Mironov V. Towards organ printing: engineering an intra-organ branched vascular tree. Expert Opin Biol Ther 2010;10(3):409-20.
9.   Lemire JM, Covin CW, White S, Giachelli CM, Schwartz SM. Characterization of cloned aortic smooth muscle cells from young rats. Am J Pathol 1994;144(5):1068-81.
10.   Lemire JM, Potter-Perigo S, Hall KL, Wight TN, Schwartz SM. Distinct rat aortic smooth muscle cells differ in versican/PG-M expression. Arterioscler Thromb Vasc Biol 1996;16(6):821-9.
11.   Gwyther TA, Hu JZ, Billiar KL, Rolle MW. Directed cellular self-assembly to fabricate cell-derived tissue rings for biomechanical analysis and tissue engineering. J Vis Exp 2011(57), doi: 10.3791/3366.
12.   Livoti CM, Morgan JR. Self-assembly and tissue fusion of toroid-shaped minimal building units. Tissue Eng Part A 2010;16(6):2051-61.
13.   Gray C, Oliva T, Christakis A, Rolle M, Billiar K. Design of a versatile, inexpensive vessel burst pressure measurement device. Northeast Bioengineering Conference, Boston, MA, 2009.
14.   Kelm JM, Lorber V, Snedeker JG, Schmidt D, Broggini-Tenzer A, Weisstanner M, Odermatt B, Mol A, Zünd G, Hoerstrup SP. A novel concept for scaffold-free vessel tissue engineering: self-assembly of microtissue building blocks. J Biotechnol 2010;148(1):46-55.
15.   Norotte C, Marga FS, Niklason LE, Forgacs G. Scaffold-free vascular tissue engineering using bioprinting. Biomaterials 2009;30(30):5910-7.
16.   Dean DM, Napolitano AP, Youssef J, Morgan JR. Rods, tori, and honeycombs: the directed self-assembly of microtissues with prescribed microscale geometries. FASEB J 2007;21(14):4005-12.
17.   Damon BJ, Mezentseva NV, Kumaratilake JS, Forgacs G, Newman SA. Limb bud and flank mesoderm have distinct "physical phenotypes" that may contribute to limb budding. Dev Biol 2008;321(2):319-30.
18.   Tejavibulya N, Youssef J, Bao B, Ferruccio TM, Morgan JR. Directed self-assembly of large scaffold-free multi-cellular honeycomb structures. Biofabrication 2011;3(3):034110.
19.   Youssef J, Bao B, Ferruccio T-M, Morgan J. Micromolded Nonadhesive Hydrogels for the Self-Assembly of Scaffold-Free 3D Cellular Microtissues. In: Berthiaume F, Morgan J, editors. Methods in Bioengineering: 3D Tissue Engineering. Norwood, MA: Artech House; 2010. p 151-166.
20.   Steinberg MS, Takeichi M. Experimental specification of cell sorting, tissue spreading, and specific spatial patterning by quantitative differences in cadherin expression. Proc Natl Acad Sci U S A 1994;91(1):206-9.
21.   Bao B, Jiang J, Yanase T, Nishi Y, Morgan JR. Connexon-mediated cell adhesion drives microtissue self-assembly. FASEB J 2010.
22.   Duguay D, Foty RA, Steinberg MS. Cadherin-mediated cell adhesion and tissue segregation: qualitative and quantitative determinants. Dev Biol 2003;253(2):309-23.
23.   Napolitano AP, Chai P, Dean DM, Morgan JR. Dynamics of the self-assembly of complex cellular aggregates on micromolded nonadhesive hydrogels. Tissue Eng 2007;13(8):2087-94.
24.   Hong H, Stegemann JP. 2D and 3D collagen and fibrin biopolymers promote specific ECM and integrin gene expression by vascular smooth muscle cells. J Biomater Sci Polym Ed 2008;19(10):1279-93.
25.   Hajdu Z, Mironov V, Mehesz AN, Norris RA, Markwald RR, Visconti RP. Tissue spheroid fusion-based in vitro screening assays for analysis of tissue maturation. J Tissue Eng Regen Med 2010;4(8):659-64.
26.   L'Heureux N, Pâquet S, Labbé R, Germain L, Auger FA. A completely biological tissue-engineered human blood vessel. FASEB J 1998;12(1):47-56.
27.   Ofek G, Revell CM, Hu JC, Allison DD, Grande-Allen KJ, Athanasiou KA. Matrix development in self-assembly of articular cartilage. PLoS One 2008;3(7):e2795.
28.   Throm AM, Liu WC, Lock CH, Billiar KL. Development of a cell-derived matrix: effects of epidermal growth factor in chemically defined culture. J Biomed Mater Res A 2010;92(2):533-41.
29.   Ahlfors JE, Billiar KL. Biomechanical and biochemical characteristics of a human fibroblast-produced and remodeled matrix. Biomaterials 2007;28(13):2183-91.
30.   Grassl ED, Oegema TR, Tranquillo RT. A fibrin-based arterial media equivalent. J Biomed Mater Res A 2003;66(3):550-61.
31.   Mironov V, Visconti RP, Kasyanov V, Forgacs G, Drake CJ, Markwald RR. Organ printing: tissue spheroids as building blocks. Biomaterials 2009;30(12):2164-74.
32.   Fleming PA, Argraves WS, Gentile C, Neagu A, Forgacs G, Drake CJ. Fusion of uniluminal vascular spheroids: a model for assembly of blood vessels. Dev Dyn 2010;239(2):398-406.

33. Dean DM, Morgan JR. Cytoskeletal-mediated tension modulates the directed self-assembly of microtissues. Tissue Eng Part A 2008;14(12):1989-97.
34. Foty RA, Steinberg MS. The differential adhesion hypothesis: a direct evaluation. Dev Biol 2005;278(1):255-63.

Chapter 5: Spontaneous aggregation and self-assembly of human smooth muscle cells to create engineered vascular tissues

5.1 Introduction

We have previously described a new method to generate 3D, scaffold-free, cell-derived tissue rings based on facilitated cellular self-assembly.[1] This method allows us to aggregate cells from a cell suspension into tissue rings which can be used to study vascular tissue function, or can be fused together to generate tube-shaped vascular constructs.

All of our initial studies utilized rat smooth muscle cells (SMCs) to generate self-assembled cell ring constructs. The rat SMCs used in these studies are a stable cell line (not immortalized) that was created as described in Lemire et al.[2,3] The rationale for using these cells was that they are relatively easy to maintain and have a shorter doubling time than primary SMCs. This was especially important given the large number of cells we needed to generate many batches of tissue rings to create and analyze the tissue ring fabrication system. While non-human cell types are often used to generate tissue engineered vascular constructs, they are not an ideal cell source to use when building vascular grafts for human patients. In order to generate transplantable vascular grafts, vascular tissue constructs need to be generated only from human cells.[4-6] Both human fibroblasts and human bone marrow cells have already been used to generate clinically transplantable grafts.[5,6] However, to recapitulate human vascular physiology *in vitro*, SMCs are the cell type of choice.

The goal of this chapter of the thesis is to determine whether or not self-assembled cell ring generation can be achieved using primary human SMCs. For the tissue ring system to be a more physiologically relevant model of human vasculature, the successful use of human SMCs to create tissue rings is essential. However, one of the challenges associated with human SMC culture is the difficulty in obtaining large quantities of these cells from patients. Also, their slow proliferative rates make them a more difficult cell type to work with for both experimental and clinical use.[7,8] One benefit of the self-assembled cell ring system is the ability to generate tissue with fewer cells and less time than would be required for culture and assessment of vascular tissue tubes. The ring model can thus serve as a "high-throughput" method to generate vascular tissue and test the effect of various culture conditions on tissue structure and function.[9,10] However, the current method of generating cell rings still requires 500,000

cells or more for each tissue ring sample.[1,10] In order to decrease this cell seeding number and make the tissue ring model an even more efficient tool, we also aimed to decrease the seeding well dimensions in order to decrease the initial cell seeding number needed for cell ring self-assembly, as demonstrated in other studies.[11] Decreasing the initial cell seeding number would make the ring system a more useful tool to study vascular structure and function *in vitro*.

In this chapter, we determined that, similar to our findings with rat SMCs, human SMCs are capable of self-assembling into ring-shaped structures and can remodel and fuse together to form tissue tubes. We also showed that we can decrease the number of cells required for cellular self-assembly into rings by reducing the trough width in the ring-shaped agarose cell seeding wells. This makes the ring system more "high-throughput" by reducing the amount of cells, reagents, and other resources required to generate these cell-derived tissue constructs.

5.2 Materials and Methods

5.2.1 Human and rat smooth muscle cell culture

Rat aortic smooth muscle cells (rat SMCs; WKY-3M22) were cultured in growth medium (DMEM, 10% fetal bovine serum, and 1% penicillin-streptomycin) as described previously. Human coronary artery smooth muscle cells (human SMCs; purchased from Lonza, Lot# 2F1320 – 20 year old male donor) were cultured and maintained in smooth muscle cell growth medium (SmGM-2; Lonza). All cells were maintained at 37°C and 5% CO_2 and passaged at 90% confluence.

5.2.2 Cell-derived tissue ring generation

Agarose cell seeding wells (2 mm inner diameter) were prepared as described previously (See Chapter 3).[1] The agarose was released from the PDMS, agarose was separated into wells, and each agarose well was placed into a well of a 12-well plate.[10] Rat SMC rings were seeded at 500,000 cells/well and human SMCs were seeded at 750,000 cells/well. The SMC-seeded agarose wells were left in the incubator for one day to allow cell aggregation prior to the first media exchange. Media was then exchanged every 48 hours thereafter throughout the culture duration.

5.2.3 Digital imaging for non-contact thickness measurements of tissue rings

The tissue rings were removed from the agarose wells and transferred to a PBS bath at room temperature. Each tissue ring was centered and focused under the high resolution image acquisition camera (DVT series 600-Model 630). Four measurements were taken at four distinct positions along the circumference

of the ring using Framework 2.4.6 software (DVT Corporation).[10] These values were averaged to yield a mean thickness value for each sample. Ring thickness values are expressed as the mean ± S.D.

5.2.4 Uniaxial tensile testing

Mechanical properties of rings were tested by using a uniaxial tensile testing machine (ElectroPuls E1000; Instron, Norwood, MA) as previously described (see Chapter 3).[1] The test ran 8 precycles from 5mN to 50kPa stress and then the sample was pulled to failure at a rate of 10 mm/min (n=3). Engineering stress and grip-to-grip strain were analyzed using MATLAB (The MathWorks, Inc., Natick, MA) to yield ultimate tensile stress (UTS), maximum tangent modulus (MTM), and failure strain. For each parameter, the data was averaged and represented as mean ± SD. This data was then compared to the mechanical parameters calculated for 14 day-old 2mm rat SMC rings in Chapter 3.

5.2.5 Histological analysis of tissue ring structure and morphology

Four untested human SMC tissue ring samples were fixed in a 10% neutral buffered formalin solution for 2 hours, embedded in paraffin, and sectioned at 5 μm thickness. The sections were stained with hematoxylin and eosin (Newcomers Supply), Fast Green / Picrosirius Red (Sigma), Masson's Trichrome (Newcomers Supply), and Movat's Pentachrome (Newcomers Supply). All samples were viewed with an upright microscope (Leica DMLB2) and images were acquired with a digital camera (Leica DFC 480).

5.2.6 Tissue tube generation

Tissue tubes were generated by removing tissue rings from their agarose wells and transferring them onto silicone tubing mandrels.[10] All tissue rings (either rat SMC rings or human SMC rings) were cultured for one day prior to removal from the agarose well. Three rings were placed in contact on the silicone mandrel and allowed to fuse together for 7 days. Each day throughout culture, the angle between rings, tissue tube thickness, and the length of the tubes was measured. Two-four fusion angle measurements, two thickness measurements, and two length measurements were obtained for each tube sample at each time point as described in Section 4.2.5. The values obtained from four tube samples for each group (human SMC vs. rat SMC) were averaged together to yield a mean ± SD.

5.2.7 Mold re-design to reduce seeding well dimensions

A new cell-seeding well was designed in CAD; modified from the original mold to alter seeding well dimensions (illustrated in Figure 5.1). The new design was then milled into polycarbonate using CNC machining. The resulting polycarbonate mold was used to generate multiple PDMS templates which were used to make agarose cell seeding wells. The primary change was that the width of the new seeding well trough was narrowed from 3.75mm (in the original mold design[1]) to 2 mm in the new mold. The rounded bottom was conserved in the new, narrow mold. Also a 45° chamfer was added to the top of

each of the wells to increase the ease of pipetting the cell suspension into the wells (Figure 5.1). Further, the seeding wells were placed closer together so that 5 wells could fit into one well of a 6-well plate (shown in Results, Figure 5.4). This change also allowed for uniform agarose volume with each set of wells compared to the inexact method of hand-cutting used in the original mold.[10]
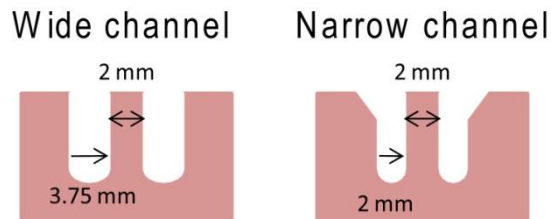
Figure 5.1 – Changes to agarose well seeding dimensions. The original mold has a trough width of 3.75 mm, whereas the re-designed, narrow channel mold has a trough width of 2 mm. With the decrease in trough width, we are able to seed fewer cells to yield a ring.

5.2.8 Measurement of critical cell seeding number for cell ring self-assembly

To determine the minimum critical number of seeded cells required to form self-assembled cell rings in the re-designed agarose wells, rat SMCs were seeded in agarose wells at varying concentrations (100,000, 200,000, 300,000 and 500,000 rat SMCs/well) into the narrow molds for the rat SMC study or the narrow and wide molds for the human SMC study. We also seeded the newly re-designed molds with human SMCs (seeding concentrations; 300,000, 400,000, 500,000, and 750,000). Wells were left undisturbed for one day after which the number of rings that formed at each cell concentration was counted. The data are presented as a percentage of the number of rings formed relative to the number of wells seeded (n=5 rings seeded per group) at each cell seeding concentration.

5.2.9 Statistical methods and analysis

A t-test was used to analyze the effect of differences in SMC source on thickness and the mechanical properties (n=3 for human SMC rings, n=6 for rat SMC rings). A two-way analysis of variance (ANOVA) with Holm-Sidak post hoc analysis was used compare fusion angle, thickness, and length of tissue tubes from each group as a function of time. SigmaPlot software (Version 11.0 Systat Software, Inc.) was used to perform the statistical tests and to identify significant differences ($p < 0.05$ considered significant).

5.3 Results

5.3.1 Rings form from human SMCs

Similar to observations with the rat SMCs, human SMCs consistently self-assembled and formed rings within 24 hours of cell seeding in agarose wells. The rings contracted around the center posts and appeared uniform in thickness around their circumference. Human SMC rings were removed from their wells after 14 days in culture. Upon removal, the thickness was measured and uniaxial tensile testing was performed (Table 5.1). The average thickness of the human SMC rings was 520±60 µm (significantly lower than rat SMC rings at 940±120 µm; p<0.05). The ultimate tensile strength of the human SMC rings was significantly higher (160±30 kPa; p<0.05) than rat SMC rings cultured from the same duration with the same post diameter (97±30 kPa). The MTM of the rings generated from human SMCs was lower than that of rat SMCs (270 kPa compared to 497 kPa), but the failure strain was greater (0.92 mm/mm compared to 0.5 mm/mm).

Mechanical Properties of human SMC rings

	n	Cell number (cells/ring)	Thickness (µm)	UTS (kPa)	MTM (kPa)	Strain (mm/mm)
Human SMC rings	3	750,000	520±60	160±30*	270±20*	0.92±0.08*
Rat SMC rings	6	660,000	940±120	97±30	497±91	0.50±0.08

Table 5.1 – Mechanical properties of human SMC rings compared to rat SMC rings. All rings were 2 mm in diameter and cultured for 14 days.[10] The rat SMC ring data was reported in Chapter 3 and ref. 1. * indicates statistical significance (p<0.05) between the human SMC ring data and the rat SMC data.

5.3.2 Histology of human SMC rings

Representative photomicrographs of 2 mm human SMC rings are shown in Figure 5.2. All samples had a high cell density with rounded nuclei and an even distribution of cells throughout the tissue. There does not appear to be circumferential alignment of the cells, based on the rounded nuclei observed throughout the tissue (however, this was not quantified). To more closely examine the composition of the tissues, histochemical stains were used to analyze ECM components (Figure 5.2). Masson's trichrome and Fast Green/Picrosirius Red staining indicated collagen deposition (which qualitatively appeared higher than previously observed in rat SMC rings).[1] Movat's pentachrome staining also showed high levels of glycosaminoglycans throughout the tissue (blue stain, Figure 5.2D,H).
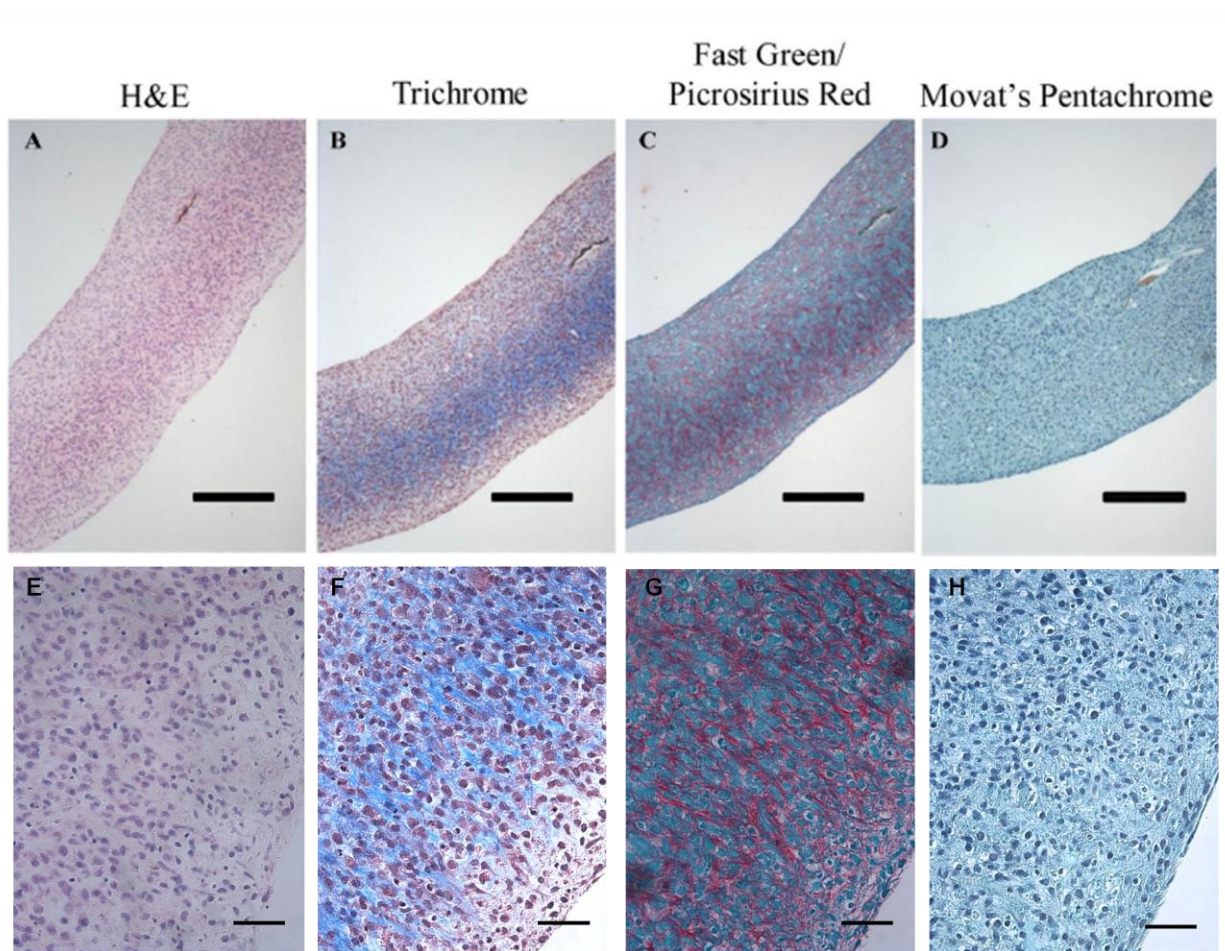
Figure 5.2 – Human smooth muscle cell tissue ring morphology. H&E-stained section (A,E); Trichrome (B,F, blue=collagen), Fast Green/Picrosirius Red (C,G, red=collagen), and Movat's Pentachrome (D,H, blue=glycosaminoglycans, yellow=collagen) show ECM present in the 2 mm human SMC tissue rings (cultured for 14 days, representative of 4 histological samples). Scale = 200 µm (A-D) or 50 µm (E-H)

5.3.3 Human SMC rings fuse to make tissue tubes

To assess the ability of human SMC rings to fuse into tubes relative to rat SMC rings, rings made from both sources of SMCs were cultured for one day prior to removal of aggregated rings from the agarose seeding wells. Tissue rings were then transferred onto silicone tubing, and placed in fusion culture for 7 days. After one day of culture, human SMC rings were less tightly contracted around the center post than we observed for one day-old rat SMC rings, but could still be removed from the posts and transferred onto the silicone mandrels without breaking. The individual ring margins of the fused rings became less apparent with time in culture as evidenced by an increase in fusion angle (Figure 5.3).   Fusion occurred rapidly over the first 4 days of culture with human SMC tubes, but slowed thereafter compared to the rat SMC tubes. The fusion angle at the rat SMC ring margins continued to increase between days 5 and 7, at

which points the fusion angles were statistically higher than in the human SMC tubes (Figure 5.3). The thickness of the human SMC tubes was greater at day 0, but decreased throughout the fusion culture. The thickness of the rat SMC tubes increased over time. The length of the human SMC tubes was statistically greater than the thickness of rat SMC tubes at days 0-4 and at day 6. Histological analysis of the human SMC tubes showed evidence of tissue fusion in all samples, although the ring margins were still visible (Figure 5.3D).
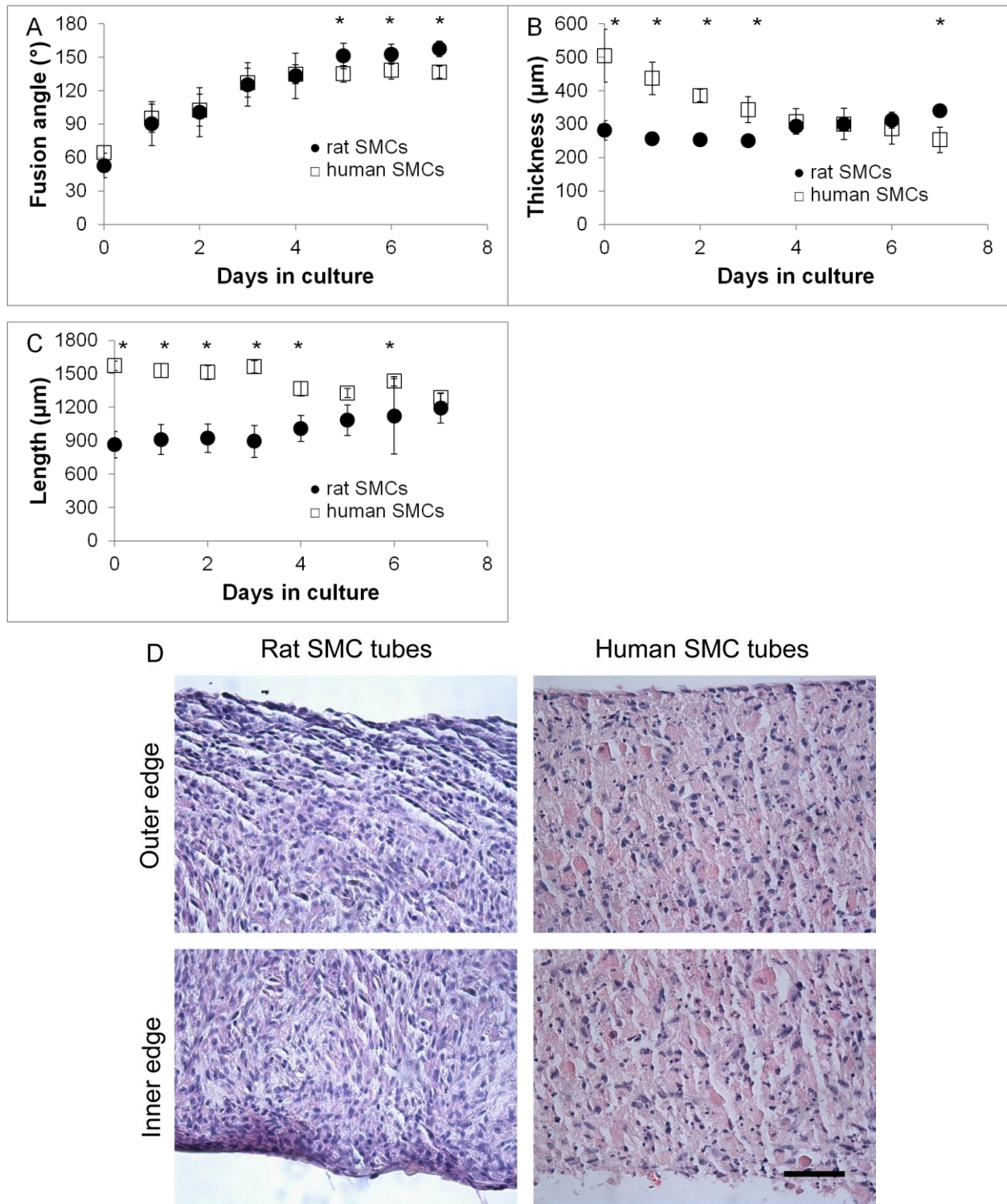
Figure 5.3 – Fusion measurement of human SMC tissue tubes compared to rat SMC tissue tubes. Comparison of rat SMC ring fusion (●) with human SMC ring fusion (□). Graphs of fusion angle (A), tube thickness (B), and tube length (C) as a function of days in culture. Asterisks indicate statistical difference between groups, p<0.05, n=4. Representative photomicrographs stained with H&E are shown in (D). Images show morphology along the outer

edge of the tube (in direct contact with culture media) and along the inner edge (in contact with the silicone tube). All tubes were cultured as rings for 1 day followed by 7 days of fusion culture. Scale = 200 µm.

5.3.4 Re-design of polycarbonate mold to lower the initial cell seeding concentration

In an effort to reduce the number of cells required to generate human SMC tissue rings, we modified the mold to decrease the seeding channel width in the agarose wells. The seeding trough width of each individual cell seeding well was decreased from 3.75 mm (wide channel) to 2 mm (narrow channel) to help minimize the cell number required for cellular self-assembly and ring fabrication. In addition, we also changed the design so that each agarose cast contained five seeding wells, and fit into 1 well of a 6-well plate. Images of the wide channel (original) and narrow channel (re-designed) molds are shown in Figure 5.4. Another consequence of making these modifications to the mold design was that we decreased the amount of material (PDMS, agarose, culture medium) required to create the cell seeding wells. Table 5.2 gives an overview of the total material savings with the new mold design.
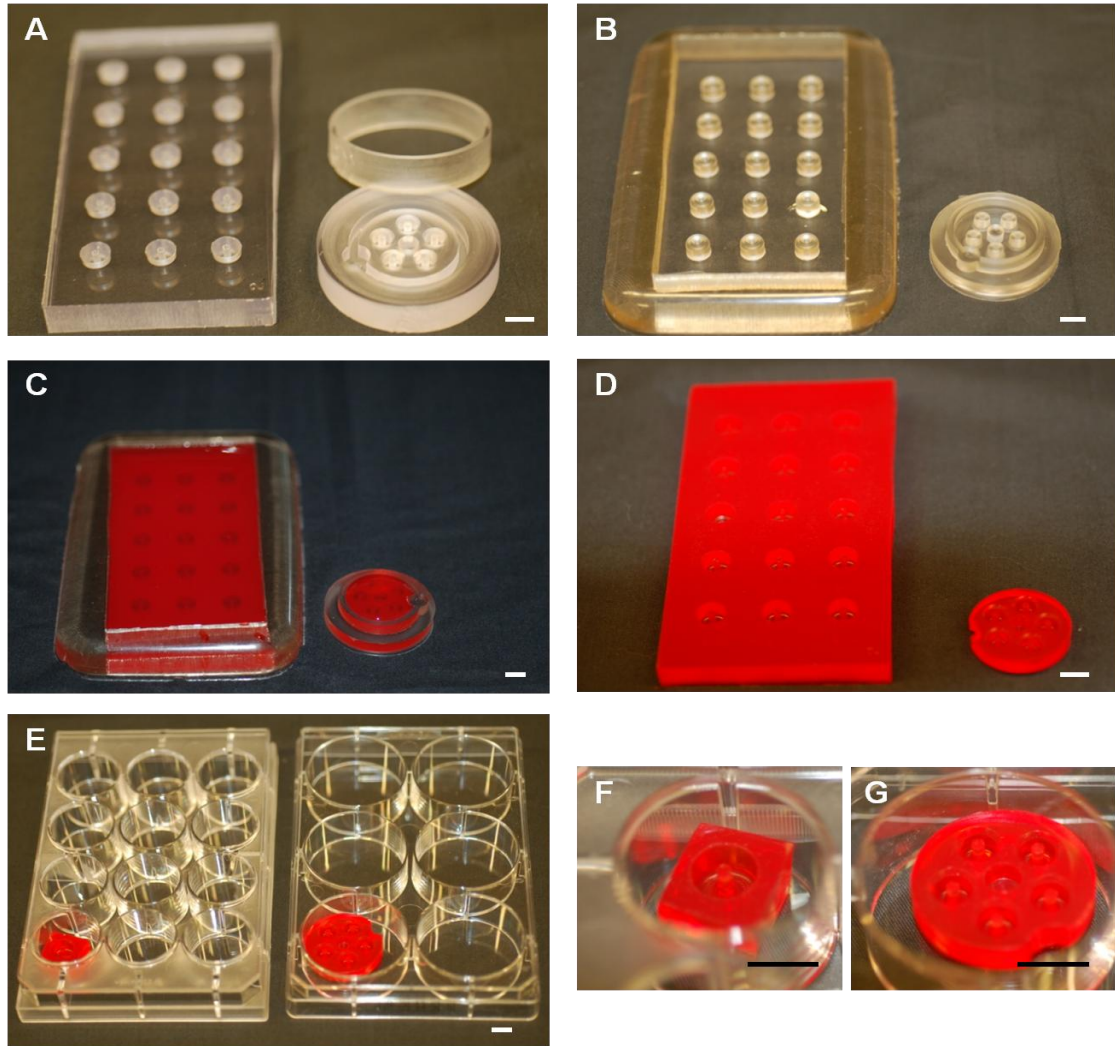
Figure 5.4 – Re-design of the mold with narrower seeding well channel width and less material. The milled polycarbonate mold of both the original, wide channel mold and the re-designed, narrow channel mold are shown in (A) along with the PDMS templates (B), the agarose cast in the PDMS templates (C), the removed agarose (D), individual wells in well-plates (E), and a close-up of the original seeding well (F) and the modified agarose wells (G). Note that individual original agarose wells fit into one well of a 12 well plate, whereas the new modified wells fit into a 6-well plate (F). Scales = 1cm

Material reduction with modified mold design

	Rings/ well	Media/ well (mL)	PDMS/ mold (g)	PDMS/ well (g)	Agarose/ PDMS mold (mL)	Agarose/ well (mL)
Wide channel mold	1	6	120	8	50	3.3
Narrow channel mold	5	3	14	2.8	2.8	0.6
% Decrease		50%	88%	65%	94%	81%

***Table 5.2** – **Total material required for agarose well fabrication with the re-designed mold vs. the original mold**.* The re-designed mold decreased the amount of material required at each step of the agarose well fabrication process.

We predicted, based on previous reports, that narrower seeding channels would allow us to lower the critical cell number required for self-assembly and ring formation.[11] To test this, we seeded agarose wells with decreasing amounts of rat SMCs than we previously reported (100,000-500,000 cells/ring) and counted the number of rings that successfully formed at each cell seeding amount. We found that we could decrease the number of rat SMCs from 500,000 cells to 200,000 cells per ring in the re-designed mold (Figure 5.5A). Seeding agarose wells with 100,000 cells per well did not yield any rings, and we therefore concluded that this was not a sufficient starting quantity for cellular self-assembly. This experiment was completed twice and the mean percentage of rings formed between the two experiments is reported in Figure 5.5A. Of note, the number of rings that formed in the second experiment increased for all groups (except 100,000 cells/ring), possibly due to increased user familiarity with the new seeding mold.

Assessment of minimum cell seeding number was repeated with human SMCs. The initial cell seeding numbers ranged from 300,000 cell/ring to 750,000 cells/ring, which was previously the lowest seeding concentration we used for human SMC ring aggregation.[10] We compared this range of seeding densities using both the original wide channel mold and the modifier-designed narrow channel mold, and found that human SMCs formed rings in the new, narrow mold at starting seeding concentrations as low as 300,000 cells/ring (Figure 5.5B).
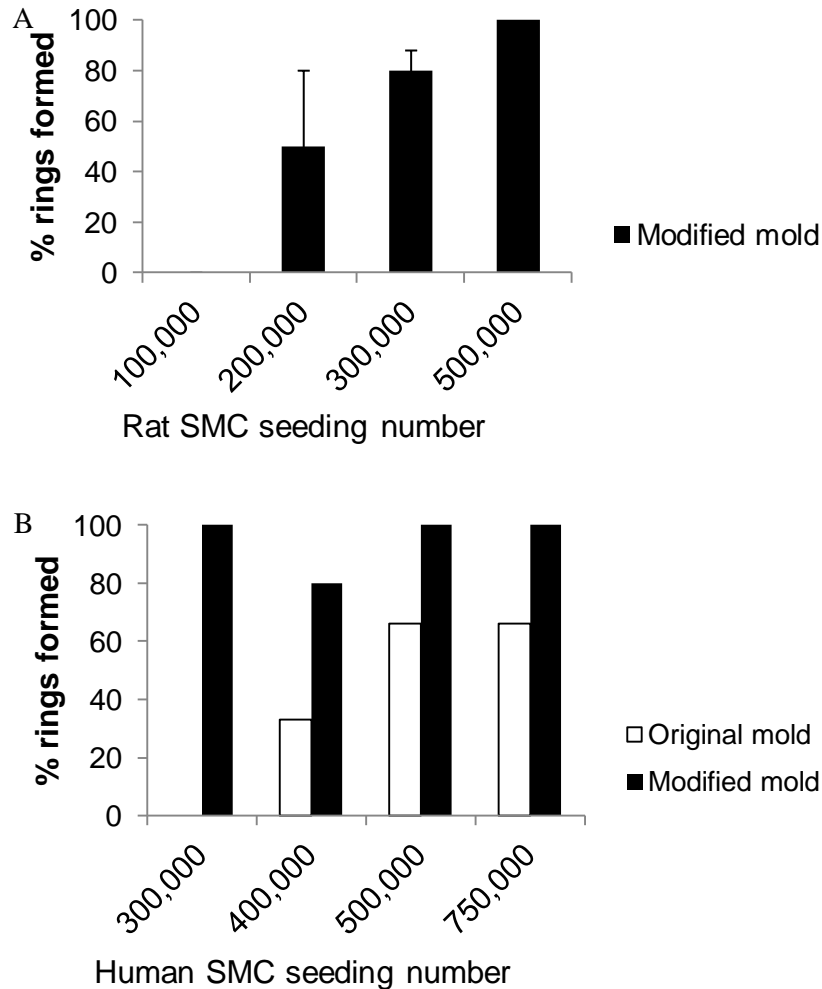
Figure 5.5 – Percentage of rings formed in original and re-designed agarose cell seeding wells. Varied concentrations of rat SMCs were seeded in re-designed, narrow trough wells (A). Human SMCs were seeded in re-designed, narrow trough wells and compared to the original, wider channel wells (B). The rat SMC study was performed twice. The average percentage of rings formed is graphed as a function of number of cell seeded (n=7 rings per group per experiment). The experiment with human SMCs was only completed once with n=3-5 rings per group.

5.4 Discussion

In this study, we found that the self-assembled cell ring system can be applied to the generation of primary human SMC rings, as well as rat SMC rings. We have demonstrated that primary human cells are capable of self-assembling into tissue rings and that these rings are strong compared to rat SMC rings we have generated previously[9] and vascular tissue generated by other tissue engineering approaches.[9,12,13] Self-assembly of human SMCs has been demonstrated in spheroids before,[14-16] but not in such large

tissues. Here we have generated tissue rings of clinically relevant size (2 mm inner diameter) which can be used to evaluate the strength and composition of human SMC-derived tissue constructs. Further, we found that human SMC rings can be stacked together and fused to generate vascular tissue tubes *entirely* from human cells (without exogenous scaffolds), which has been achieved by only a few other groups.[4,17] The application of cellular self-assembly to form rings and fused tubes may ultimately transform our system into a more useful tool for building transplantable grafts.

In comparing this study to our previous work, we found that similar to the self-assembled rat SMC rings, human SMC rings also fuse together to form tissue tubes. The rate at which they fuse is slower than that with rat SMC rings; however at the end of 7 days in fusion culture the human SMC rings had fused into cohesive tissue tubes. Interestingly, the thickness and the length of the human SMC tubes decreased over time (something not observed with the rat SMC rings). This could indicate that the tissues assemble and compact at a slower rate than corresponding rat SMC rings. Further studies are required to investigate the changes in mechanical properties, overall morphology, and ECM composition of the human SMC rings over time.

Given the difficulty in obtaining large quantities of human SMCs for cell self-assembly and ring formation studies, we modified the agarose seeding well dimensions to generate rings from the fewest possible number of cells. The original mold design required a relatively high critical mass of cells to achieve cellular self-assembly and ring formation. The seeding channel width of the original mold was 3.75 mm and required 500,000 rat SMCs or 750,000 human SMCs per ring. This high cell number led to thick tissue rings (0.94 mm for rat SMC rings and 0.52 mm for human SMC rings) which, according to the published literature, exceeded diffusion limitations (~150-200 μm)[18] and may have contributed to apparent cell death observed at the centers of the tissue rings. In our re-designed mold, we decreased the seeding trough width from 3.75 mm wide to 2 mm wide while maintaining a 2 mm post. This led to a 30% decrease in the cell seeding circumference, which allowed us to seed fewer cells, and still achieve cell aggregation and complete ring formation. In a similar cell seeding system, Livoti et al. estimated the minimal number of cells required to form a toroid is approximately 5-10 cells/μm of circumference of the post diameter, based on their mold dimensions (although their trough width was only 400 μm, the calculated number of cells/μm is normalized to the size of the post diameter).[11] Translating to our system's dimensions, this would suggest a minimum cell seeding density of our rings at 31,000-63,000 cells/ring. This is below the range of cell densities we tested, but we did not observe any ring formation with our 100,000 cells/ring group. The minimum cell number required for cellular self-assembly may

also depend on cell type. We seeded SMCs in these wells to form tissue rings whereas the above mentioned study used rat hepatocytes.

In addition to decreasing the initial cell seeding number, the new mold design decreased the amount of material (polycarbonate, PDMS, and agarose) required to generate each well. This improvement reduced time and costs, allowing for more efficient generation of cell-derived tissue rings.

Cell source is a critical consideration in designing vascular grafts. Human smooth muscle cells are an obvious choice as they are the cells that populate the medial layer of native human arteries and veins; however, due to the relative difficulty of obtaining human SMCs, their slow doubling time, and short proliferative life-span, they are not the most attractive cell source for implantable grafts.[7,8] Also studies utilizing adult human SMCs to generate vascular grafts have found that the grafts do not attain sufficient mechanical strength for implantation.[19] Tissue engineered vascular grafts have been used successfully in clinical applications when generated from other cell sources (e.g., dermal fibroblasts and bone marrow mononuclear cells).[5,6] For example, fibroblast-derived cell-sheet engineered grafts have been used for low flow applications for arteriovenous fistulas.[5] Although this approach did not use vascular SMCs, the resulting graft functioned properly *in vivo*. In another example, bone marrow mononuclear cells seeded directly onto synthetic polymer scaffold were used successfully in pediatric applications (even without the pre-culture of the graft with cells on it).[20] These studies suggest that vascular smooth muscle cells are not the only cell type that is capable of generating clinically useful vascular grafts.

Observations have led researchers to believe that cells will remodel grafts *in vivo;* therefore, the exact structure of the desired tissue does not need to be intact prior to implantation.[21-23] In fact, starting cell source (or even the presence of cells) may not be critical design criteria at all when developing implantable grafts because host cells have been found to re-populate tissues *in vivo*.[20,21,24] Recently decellularized approaches to vascular engineering have emerged as promising alternatives to living tissues. For example, a frozen, decellularized vascular graft generated from autologous fibroblasts and endothelial cells was successfully implanted into humans.[25] After eight weeks *in vivo*, the graft still functioned properly, which suggested that this method can be used to generate "off-the-shelf" autologous vessels.[25] In another example, allogeneic vascular SMCs were cultured on a PGA scaffold for 10 weeks in a bioreactor prior to decellularization.[26] The grafts were then endothelialized and implanted in a porcine model and remained patent for 30 days.[26] The decellularized approach is clinically appealing in that it decreases the long wait times required for living vessels to reach substantial strength for

implantation.[25,26]   Rather, decellularized vessels can be removed from storage and implanted almost immediately lending this method to clinical promise.

Although human SMCs are associated with limitations and have not been used clinically in vascular grafts, there is precedent for using them for tissue engineering applications.[8,16,27] SMCs contribute to the ECM synthesis and the vasoactivity of the vascular media. SMC contribution to vascular physiology makes these cells a critical component when building tissues to serve as *in vitro* models of vascular tissue, as they need to closely mimic vascular structure and function. Therefore, the studies outlined in this chapter focused on translating the ring-based model system for use with human SMCs.

In summary, we have demonstrated that primary human SMCs can aggregate and spontaneously contract to form self-assembled tissue rings similar to our earlier reports of rat SMCs.[9,10] The cells within these rings are capable of remodeling the tissue to fuse into tube-shaped structures. These findings, combined with our additional modifications to the cell-seeding wells, will allow us to use this platform technology as a means of generating primary human SMC-derived tissue to be used as both an *in vitro* research tool as well as a novel method for developing vascular grafts.

5.5 References

1.   Gwyther TA, Hu JZ, Christakis AG, Skorinko JK, Shaw SM, Billiar KL, Rolle MW. Engineered vascular tissue fabricated from aggregated smooth muscle cells. Cells Tissues Organs 2011;194(1):13-24.
2.   Lemire JM, Covin CW, White S, Giachelli CM, Schwartz SM. Characterization of cloned aortic smooth muscle cells from young rats. Am J Pathol 1994;144(5):1068-81.
3.   Lemire JM, Potter-Perigo S, Hall KL, Wight TN, Schwartz SM. Distinct rat aortic smooth muscle cells differ in versican/PG-M expression. Arterioscler Thromb Vasc Biol 1996;16(6):821-9.
4.   L'Heureux N, Pâquet S, Labbé R, Germain L, Auger FA. A completely biological tissue-engineered human blood vessel. FASEB J 1998;12(1):47-56.
5.   L'Heureux N, McAllister TN, de la Fuente LM. Tissue-engineered blood vessel for adult arterial revascularization. N Engl J Med 2007;357(14):1451-3.
6.   Shin'oka T, Imai Y, Ikada Y. Transplantation of a tissue-engineered pulmonary artery. N Engl J Med 2001;344(7):532-3.
7.   Poh M, Boyer M, Solan A, Dahl SL, Pedrotty D, Banik SS, McKee JA, Klinger RY, Counter CM, Niklason LE. Blood vessels engineered from human cells. Lancet 2005;365(9477):2122-4.
8.   McKee JA, Banik SS, Boyer MJ, Hamad NM, Lawson JH, Niklason LE, Counter CM. Human arteries engineered in vitro. EMBO Rep 2003;4(6):633-8.
9.   Adebayo O, Gwyther T, Hu J, Billiar K, Rolle M. Vascular smooth muscle cell derived tissue rings exhibit greater tensile strength than smooth muscle cells in fibrin or collagen gels. in submission.
10.   Gwyther TA, Hu JZ, Billiar KL, Rolle MW. Directed cellular self-assembly to fabricate cell-derived tissue rings for biomechanical analysis and tissue engineering. J Vis Exp 2011(57), doi: 10.3791/3366.
11.   Livoti CM, Morgan JR. Self-assembly and tissue fusion of toroid-shaped minimal building units. Tissue Eng Part A 2010;16(6):2051-61.

12.   Seliktar D, Black RA, Vito RP, Nerem RM. Dynamic mechanical conditioning of collagen-gel blood vessel constructs induces remodeling in vitro. Ann Biomed Eng 2000;28(4):351-62.

13.   Rowe SL, Stegemann JP. Interpenetrating collagen-fibrin composite matrices with varying protein contents and ratios. Biomacromolecules 2006;7(11):2942-8.

14.   Dean DM, Napolitano AP, Youssef J, Morgan JR. Rods, tori, and honeycombs: the directed self-assembly of microtissues with prescribed microscale geometries. FASEB J 2007;21(14):4005-12.

15.   Napolitano AP, Chai P, Dean DM, Morgan JR. Dynamics of the self-assembly of complex cellular aggregates on micromolded nonadhesive hydrogels. Tissue Eng 2007;13(8):2087-94.

16.   Norotte C, Marga FS, Niklason LE, Forgacs G. Scaffold-free vascular tissue engineering using bioprinting. Biomaterials 2009;30(30):5910-7.

17.   Kelm JM, Lorber V, Snedeker JG, Schmidt D, Broggini-Tenzer A, Weisstanner M, Odermatt B, Mol A, Zünd G, Hoerstrup SP. A novel concept for scaffold-free vessel tissue engineering: self-assembly of microtissue building blocks. J Biotechnol 2010;148(1):46-55.

18.   Curcio E, Salerno S, Barbieri G, De Bartolo L, Drioli E, Bader A. Mass transfer and metabolic reactions in hepatocyte spheroids cultured in rotating wall gas-permeable membrane system. Biomaterials 2007;28(36):5487-97.

19.   Dahl SL, Rhim C, Song YC, Niklason LE. Mechanical properties and compositions of tissue engineered and native arteries. Ann Biomed Eng 2007;35(3):348-55.

20.   Hibino N, Shin'oka T, Matsumura G, Ikada Y, Kurosawa H. The tissue-engineered vascular graft using bone marrow without culture. J Thorac Cardiovasc Surg 2005;129(5):1064-70.

21.   Matsumura G, Hibino N, Ikada Y, Kurosawa H, Shin'oka T. Successful application of tissue engineered vascular autografts: clinical experience. Biomaterials 2003;24(13):2303-8.

22.   Watanabe M, Shin'oka T, Tohyama S, Hibino N, Konuma T, Matsumura G, Kosaka Y, Ishida T, Imai Y, Yamakawa M and others. Tissue-engineered vascular autograft: inferior vena cava replacement in a dog model. Tissue Eng 2001;7(4):429-39.

23.   Pandis L, Zavan B, Bassetto F, Ferroni L, Iacobellis L, Abatangelo G, Lepidi S, Cortivo R, Vindigni V. Hyaluronic acid biodegradable material for reconstruction of vascular wall: a preliminary study in rats. Microsurgery 2011;31(2):138-45.

24.   Zavan B, Vindigni V, Lepidi S, Iacopetti I, Avruscio G, Abatangelo G, Cortivo R. Neoarteries grown in vivo using a tissue-engineered hyaluronan-based scaffold. FASEB J 2008;22(8):2853-61.

25.   Wystrychowski W, Cierpka L, Zagalski K, Garrido S, Dusserre N, Radochonski S, McAllister TN, L'heureux N. Case study: first implantation of a frozen, devitalized tissue-engineered vascular graft for urgent hemodialysis access. J Vasc Access 2011;12(1):67-70.

26.   Quint C, Kondo Y, Manson RJ, Lawson JH, Dardik A, Niklason LE. Decellularized tissue-engineered blood vessel as an arterial conduit. Proc Natl Acad Sci U S A 2011;108(22):9214-9.

27.   Grassl ED, Oegema TR, Tranquillo RT. A fibrin-based arterial media equivalent. J Biomed Mater Res A 2003;66(3):550-61.

Chapter 6: Preliminary studies to optimize cell source, contraction, and ECM synthesis in cell-derived vascular tissue

6.1 Introduction

This thesis focused on the development of a new model system to generate 3D cell-derived tissues by cellular self-assembly, and to study their biomechanics and ECM composition. With this method, we are able to take cells in suspension and directly generate 3D tissue constructs by simply placing cells into non-adhesive wells. The resulting tissues more closely resemble native tissue in that they are derived entirely from cells and the ECM they produce. However, our engineered vascular constructs lack important elements (such as elastin-rich ECM and contractile SMCs) required for true recapitulation of native vascular structure and function.

Recently there have been several reports of grafts with substantial mechanical properties and burst pressures which exceed 2000 mmHg (saphenous vein).[1,2] However, few reports include information about compliance of the vessels. Those who do address compliance, find their values below that of native vessels.[3-5] For example, upon implantation, cell-sheet based vascular grafts have a compliance of only 1/3 that of native controls (11.5% /100mmHg), but after 6 months *in vivo*, remodeling of the graft occurs which results in compliance measurements comparable to those values of native arteries (8.8% /100mmHg).[3] The medial layer of blood vessels consists of layers of elastic fibers which help lead to compliant tissue. Elastin has proven to be a difficult protein to incorporate into engineered tissue because adult SMCs do not readily synthesize the protein. However, there are many researchers attempting to generate more compliant grafts by increasing elastin synthesis and elastic fiber assembly through the use of alternative cell types or soluble factor addition.[6,7] As of yet, there have been few reports of engineered vascular grafts with levels of elastic fibers similar to native arteries. The incorporation of elastin will be critical, however, because controlling compliance prior to implantation is critically important because a mis-match in mechanical properties at the anastomosis site can lead to occlusion and a decrease in patency.[8]

Another factor limiting the use of tissue engineered vascular grafts is their low contractility compared to native blood vessels. One approach to analyzing the contractile properties of grafts is by immunostaining for specific contractile proteins within SMCs (such as smooth muscle alpha actin, SMA; calponin, CALP; or myosin heavy chain, MHC). While many researchers probe to see if these contractile proteins are present, only a subset of studies have examined the *functional* effects of their presence on vascular contractility.[1,7,9-11] For example, Peng *et al.* demonstrated that sub-intestinal submucosal vascular grafts populated with hair follicle-derived smooth muscle cells produce contractile forces) in response to potassium chloride treatment, but only at 7.5% of the force generated by native vessels (17.5 kPa.[7] SMCs seeded onto PGA scaffolds contract in response to prostaglandin (a mediator of SMC contraction), but only reach 5% of the response of control vessels after 8 weeks in culture.[1] Although there has been some success in generating vascular tissues which express contractile SMC proteins, the correlation of protein expression to functional contractility of the tissues is largely unknown or if tested, falls short of that present in native vasculature.

Finding the proper culture parameters that give rise to these missing elements (such as elastin and contractile proteins) remains a challenge. We propose that through the use of this system we can better screen combinations and concentrations of factors which promote ECM synthesis and SMC contraction in engineered cell-derived tissue. Further, with this system we can explore the use of alternative cell sources for vascular tissue engineering. Below is a description of how the ring system may be utilized to explore each of these features.

6.2 Plasticity of SMC phenotype (Quiescent vs. Synthetic)

Smooth muscle plays a role in a variety of systems *in vivo*. To perform their diverse functions throughout development and in stable adult tissues, SMC phenotype spans a continuum from contractile and quiescent to proliferative and synthetic.[12] "Quiescent" SMCs are able to respond by contracting and relaxing to small molecule signals (such as acetylcholine and norepinepherine) because they contain a fully functional contractile apparatus.[13] Unlike other muscle cells, their contractile network is multi-directional throughout the cells allowing them to contract simultaneously in both the circumferential and longitudinal directions to help propagate the contraction and blood flow down the vasculature. The contractile apparatus consists of a network of fibrillar cytoplasmic proteins including smooth muscle α-actin (SMA), calponin (CALP), SM-22α, caldesmon, smoothelin, and myosin heavy chain (MHC).[14] Quiescent SMCs also contain little connective tissue and ECM, and, in culture, adopt a fusiform or "spindle-like" morphology.[15] The opposite end of the continuum contains "synthetic" SMCs. These cells

contain very little contractile machinery and as such, are unable to produce much contraction. These synthetic SMCs have been found to express caldesmon, vimentin, and non-muscle myosin heavy chain.[16,17] In culture, these cells adopt a "hill-and-valley" morphology where they are more spread out and can grow on top of each other into multi-layers.[15] Synthetic SMCs are also associated with high levels of proliferation and ECM synthesis (rich in glycosaminoglycans and sulfated proteoglycans).[18] Figure 6.1 shows a schematic of the spectrum of SMC phenotypes. (Further description of phenotype characteristics reviewed in[14]).

Figure 6.1 – SMC phenotype continuum. This diagram summarizes the characteristics of both the quiescent and the synthetic SMC phenotypes. The quiescent phenotype is characterized mainly by expression of SMC contractile protein markers (SMA, CALP, and MHC). The synthetic phenotype is characterized mainly by proliferation, loss of contractile protein expression, and synthesis of glycosaminoglycans and sulfated proteoglycans. SMCs can exist anywhere along the continuum with varying relative expression of these identifying markers.

Healthy adult vascular SMCs generally maintain a quiescent phenotype. However, cultured SMCs adopt a synthetic phenotype, similar to that found in vascular pathologies such as restenosis and atherosclerosis.[19,20] In this pathological state, SMCs lose expression of contractile proteins, become highly proliferative, and synthesize ECM molecules such as versican and hyaluronan.[15,20,21] Several

external stimuli including soluble factors (detailed below), ECM cues, and mechanical stimulation have all been found to help switch cultured SMCs from the synthetic phenotype to a quiescent phenotype (an event called "phenotype switching", reviewed in[14,22]).

Soluble signaling factors can be potent mediators of SMC phenotype. Several factors have been implicated in shifting SMCs toward the proliferative synthetic phenotype such as platelet derived growth factor (PDGF), fibroblast growth factor (FGF-2), insulin-like growth factor (IGF), epidermal growth factor (EGF), angiotensin II (Ang-II), and thrombin.[23-26] However, other soluble factors have been implicated in shifting cultured SMCs back toward a contractile phenotype; TGFβ-1, heparin, IGF-1, and Ang II.[23,24,27-32] This suggests that SMCs are a plastic cell type, and that with proper environmental cues, can be manipulated both into and out of a contractile phenotype.

Mechanical stimulation has also been found to play a major role in determining the phenotypic fate of SMCs. As SMCs are exposed to constant cyclic loading *in vivo*, several researchers have attempted to recapitulate that behavior *in vitro*. Cyclic mechanical strain has increased the content of SMA positive cells observed within the engineered vessel wall.[33] In addition to affecting the phenotype of SMCs, mechanical strain has also been shown to stimulate production of ECM molecules such as collagen or elastin *in vitro*.[34,35] As a result many researchers utilize biomechanical loading as part of their culture regime for tissue engineered vascular grafts.[1,9,36-40]

Finally, extracellular matrix molecules also help control the phenotype of cultured SMCs. Fibronectin, for example, has been implicated in the loss of SMC contractile phenotype,[41] although laminin plays a critical role in maintaining contractile protein expression, or at least delaying the switch to a synthetic phenotype in cultured cells.[41,42] Factors implicated in phenotypic switching are outlined in a schematic shown in Figure 6.2.
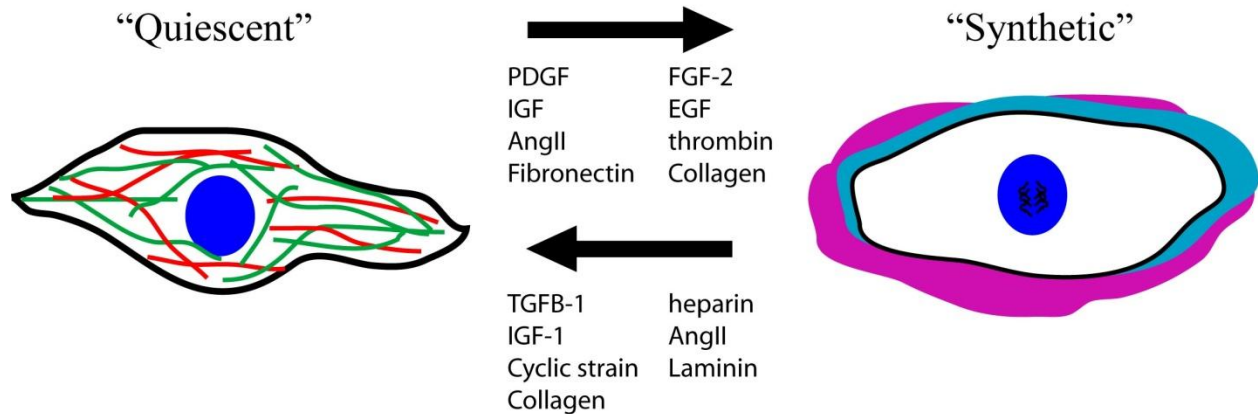
Figure 6.2 – Factors implicated in switching SMC phenotype. Several factors including soluble additives, ECM molecules, and mechanical loading can switch SMCs between quiescent and synthetic phenotypes.

Smooth muscle cell phenotype is of critical importance when developing engineered tissue to be used as vascular tissue models *in vitro*. In order to obtain sufficient quantities of cells to populate engineered tissues, SMCs must be capable of proliferating. However, for engineered vascular tissue to achieve physiological contraction, the SMCs must exist in a quiescent phenotype where SMCs need to express SMA, CALP, MHC, etc. to help aide in the vascular contraction. This paradigm forces engineers to understand and control factors which shift cells between phenotypes as needed.[39] If engineers understand these conditions, culture environment can be exploited through the use of a biphasic approach where first cell are cultured under growing conditions followed by a differentiation period into contractile SMCs. In all, there are many factors that contribute to the phenotypic state of SMCs, and we believe that the ring system described in this thesis is capable of screening through these factors to determine which combinations and concentrations lead to optimal tissue growth for building ideal vascular tissue.

6.2.1 Quiescent, contractile SMCs in engineered vascular tissue

Although smooth muscle cell phenotype is a critical parameter to consider when generating vascular tissue, we have not observed the presence of smooth muscle cell markers in our cell-derived tissue rings. To demonstrate this, Figure 6.3 shows smooth muscle alpha actin (SMA) staining of human SMC tissue rings cultured for 14 days in two different media formulations (Figure 6.3 A, B; SmGM-2, Lonza; or "base medium", 1:1 DMEM:Ham's F12, 10% Fetal Clone III, 1% penicillin-streptomycin). The rings cultured in SmGM-2 are the same rings that were discussed in Chapter 5 of this thesis. For comparison in this experiment there were three 2 mm rings (750,000 cells/ring) grown in each of the different types of

medium (SmGM-2 and base medium). The immunostaining was compared to positively marked blood vessels found in a human skin control (Figure 6.3D). As seen in the photomicrographs, there was no SMA expression found in human SMC rings cultured in either media formulation. In fact, throughout this work we did not observe SMA expression in any of our tissue rings generated from either human SMCs or rat SMCs (data not shown). This suggests that the cells we have in our self-assembled rings may be in their synthetic phenotype rather than a contractile phenotype. This hypothesis is in agreement with our earlier histology staining where we observed abundant GAG deposition within our rings. The lack of SMA expression coupled with the abundant GAGs lead us to believe that our tissue rings are full of SMCs in their synthetic state. Therefore, we believe that we will need to add additional media supplements to increase SMC contractile protein expression and change the cells into quiescent cells.
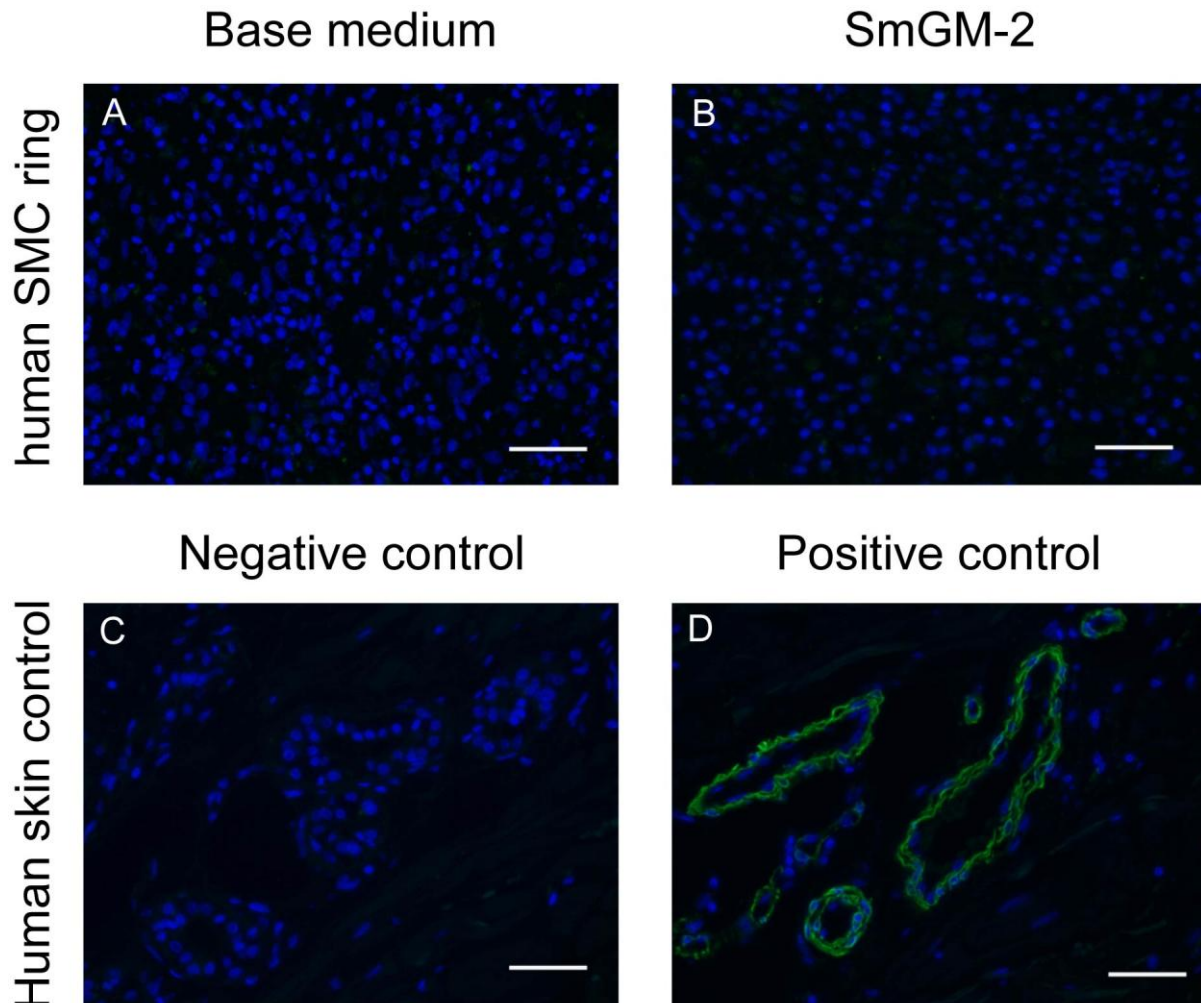

Figure 6.3 – Photomicrographs of SMA-stained human SMC rings. Tissue rings cultured in base medium (1:1 DMEM:Ham's F12, 10% Fetal Clone III, 1% penicillin-streptomycin, A) or SmGM-2 (Lonza SMC growth media, B) compared to human skin control (negative, C; positive, D). Green: SMA, Blue: nuclei. Scale = 50 μm.

The human SMCs used to generate human SMC rings are commercially available from Lonza. According to the manufacturer, these cells are only *guaranteed* to grow and maintain their smooth muscle cell phenotype in their proprietary smooth muscle cell growth medium (SmGM-2). Ultimately, we would like to move away from culturing these cells in proprietary medium and into a chemically defined medium of which we know exact component concentration and composition. Although we have not yet reached this goal, we have tried growing these cells in other media formulations. The most basic formulation we have used is base medium (consisting of 1:1 DMEM:Ham's F12, 10% Fetal Clone III, 1% penicillin-streptomycin). We have also added growth factors to this base media to try to encourage better cell growth. For example, we have supplemented this base media with 4 ng/ml FGF-2 to enhance cell proliferation (this media is called +FGF media).

To test the effect of these media formulations on the human SMC growth and, we began by culturing cells on coverslips in the three different media (base media, SmGM-2, and +FGF media). To test this, 10,000 human SMCs were seeded onto glass coverslips placed into each well of a 24-well plate. The cells were seeded in the different media formulation and cultured for 7 days before fixing and immunostaining for smooth muscle alpha actin (SMA), and Hoechst to visualize nuclei. Five to ten images were taken per coverslip (3-7 coverslips per media condition), and the number of nuclei and the number of SMA positive cells were counted.

We found that when cultured in SmGM-2, human SMCs proliferate faster (higher cell counts) than when cultured in the base medium (data not shown). However, we have found that by supplementing the base media with 4 ng/ml FGF-2 (+FGF media), we increased human SMC proliferation compared to the base medium (data not shown). These findings are in agreement with other published reports which also suggest that FGF-2 promotes SMC proliferation.[43-45] We also observed differences in SMA expression between human SMCs cultured in the three different media formulations (base media, +FGF, or SmGM-2). For example, human SMCs cultured in base media have a higher percentage of SMA positive cells (Figure 6. 4A,B) than human SMCs cultured in +FGF medium (Figure 6.4A,C). Further, human SMCs cultured in SmGM-2 have a higher percentage of SMA-positive cells than cells cultured in +FGF media, but fewer positively stained cells than SMCs cultured in base media (data not shown). Therefore, it seems that the SmGM-2 media is not particularly effective at expanding human SMCs or switching them into a contractile phenotype.
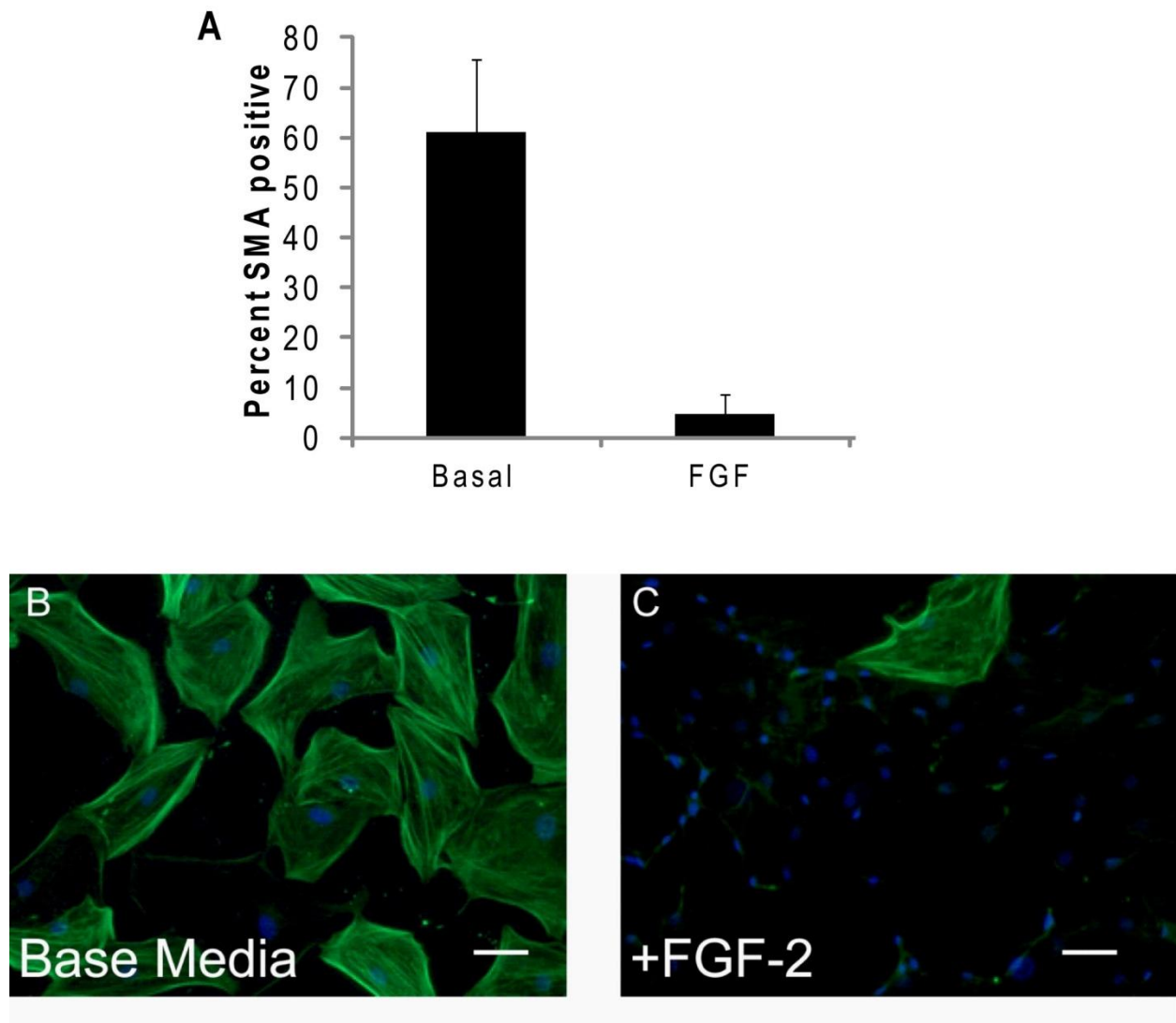
Figure 6.4 – SMA expression in human SMCs cultured with or without FGF-2. Human SMCs cultured on glass coverslips for 7 days in medium with or without FGF-2. The number of smooth muscle alpha actin (SMA)-positive cells was counted in each condition. Quantification of the percentage of positive cells is shown in the graph (A) SMA labeling is shown in green in human SMCs cultured in base medium (B) or FGF-2 media (4 ng/ml) (C). Blue = nuclei, Scale = 50μm. (mean±SD, n=3, $p < 0.05$)

These results are interesting because the "base medium" which resulted in elevated levels of SMA staining on coverslips, did not result in any SMA-positive staining in human SMC tissue rings ("base medium", Figure 6.3A). This suggests that while SMC phenotype modulation can be achieved by a single growth factor addition in 2D, the same results are not realized with 3D tissue. This provides an argument for moving forward in a 3D screening system like the self-assembled rings for future studies on

smooth muscle cell phenotype. We anticipate that through the use of the ring model we can systematically evaluate the effects of various combinations and concentrations of factors leading to increased SMC contractile protein expression. Further, we can also use these rings to evaluate the contractile forces generated by SMC-derived tissues.

Regardless of the lack of contractile expression to date, we have developed this ring-based system with the intention of conducting functional myography to test the contractile potential of the rings. To determine whether contractility tests are feasible with this system, we have cultured rat SMC rings for 7 days and then mounted them on a wire myograph system (DMT, Model 610M). Figure 6.5 shows force traces produced by both a ring segment from a mouse aorta and one of our rat SMC tissue rings. The vessels and rings were both stimulated with potassium-rich physiological salt solution (KPSS) to induce contraction. The mouse aorta displays a normal force trace in which the vessel contracts upon exposure to the KPSS, whereas the rat SMC rings don't appear to produce any force.
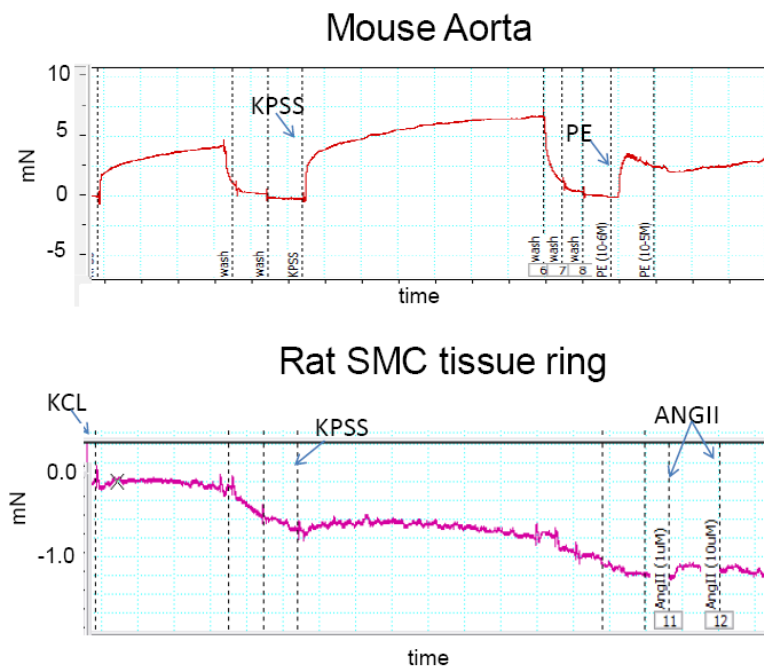

Figure 6.5 – Contraction force measured by myography. Force traces generated by myography of a mouse aorta and a 2 mm, 7-day-old rat SMC ring. Rings were stimulated with potassium-rich physiological salt solution (KPSS), Phenylephrine (PE), or Angiotensin II (ANG II) to stimulate contraction. (*Note the scale of the y-axis differs in the two traces)

Although we have not yet fabricated tissue rings that generate force or express smooth muscle contractile proteins, we have shown that with our system we can fabricate cell-derived ring constructs which are size and shape appropriate for contraction studies. Future studies can further examine the affects of various factors on the ability of tissue rings to generate contractile proteins and ultimately contractile function. For example, L'Heureux et al. showed that cell-derived tissue tubes generated from vascular SMCs cultured in 50 μg/ml of ascorbic acid and 0.5% serum can produce contractile force in response to vasoconstrictor agonists.[11] Although these vessel segments were cultured for >3 months, we may be able to use the same culture media composition with SMCs in out self-assembled rings to produce contractile forces. We can also perform protein analysis to determine where along the phenotype spectrum our cells are located. For example, we can examine not only the above mentioned contractile proteins (SMA, CALP, MHC) but also look at ion channel expression to determine if proteins that aide in vascular responsiveness are present in our cells. In all, we can use these self-assembled rings to analyze contractile potential of cell-derived vascular constructs.

6.3 Extracellular matrix found in the vascular media (Elastin)

Another critical component to building engineered vascular tissue is the extracellular matrix (ECM). Native vascular medial layers are rich in both collagen and elastin. Collagen helps to provide the strength and structure to the vessels whereas elastin provides compliance and elastic recoil to the vessels. While researchers have made great strides in building grafts with substantial collagen content and high burst pressures, sufficient elastin production remains elusive.[46-48] Elastin is the most abundant protein found in muscular arteries and not only plays an important role in compliance,[49] but also in the structure[50] and elastic recoil[51] of the blood vessel and helps control smooth muscle cell phenotype and limit proliferation.[52]

Elastin is formed when its soluble precursor, tropoelastin, is cross-linked with fibrillins, fibulins, and other micro-fibril associated glycoproteins to form elastic fibers.[53] These fibers are found concentrated in lamellae throughout the medial layer in between layers of smooth muscle cells. Elastin is primarily produced throughout development where it is cross-linked into the elastic fibers. Elastin is a very stable protein with a half-life that approaches the age of the animal.[54] Therefore, there is very little elastin turn-over and little elastin synthesis in adult vessels. This generates a problem when engineers look to use adult SMCs as a cell source for their vascular grafts because of the lack of elastin synthesis. Therefore, most tissue engineered grafts that lack elastic fibers have low patency rates due to thrombosis,[55,56] intimal

hyperplasia,[57] and aneurysm[47]. Many attempts to engineer grafts with SMCs have generated small levels of elastin synthesis,[58] but not the levels found in native artery.[49] Neonatal SMCs have been shown to produce elastic fibers more readily than adult SMC cells, but may not be a clinically useful cell type for adult vascular grafts due to lack of availability.[58,59] Recently, there have been multiple reports of tissue engineered vascular grafts with elastin production,[6,7,60,61] but characterization of the contribution of elastin to their mechanical properties remains unknown.

6.3.1 Cell derived elastin-rich rings

One possible application of our cell-based system is to study the biomechanics of elastin-rich tissue. We can monitor how elastin production, secretion, and cross-linking in to the ECM affect the compliance of self-assembled tissues. As described above, inducing adult cells to generate elastin in culture has proven difficult, therefore in preliminary studies (to show proof-of-concept) we chose to use neonatal elastogenic cells to generate elastin-rich tissue rings. We could then determine if our ring system is capable of differentiating changes in mechanical properties due to increased elastic fiber content. Further, we could use this cell-derived approach as a means of "tuning" the mechanical properties by altering proportions of elastin-producing cells with another cell type. If successful, that would yield increased compliance with increased elastic fiber content due to a higher proportion of elastin producing cells.

As preliminary work, we generated tissue rings from neo-natal rat lung fibroblasts (RFL-6 cells, ATCC, CCL-192), a cell type well known for producing abundant amounts of elastin.[62,63] In our study, we tried to modulate the mechanical properties of the tissue rings by changing the amount of elastin. To do this, we attempted to create tissue rings by co-seeding various proportions of RFL-6 cells with rat SMCs (0%, 50%, 75%, or 100% RFL-6 cells). By increasing the percentage of RFL-6 cells, we were hoping to generate constructs that contained more elastin and ultimately greater compliance. Five tissue rings were produced for each proportion as described in Chapter 4 with 500,000 cells per 2 mm ring, cultured for 7 days. All proportions of cells aggregated to form rings, but the rings generated entirely from RFL-6 cells only loosely contracted around the center post and appeared "lumpy" with thick and thin regions around the circumference. Upon removal from the wells the rings made entirely from RFL-6 cells were extremely fragile and did not remain intact. Histological staining for elastin showed that co-cultured rings did not express the protein, no matter the ratio of cell types (see Figure 6.6). Conversely, the rings completely generated from RFL-6 cells produced an over-abundance of elastin which, we believe, led to our inability to manipulate the rings and perform mechanical analysis.
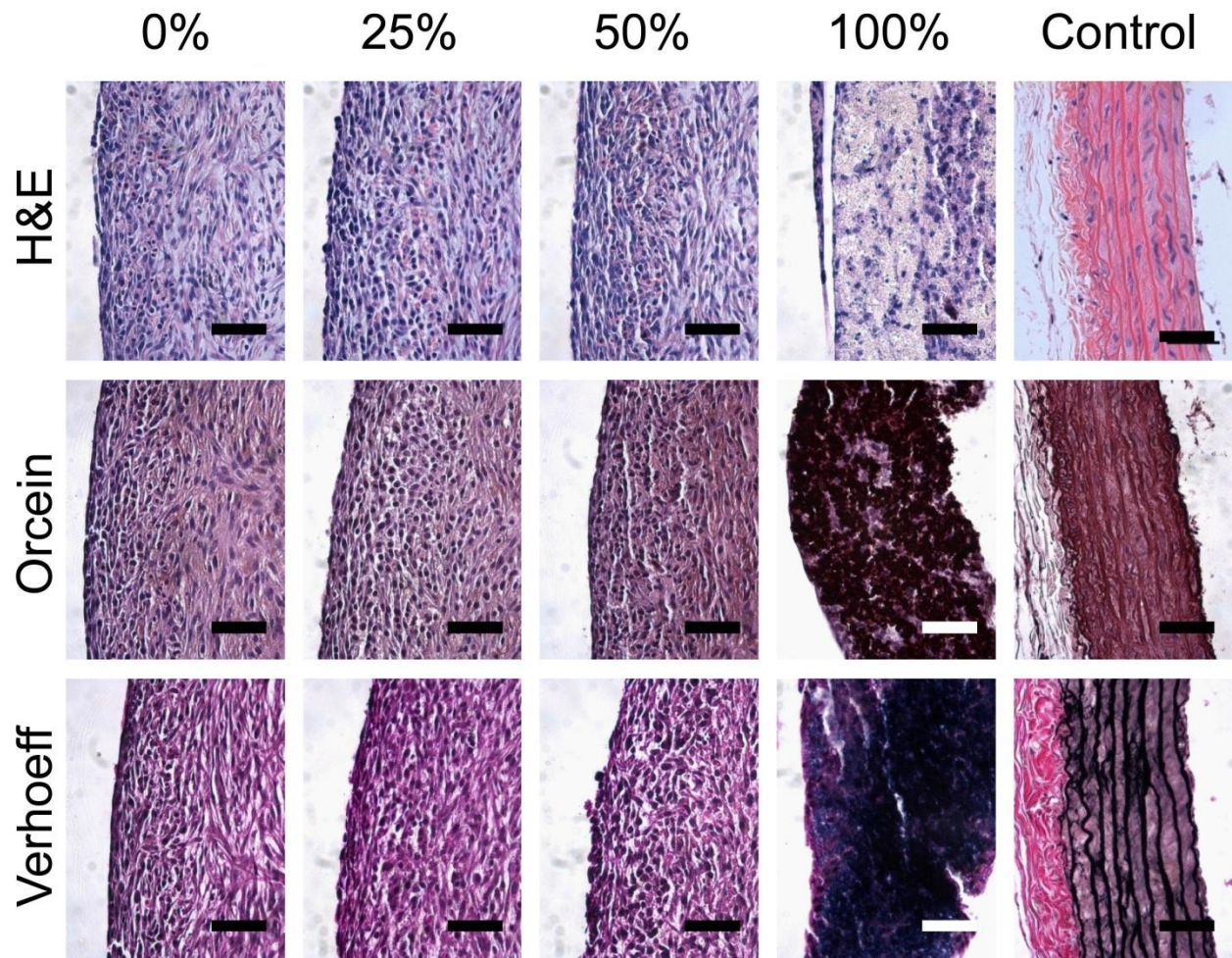
Figure 6.6 – Histomorphometry of tissue rings co-cultured from rat SMCs and RFL-6 cells. Co-seeded 2mm rings were cultured for 7 days. The percentage above the images indicated the percentage of RFL-6 cells seeded in the ring. Paraffin-embedded sections were stained with H&E, Orcein (dark purple=elastin), and Verhoeff van Geison (black=elastin). Scale = 50µm

While the 100% RFL-6 group was too fragile to test, the 0%, 25% and 50% RFL-6 groups were removed from their wells and uniaxially tested to obtain mechanical data (similar to as described in Chapter 3). Interestingly, the ultimate tensile strength and stiffness of the rings with RFL-6 cells were greater than those composed solely of smooth muscle cells (0% RFL-6, Figure 6.7B, C). This could in part be due to an increase fibroblast population within these tissues as fibroblasts are known to produce abundant ECM and generate strong cell-derived structures.[3,64-66] Further supporting this idea is the increase in thickness observed in the rings co-cultured with fibroblasts compared to SMC-only rings (Figure 6.7A).
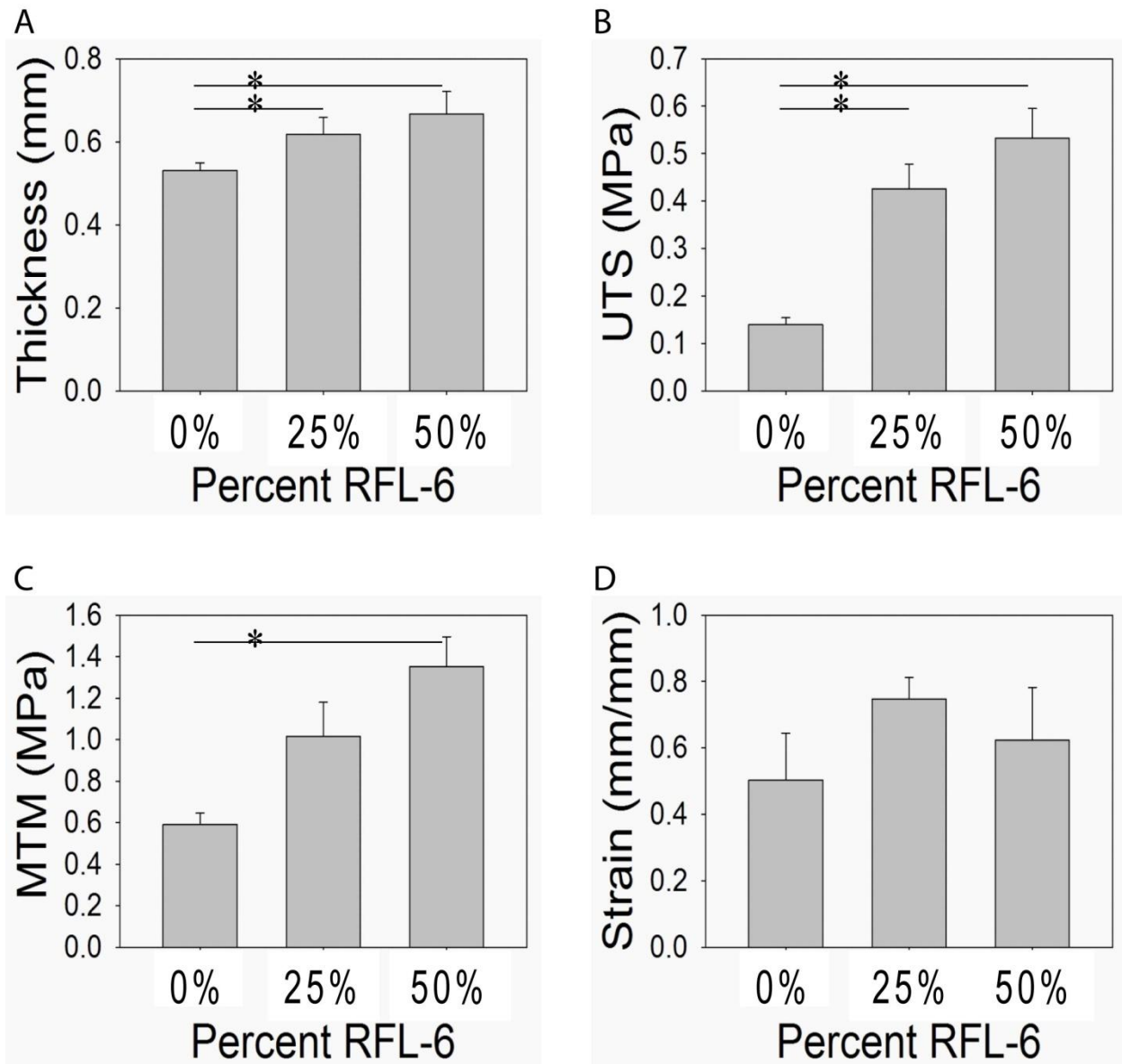
Figure 6.7 – Mechanical analysis of rings co-cultured with rat SMCs and RFL-6 cells. Mechanical testing parameters as a function of percent RFL-6 cells in the co-culture. The data is represented as mean ± SD, n=3. *= p<0.05

Although not successful in achieving our goal of creating tissue rings with elevated elastin content, this study demonstrates that we are able to utilize the tissue ring system to alter the ECM composition of our tissues and measure changes in the biomechanical and histological properties.

Throughout the course of these studies, however, we did observe some limitations to the current system. We currently use a 1N load cell for uniaxial tensile testing. This may not be sufficient to cover the range of loads necessary for stronger tissues. Because one future goal is to increase collagen content and

overall tissue strength, some modifications to current testing protocols such as changing the load cell and pre-cycling regimen may be necessary to accommodate stronger tissues. Additionally, the current method for testing our tissues monitors force and displacement of the grips on which we mount the rings. We then take these measurements and calculate *failure* properties of our tissues. To do this, we calculate engineering stress based on measured initial thickness, and engineering strain based globally on the displacement of the grips. However, we are interested in understanding how our tissues behave under physiological loads, therefore in future studies we need to examine their *sub-failure* properties. The current method of obtaining global failure mechanical data is not ideal for assessing sub-failure properties of the tissue rings. Therefore, we may need to modify the testing protocol to include local tracking of the tissue which will help us calculate local strain and sub-failure compliance. One method to achieve this is to attach dots on the surface of the tissue ring and video record displacement of the markers. This will give us information about the local strain in certain regions of the tissue and yield a more accurate representation of tissue sub-failure mechanics.

6.4 Sources of cells suitable for vascular tissue engineering

Finally, the source of cells used to generate tissue-engineered blood vessels is also an important design parameter. Most *in vivo* studies have used autologous cells or have implanted allogeneic or xenogeneic cells into immuno-compromised animals. Vascular smooth muscle cells harvested from autologous vessels are an obvious option because they are the cells found in the medial layer of native vessels. While they have been the widely used cell source for experimental vascular tissue engineering studies, obtaining human SMCs requires a tissue biopsy from a patient's vein or artery, which causes pain and morbidity at the donor site. Further, patients who are candidates for vessel grafts are typically older and have more cardiovascular disease risk factors than the young, healthy donors from which cells are obtained for most experimental studies. SMCs from older patients were shown to have a limited proliferative capacity, and a decreased ability to synthesize collagen and elastin.[48,67] The limited life span of adult SMCs has proven to be a major stumbling block in their use in regenerative medicine.

The engineering of cells to overexpress human telomerase reverse transcriptase (hTERT) has considerably lengthened the lifespan of many cell types. hTERT is an enzyme that couples with an RNA primer inside the cell to provide a telomere-extending capability, to reverse the natural telomere shortening that occurs upon cell replication. Interestingly, SMC life span could be extended for several passages by overexpressing human telomerase reverse transcriptase (hTERT),[67] but this approach introduces concerns of the use of genetic manipulation and the potential for malignancy. Recently, a

chimeric fusion between TERT and a DNA binding protein (pot1) has been described giving rise to the hope of transiently expressing hTERT in adult cells without the need for retro- or lenti- viral expression.[68] While this fusion protein has increased the lifespan of SMCs in vitro, its potential for vascular tissue engineering is unrealized.[68]

Alternatively, other vascular cells such as fibroblasts and endothelial cells are more readily obtained in clinically useful quantities from autologous tissues such as skin biopsies. A single dermal biopsy can provide sufficient numbers of cells to create cell-sheet-based vascular grafts, regardless of patient age, cardiovascular disease status, and other risk factors.[3,69,70] Multiple sources of endothelial cells have been investigated for the intimal lining of vascular grafts, including microvascular endothelial cells from autologous adipose tissue;[71] however, a patient-matched, expandable source of vascular SMCs has not yet been established.

This challenge has led to the investigation of alternative cell sources, including stem cells. Over the past decade, cells from bone marrow,[39,72-78] adipose tissue,[79,80] muscle,[81,82] and hair follicles[83,84] have been isolated and seeded onto scaffolds to create vascular grafts. Many of these stem cell sources have been shown to differentiate along a SMC lineage. Cells isolated from the bone marrow, including freshly purified mononuclear cells,[85] multipotent adult progenitor cells,[75] and adherent mesenchymal cells,[39,72] are the predominant stem cell sources that have been studied to date. Bone-marrow-derived mesenchymal stem cells (MSCs) have been used after a period of cell culture to differentiate them into SMCs, although they have also been used fresh, without ex vivo culture, which is advantageous for clinical use.[85] Additionally, these cells have proven to be a valuable model cell type for animal studies because they can be isolated from many species. Most strategies for selection and differentiation rely on evidence of expression of genes that are characteristic of differentiated, contractile SMCs. The most common early marker used to identify SMCs is smooth muscle a-actin (SMA); however, it is also expressed in myofibroblasts and therefore is not specific.[86] More stringent criteria include expression of another early contractile protein, calponin (CALP), which is restricted to SMCs, transcription factors such as SM22a, and proteins expressed at later stages of differentiation, including smooth muscle myosin heavy chain. Most studies rely on a combination of gene expression, contractile protein synthesis, and functional contraction assays as evidence of SMC differentiation from progenitor cells.

6.4.1 Human mesenchymal stem cells for use in vascular tissue engineering

Because others have demonstrated that bone marrow-derived MSCs are able to differentiate into SMCs, we chose to explore their differentiation potential and utility as a starting cell source for our vascular

tissue engineering studies. There does not appear to be a single protocol for differentiating stem cells into SMCs, as different groups use different methods.[39,76,87,88] We began by culturing human bone-marrow derived mesenchymal stem cells (hMSCs, Lonza, passage 5-9, donor: male 21 years old) on glass coverslips for 7 days in mesenchymal stem cell growth media (MSCGM, Lonza). At the conclusion of culture the cells were stained for SMA and CALP (mouse monoclonal antibodies from Dako). Figure 6.8 shows positively stained MSCs cultured on glass coverslips. While not 100% of the cells expressed SMC contractile proteins, there are many in which the organized, filamentous protein staining was observed.
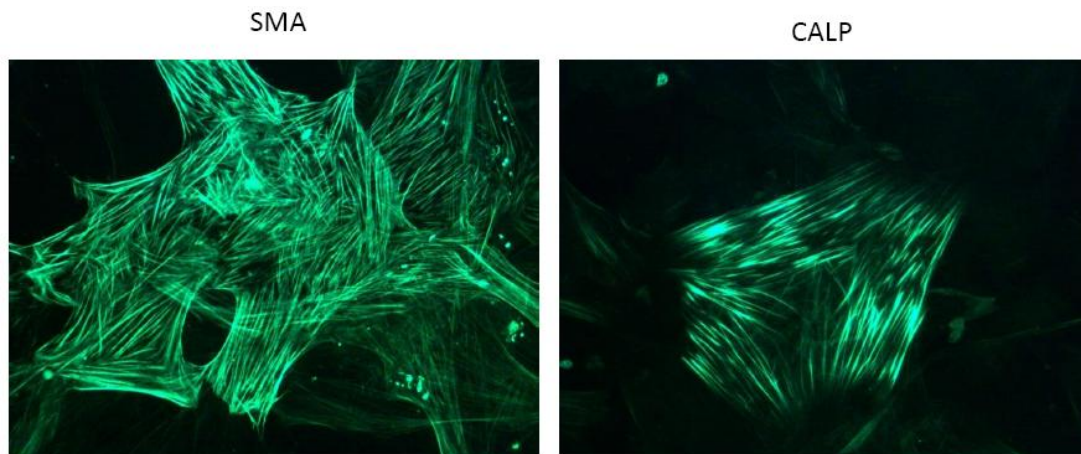
Figure 6.8 – MSCs can differentiate and express SMA and CALP. MSCs cultured on glass coverslips in MSCGM for 7 days express smooth muscle alpha actin (SMA) and calponin (CALP.)

Our immunostaining results indicated that there were some SMA-positive MSCs in our cultures; therefore we went on to quantify the percentage of SMA-positive cells. Additionally, in an effort to increase the number of cells expressing SMA, we treated the MSCs with varying doses of TGF-β1 (0-10 ng/ml), a factor which has been implicated in promoting SMC contractile protein expression either by itself or in combination with other cytokines.[39,74,75] To do this, MSCs were cultured on glass coverslips for 7 days in medium (MSCGM or 1:1 Ham's F12 and DMEM, 10% Fetal Clone III (HyClone), 1% Penecillin-Streptomycin (Mediatech)) with varying concentrations of TGF-β1 or FGF-2). The coverslips (3-7 per group) were then stained for SMA and five images per coverslip were acquired. The number of SMA-positive cells and the total number of cells were counted and averaged between the five images. Then number of SMA-positive cells was divided by the total number of cells in the field of view to yield the percentage of positive cells in each treatment group. Figure 6.9 shows a graph of the percentage of SMA-positive MSCs expressed as mean ± SD. The addition of 1 ng/ml TGF-β1 increased levels of SMA staining to approximately 70% compared to the 30% baseline of culture in MSCGM media.
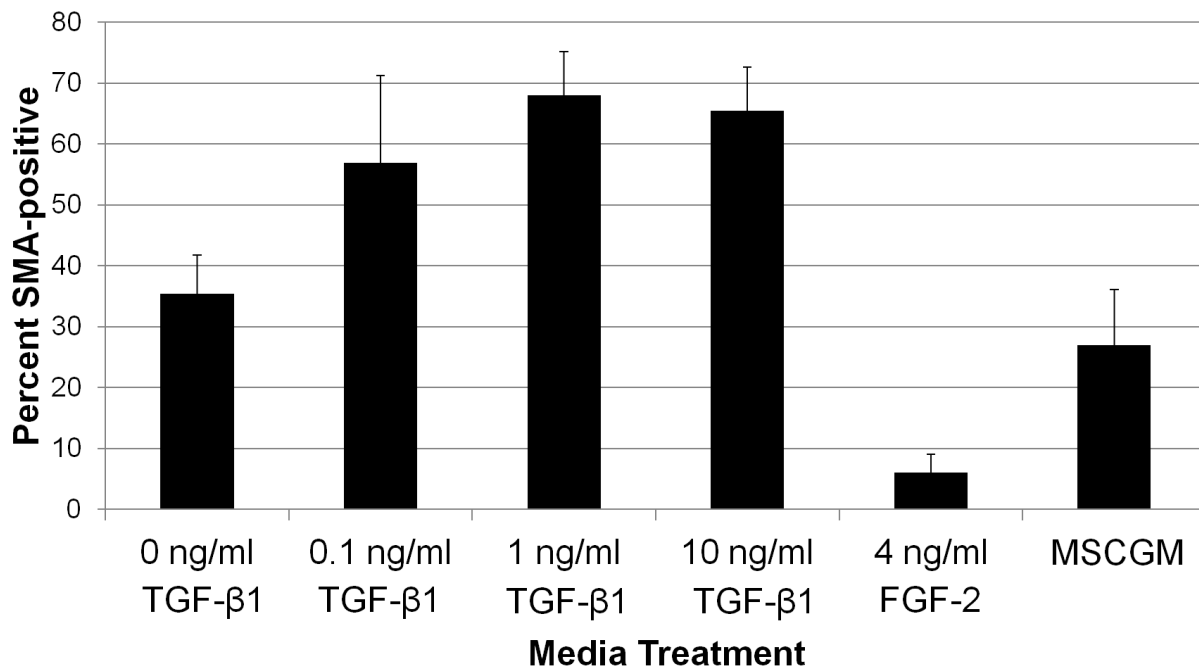
Figure 6.9 – MSCs express SMA in media with TGF-β1. MSCs were seeded on glass coverslips and cultured for 7 days in MSCGM or in base media (1:1 DMEM:Ham's F12, 10% Fetal Clone III, 1% penicillin-streptomycin) supplemented with either TGF-β1 or FGF-2. The percentage of cells expressing smooth muscle alpha actin (SMA) was calculated and compared between conditions. Data expressed as mean ±SD. n=3-7 per group.

To further understand if MSCs could generate cell-derived 3D vascular tissues, we decided to see if they would self-assemble into rings in our system.[89] Rings were seeded as described in Chapter 5 for human SMCs, with 750,000 MSCs seeded per 2 mm ring. Within 2 days of seeding, MSCs aggregated to form rings, although they were not as tightly contracted around the center posts as we have observed with SMCs. The rings were fragile after 2 weeks of culture and although we were able to mount the rings on the tensile testing device, we could not obtain mechanical data. The rings were unable to register readable forces on the current 1N load cell, however, were extremely extensible and stretched over 3 times their original length before failure. Histological analysis did not indicate much expression of collagen, GAGs, or SMA throughout the tissue.

Together, these data suggests that MSCs (or potentially other stem cells) are a possible cell source for vascular engineering. Studying factors which promote stem cell differentiation, however, may be best carried out in a 3D environment, which our tissue ring system provides. Although rings generated from human MSCs were not strong enough for mechanical studies when cultured the way we did (14 days in

MSCGM), we may be able to alter the culture conditions by supplementing the media or by adding mechanical conditioning to increase the ring strength and allow for mechanical analysis.

6.5 Conclusions

In all, we have developed a system in which we utilize cellular self-assembly to generate 3D tissues. We have shown ways in which we may be able to use this system to evaluate contractile SMC phenotype and function, ECM and elastin composition and biomechanics of rings, as well as alternative smooth muscle cell sources. Although we have not identified the culture conditions that lead to a quiescent phenotype switch or elastin synthesis in SMCs, we have developed a tool which can be used to systematically measure the effects of culture parameters on tissue structure and function. We believe that by changing the way we culture these rings by adding supplements to the media or combining mechanical stimulation throughout culture we may better be able to achieve proper cell phenotype and ECM deposition.

6.6 References

1. Niklason LE, Gao J, Abbott WM, Hirschi KK, Houser S, Marini R, Langer R. Functional arteries grown in vitro. Science 1999;284(5413):489-93.
2. Chue WL, Campbell GR, Caplice N, Muhammed A, Berry CL, Thomas AC, Bennett MB, Campbell JH. Dog peritoneal and pleural cavities as bioreactors to grow autologous vascular grafts. J Vasc Surg 2004;39(4):859-67.
3. Konig G, McAllister TN, Dusserre N, Garrido SA, Iyican C, Marini A, Fiorillo A, Avila H, Wystrychowski W, Zagalski K and others. Mechanical properties of completely autologous human tissue engineered blood vessels compared to human saphenous vein and mammary artery. Biomaterials 2009;30(8):1542-50.
4. Zhang L, Zhou J, Lu Q, Wei Y, Hu S. A novel small-diameter vascular graft: in vivo behavior of biodegradable three-layered tubular scaffolds. Biotechnol Bioeng 2008;99(4):1007-15.
5. Izhar U, Schwalb H, Borman JB, Hellener GR, Hotoveli-Salomon A, Marom G, Stern T, Cohn D. Novel synthetic selectively degradable vascular prostheses: a preliminary implantation study. J Surg Res 2001;95(2):152-60.
6. Lee KW, Stolz DB, Wang Y. Substantial expression of mature elastin in arterial constructs. Proc Natl Acad Sci U S A 2011;108(7):2705-10.
7. Peng HF, Liu JY, Andreadis ST, Swartz DD. Hair follicle-derived smooth muscle cells and small intestinal submucosa for engineering mechanically robust and vasoreactive vascular media. Tissue Eng Part A 2011;17(7-8):981-90.
8. Prichard HL, Manson RJ, DiBernardo L, Niklason LE, Lawson JH, Dahl SL. An early study on the mechanisms that allow tissue-engineered vascular grafts to resist intimal hyperplasia. J Cardiovasc Transl Res 2011;4(5):674-82.
9. Schutte SC, Chen Z, Brockbank KG, Nerem RM. Cyclic strain improves strength and function of a collagen-based tissue-engineered vascular media. Tissue Eng Part A 2010;16(10):3149-57.
10. Schutte SC, Chen Z, Brockbank KG, Nerem RM. Tissue engineering of a collagen-based vascular media: Demonstration of functionality. Organogenesis 2010;6(4):204-11.

11. L'Heureux N, Stoclet JC, Auger FA, Lagaud GJ, Germain L, Andriantsitohaina R. A human tissue-engineered vascular media: a new model for pharmacological studies of contractile responses. FASEB J 2001;15(2):515-24.

12. Owens GK. Regulation of differentiation of vascular smooth muscle cells. Physiol Rev 1995;75(3):487-517.

13. Gonzales RJ, Carter RW, Kanagy NL. Laboratory demonstration of vascular smooth muscle function using rat aortic ring segments. Adv Physiol Educ 2000;24(1):13-21.

14. Beamish JA, He P, Kottke-Marchant K, Marchant RE. Molecular regulation of contractile smooth muscle cell phenotype: implications for vascular tissue engineering. Tissue Eng Part B Rev 2010;16(5):467-91.

15. Rzucidlo EM, Martin KA, Powell RJ. Regulation of vascular smooth muscle cell differentiation. J Vasc Surg 2007;45 Suppl A:A25-32.

16. Aikawa M, Sivam PN, Kuro-o M, Kimura K, Nakahara K, Takewaki S, Ueda M, Yamaguchi H, Yazaki Y, Periasamy M. Human smooth muscle myosin heavy chain isoforms as molecular markers for vascular development and atherosclerosis. Circ Res 1993;73(6):1000-12.

17. Sobue K, Hayashi K, Nishida W. Expressional regulation of smooth muscle cell-specific genes in association with phenotypic modulation. Mol Cell Biochem 1999;190(1-2):105-18.

18. Merrilees MJ, Campbell JH, Spanidis E, Campbell GR. Glycosaminoglycan synthesis by smooth muscle cells of differing phenotype and their response to endothelial cell conditioned medium. Atherosclerosis 1990;81(3):245-54.

19. Acampora KB, Nagatomi J, Langan EM, LaBerge M. Increased synthetic phenotype behavior of smooth muscle cells in response to in vitro balloon angioplasty injury model. Ann Vasc Surg 2010;24(1):116-26.

20. Orr AW, Hastings NE, Blackman BR, Wamhoff BR. Complex regulation and function of the inflammatory smooth muscle cell phenotype in atherosclerosis. J Vasc Res 2010;47(2):168-80.

21. Farb A, Kolodgie FD, Hwang JY, Burke AP, Tefera K, Weber DK, Wight TN, Virmani R. Extracellular matrix changes in stented human coronary arteries. Circulation 2004;110(8):940-7.

22. Kawai-Kowase K, Owens GK. Multiple repressor pathways contribute to phenotypic switching of vascular smooth muscle cells. Am J Physiol Cell Physiol 2007;292(1):C59-69.

23. Hayashi K, Saga H, Chimori Y, Kimura K, Yamanaka Y, Sobue K. Differentiated phenotype of smooth muscle cells depends on signaling pathways through insulin-like growth factors and phosphatidylinositol 3-kinase. J Biol Chem 1998;273(44):28860-7.

24. Daum G, Hedin U, Wang Y, Wang T, Clowes AW. Diverse effects of heparin on mitogen-activated protein kinase-dependent signal transduction in vascular smooth muscle cells. Circ Res 1997;81(1):17-23.

25. Hedin U, Daum G, Clowes AW. Heparin inhibits thrombin-induced mitogen-activated protein kinase signaling in arterial smooth muscle cells. J Vasc Surg 1998;27(3):512-20.

26. Watanabe T, Pakala R, Katagiri T, Benedict CR. Serotonin potentiates angiotensin II--induced vascular smooth muscle cell proliferation. Atherosclerosis 2001;159(2):269-79.

27. Björkerud S. Effects of transforming growth factor-beta 1 on human arterial smooth muscle cells in vitro. Arterioscler Thromb 1991;11(4):892-902.

28. Hayashi K, Shibata K, Morita T, Iwasaki K, Watanabe M, Sobue K. Insulin receptor substrate-1/SHP-2 interaction, a phenotype-dependent switching machinery of insulin-like growth factor-I signaling in vascular smooth muscle cells. J Biol Chem 2004;279(39):40807-18.

29. Millette E, Rauch BH, Defawe O, Kenagy RD, Daum G, Clowes AW. Platelet-derived growth factor-BB-induced human smooth muscle cell proliferation depends on basic FGF release and FGFR-1 activation. Circ Res 2005;96(2):172-9.

30. Yoshida T, Hoofnagle MH, Owens GK. Myocardin and Prx1 contribute to angiotensin II-induced expression of smooth muscle alpha-actin. Circ Res 2004;94(8):1075-82.

31. Deaton RA, Su C, Valencia TG, Grant SR. Transforming growth factor-beta1-induced expression of smooth muscle marker genes involves activation of PKN and p38 MAPK. J Biol Chem 2005;280(35):31172-81.

32. Bingley JA, Hayward IP, Campbell JH, Campbell GR. Arterial heparan sulfate proteoglycans inhibit vascular smooth muscle cell proliferation and phenotype change in vitro and neointimal formation in vivo. J Vasc Surg 1998;28(2):308-18.

33. Stegemann JP, Nerem RM. Phenotype modulation in vascular tissue engineering using biochemical and mechanical stimulation. Ann Biomed Eng 2003;31(4):391-402.

34. Mann BK, Schmedlen RH, West JL. Tethered-TGF-beta increases extracellular matrix production of vascular smooth muscle cells. Biomaterials 2001;22(5):439-44.

35. O'Callaghan CJ, Williams B. Mechanical strain-induced extracellular matrix production by human vascular smooth muscle cells: role of TGF-beta(1). Hypertension 2000;36(3):319-24.
36. Bulick AS, Muñoz-Pinto DJ, Qu X, Mani M, Cristancho D, Urban M, Hahn MS. Impact of endothelial cells and mechanical conditioning on smooth muscle cell extracellular matrix production and differentiation. Tissue Eng Part A 2009;15(4):815-25.
37. Hahn MS, McHale MK, Wang E, Schmedlen RH, West JL. Physiologic pulsatile flow bioreactor conditioning of poly(ethylene glycol)-based tissue engineered vascular grafts. Ann Biomed Eng 2007;35(2):190-200.
38. Isenberg BC, Tranquillo RT. Long-term cyclic distention enhances the mechanical properties of collagen-based media-equivalents. Ann Biomed Eng 2003;31(8):937-49.
39. Gong Z, Niklason LE. Small-diameter human vessel wall engineered from bone marrow-derived mesenchymal stem cells (hMSCs). FASEB J 2008;22(6):1635-48.
40. Zaucha MT, Raykin J, Wan W, Gauvin R, Auger FA, Germain L, Michaels TE, Gleason RL. A novel cylindrical biaxial computer-controlled bioreactor and biomechanical testing device for vascular tissue engineering. Tissue Eng Part A 2009;15(11):3331-40.
41. Hedin U, Bottger BA, Forsberg E, Johansson S, Thyberg J. Diverse effects of fibronectin and laminin on phenotypic properties of cultured arterial smooth muscle cells. J Cell Biol 1988;107(1):307-19.
42. Moiseeva EP. Adhesion receptors of vascular smooth muscle cells and their functions. Cardiovasc Res 2001;52(3):372-86.
43. Olson NE, Chao S, Lindner V, Reidy MA. Intimal smooth muscle cell proliferation after balloon catheter injury. The role of basic fibroblast growth factor. Am J Pathol 1992;140(5):1017-23.
44. Klagsbrun M, Edelman ER. Biological and biochemical properties of fibroblast growth factors. Implications for the pathogenesis of atherosclerosis. Arteriosclerosis 1989;9(3):269-78.
45. Kinsella MG, Irvin C, Reidy MA, Wight TN. Removal of heparan sulfate by heparinase treatment inhibits FGF-2-dependent smooth muscle cell proliferation in injured rat carotid arteries. Atherosclerosis 2004;175(1):51-7.
46. L'Heureux N, Pâquet S, Labbé R, Germain L, Auger FA. A completely biological tissue-engineered human blood vessel. FASEB J 1998;12(1):47-56.
47. Opitz F, Schenke-Layland K, Cohnert TU, Starcher B, Halbhuber KJ, Martin DP, Stock UA. Tissue engineering of aortic tissue: dire consequence of suboptimal elastic fiber synthesis in vivo. Cardiovasc Res 2004;63(4):719-30.
48. Dahl SL, Rhim C, Song YC, Niklason LE. Mechanical properties and compositions of tissue engineered and native arteries. Ann Biomed Eng 2007;35(3):348-55.
49. Rosenbloom J, Abrams WR, Mecham R. Extracellular matrix 4: the elastic fiber. Faseb J 1993;7(13):1208-18.
50. Burton AC. Relation of structure to function of the tissues of the wall of blood vessels. Physiol Rev 1954;34(4):619-42.
51. Vrhovski B, Weiss AS. Biochemistry of tropoelastin. Eur J Biochem 1998;258(1):1-18.
52. Li DY, Brooke B, Davis EC, Mecham RP, Sorensen LK, Boak BB, Eichwald E, Keating MT. Elastin is an essential determinant of arterial morphogenesis. Nature 1998;393(6682):276-80.
53. Yanagisawa H, Davis EC. Unraveling the mechanism of elastic fiber assembly: The roles of short fibulins. Int J Biochem Cell Biol 2010;42(7):1084-93.
54. Shapiro SD, Endicott SK, Province MA, Pierce JA, Campbell EJ. Marked longevity of human lung parenchymal elastic fibers deduced from prevalence of D-aspartate and nuclear weapons-related radiocarbon. J Clin Invest 1991;87(5):1828-34.
55. Cinat ME, Hopkins J, Wilson SE. A prospective evaluation of PTFE graft patency and surveillance techniques in hemodialysis access. Ann Vasc Surg 1999;13(2):191-8.
56. Cho SW, Lim SH, Kim IK, Hong YS, Kim SS, Yoo KJ, Park HY, Jang Y, Chang BC, Choi CY and others. Small-diameter blood vessels engineered with bone marrow-derived cells. Ann Surg 2005;241(3):506-15.
57. Zavan B, Vindigni V, Lepidi S, Iacopetti I, Avruscio G, Abatangelo G, Cortivo R. Neoarteries grown in vivo using a tissue-engineered hyaluronan-based scaffold. FASEB J 2008;22(8):2853-61.
58. Long JL, Tranquillo RT. Elastic fiber production in cardiovascular tissue-equivalents. Matrix Biol 2003;22(4):339-50.
59. Lemire JM, Covin CW, White S, Giachelli CM, Schwartz SM. Characterization of cloned aortic smooth muscle cells from young rats. Am J Pathol 1994;144(5):1068-81.

60.	He W, Nieponice A, Soletti L, Hong Y, Gharaibeh B, Crisan M, Usas A, Peault B, Huard J, Wagner WR and others. Pericyte-based human tissue engineered vascular grafts. Biomaterials 2010;31(32):8235-44.

61.	Keire PA, L'Heureux N, Vernon RB, Merrilees MJ, Starcher B, Okon E, Dusserre N, McAllister TN, Wight TN. Expression of versican isoform V3 in the absence of ascorbate improves elastogenesis in engineered vascular constructs. Tissue Eng Part A 2010;16(2):501-12.

62.	Czirok A, Zach J, Kozel BA, Mecham RP, Davis EC, Rongish BJ. Elastic fiber macro-assembly is a hierarchical, cell motion-mediated process. J Cell Physiol 2006;207(1):97-106.

63.	Kozel BA, Rongish BJ, Czirok A, Zach J, Little CD, Davis EC, Knutsen RH, Wagenseil JE, Levy MA, Mecham RP. Elastic fiber formation: a dynamic view of extracellular matrix assembly using timer reporters. J Cell Physiol 2006;207(1):87-96.

64.	Ahlfors JE, Billiar KL. Biomechanical and biochemical characteristics of a human fibroblast-produced and remodeled matrix. Biomaterials 2007;28(13):2183-91.

65.	Throm AM, Liu WC, Lock CH, Billiar KL. Development of a cell-derived matrix: effects of epidermal growth factor in chemically defined culture. J Biomed Mater Res A 2010;92(2):533-41.

66.	Ishikawa O, Kondo A, Okada K, Miyachi Y, Furumura M. Morphological and biochemical analyses on fibroblasts and self-produced collagens in a novel three-dimensional culture. Br J Dermatol 1997;136(1):6-11.

67.	Poh M, Boyer M, Solan A, Dahl SL, Pedrotty D, Banik SS, McKee JA, Klinger RY, Counter CM, Niklason LE. Blood vessels engineered from human cells. Lancet 2005;365(9477):2122-4.

68.	Petersen TH, Hitchcock T, Muto A, Calle EA, Zhao L, Gong Z, Gui L, Dardik A, Bowles DE, Counter CM and others. Utility of telomerase-pot1 fusion protein in vascular tissue engineering. Cell Transplant 2010;19(1):79-87.

69.	L'Heureux N, Dusserre N, Konig G, Victor B, Keire P, Wight TN, Chronos NA, Kyles AE, Gregory CR, Hoyt G and others. Human tissue-engineered blood vessels for adult arterial revascularization. Nat Med 2006;12(3):361-5.

70.	McAllister TN, Maruszewski M, Garrido SA, Wystrychowski W, Dusserre N, Marini A, Zagalski K, Fiorillo A, Avila H, Manglano X and others. Effectiveness of haemodialysis access with an autologous tissue-engineered vascular graft: a multicentre cohort study. Lancet 2009;373(9673):1440-6.

71.	Hewett PW. Vascular endothelial cells from human micro- and macrovessels: isolation, characterisation and culture. Methods Mol Biol 2009;467:95-111.

72.	Hashi CK, Zhu Y, Yang GY, Young WL, Hsiao BS, Wang K, Chu B, Li S. Antithrombogenic property of bone marrow mesenchymal stem cells in nanofibrous vascular grafts. Proc Natl Acad Sci U S A 2007;104(29):11915-20.

73.	Cho SW, Kim IK, Lim SH, Kim DI, Kang SW, Kim SH, Kim YH, Lee EY, Choi CY, Kim BS. Smooth muscle-like tissues engineered with bone marrow stromal cells. Biomaterials 2004;25(15):2979-86.

74.	Gong Z, Niklason LE. Use of human mesenchymal stem cells as alternative source of smooth muscle cells in vessel engineering. Methods Mol Biol 2011;698:279-94.

75.	Ross JJ, Hong Z, Willenbring B, Zeng L, Isenberg B, Lee EH, Reyes M, Keirstead SA, Weir EK, Tranquillo RT and others. Cytokine-induced differentiation of multipotent adult progenitor cells into functional smooth muscle cells. J Clin Invest 2006;116(12):3139-49.

76.	Liu JY, Swartz DD, Peng HF, Gugino SF, Russell JA, Andreadis ST. Functional tissue-engineered blood vessels from bone marrow progenitor cells. Cardiovasc Res 2007;75(3):618-28.

77.	O'Cearbhaill ED, Murphy M, Barry F, McHugh PE, Barron V. Behavior of human mesenchymal stem cells in fibrin-based vascular tissue engineering constructs. Ann Biomed Eng 2010;38(3):649-57.

78.	Hibino N, Shin'oka T, Matsumura G, Ikada Y, Kurosawa H. The tissue-engineered vascular graft using bone marrow without culture. J Thorac Cardiovasc Surg 2005;129(5):1064-70.

79.	Wang C, Cen L, Yin S, Liu Q, Liu W, Cao Y, Cui L. A small diameter elastic blood vessel wall prepared under pulsatile conditions from polyglycolic acid mesh and smooth muscle cells differentiated from adipose-derived stem cells. Biomaterials 2010;31(4):621-30.

80.	Wang C, Yin S, Cen L, Liu Q, Liu W, Cao Y, Cui L. Differentiation of adipose-derived stem cells into contractile smooth muscle cells induced by transforming growth factor-beta1 and bone morphogenetic protein-4. Tissue Eng Part A 2010;16(4):1201-13.

81.	Soletti L, Hong Y, Guan J, Stankus JJ, El-Kurdi MS, Wagner WR, Vorp DA. A bilayered elastomeric scaffold for tissue engineering of small diameter vascular grafts. Acta Biomater 2010;6(1):110-22.

82.   Nieponice A, Soletti L, Guan J, Deasy BM, Huard J, Wagner WR, Vorp DA. Development of a tissue-engineered vascular graft combining a biodegradable scaffold, muscle-derived stem cells and a rotational vacuum seeding technique. Biomaterials 2008;29(7):825-33.

83.   Liu JY, Peng HF, Andreadis ST. Contractile smooth muscle cells derived from hair-follicle stem cells. Cardiovasc Res 2008;79(1):24-33.

84.   Liu JY, Peng HF, Gopinath S, Tian J, Andreadis ST. Derivation of functional smooth muscle cells from multipotent human hair follicle mesenchymal stem cells. Tissue Eng Part A 2010;16(8):2553-64.

85.   Matsumura G, Hibino N, Ikada Y, Kurosawa H, Shin'oka T. Successful application of tissue engineered vascular autografts: clinical experience. Biomaterials 2003;24(13):2303-8.

86.   Ishiguro S, Akasaka Y, Kiguchi H, Suzuki T, Imaizumi R, Ishikawa Y, Ito K, Ishii T. Basic fibroblast growth factor induces down-regulation of alpha-smooth muscle actin and reduction of myofibroblast areas in open skin wounds. Wound Repair Regen 2009;17(4):617-25.

87.   Simper D, Stalboerger PG, Panetta CJ, Wang S, Caplice NM. Smooth muscle progenitor cells in human blood. Circulation 2002;106(10):1199-204.

88.   Le Ricousse-Roussanne S, Barateau V, Contreres JO, Boval B, Kraus-Berthier L, Tobelem G. Ex vivo differentiated endothelial and smooth muscle cells from human cord blood progenitors home to the angiogenic tumor vasculature. Cardiovasc Res 2004;62(1):176-84.

89.   Gwyther TA, Hu JZ, Billiar KL, Rolle MW. Directed cellular self-assembly to fabricate cell-derived tissue rings for biomechanical analysis and tissue engineering. J Vis Exp 2011(57), doi: 10.3791/3366.

Chapter 7: Conclusions and Future Work

7.1 Overview

The work in this thesis describes the development of a new system to generate self-assembled vascular tissue that more closely recapitulates the native vascular environment. Analogous to current trends in vascular engineering, our system generates 3D tissues entirely from cells and the ECM they produce.[1-8] However, in addition to tissue structure, we can also use our tissues to evaluate biomechanics, and contractile function. Similar to native vessels, our tissue rings are composed of vascular smooth muscle cells, have high cell densities, and have comparable size and geometries. We believe that this is a simple, straight-forward method of generating cell-derived tissue constructs that any lab could adopt without purchasing specialized equipment. The method yields robust 3D constructs in as short of a time as one week and can be used to examine the structure and function of vascular tissue (overview in Figure 7.1).
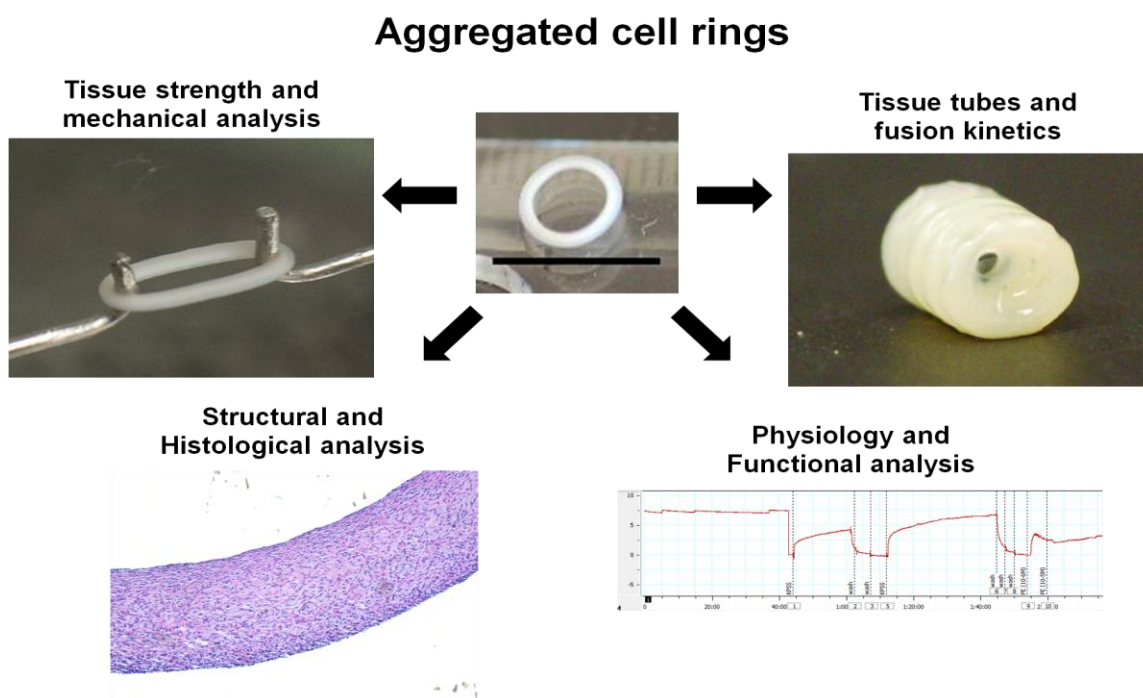

Figure 7.1 – Overview of the self-assembled cell ring system. Rings are conducive for analysis of biomechanics, structure, physiological function, and for tissue tube formation.

7.2 Advantages to the ring-based system

The cell self-assembly process illustrated here allowed for tissue generation using a straight-forward method. One drawback to generating scaffold-free tissue has been the amount of handling required to form the tissue shapes of interest.[7,9,10] However, the process described in this thesis allowed us to generate tissue in ring shapes with minimal manipulation. In order to achieve this, we developed a three step process of generating agarose cell-seeding molds.[11,12] While it takes a few steps and some time to generate the cell-seeding molds, the round-bottomed annular wells force the cells to aggregate due to gravity upon seeding.[1,3] Therefore, we can generate self-assembled rings without the need for manipulating the tissues throughout culture.

Another limitation of other scaffold-free approaches to tissue engineering is the long culture times (>3 months) required to generate handleable tissue constructs.[13-15] The method described in this thesis yields handleable tissue constructs in as little as one week of culture. While we only performed mechanical analysis on the tissues after one week in culture, we were able to remove rings from their agarose wells after only 1 day, suggesting that the aggregated tissue was robust enough for manipulation at that time. Future studies may need to culture the tissue rings for longer periods of time in an effort to increase the ECM synthesis and incorporation, leading to stronger and more compliant tissues. However, this method decreases the length of time required for the generation of handleable vascular grafts from months to weeks.

Mechanical analysis revealed that the tissue ring strength and stiffness exceeded those of similarly cultured tissue constructs generated from other commonly utilized tissue engineering techniques such as cells in collagen or fibrin gels.[16,17] This suggests that we may be better able to reach desired tissue strength faster in a cell-derived system compared to other "cell-in-gels" approaches. Interestingly, the strength of the tissue rings decreased as the rings were cultured for 2 weeks compared to 1 week. We did not observe a change in overall failure force, however due to the increase in ring thickness from 8 days to 14 days, the failure stress of the tissue decreased. This increase in thickness (outside of diffusion limitations) led to necrosis in the center of the rings by 2 weeks in culture. Another possible reason for the decrease in strength is due to the ECM composition of the rings. Glycosaminoglycans were abundant in rat SMC rings at all time points, and this matrix component does not contribute to the mechanical strength of the tissues. While there did appear to be an increase in collagen content with 2 weeks in culture, this may have been counteracted by the necrosis in the centers of the thick tissues. Future work should focus on increasing tissue strength as well as decreasing cell-seeding number and tissue thickness to alleviate the necrosis in the center of the tissue.

One approach to achieving the increase in strength and decrease in thickness could be to add a dynamic cyclic conditioning regimen to the culture of the tissue rings. Dynamic cyclic loading has been shown to help decrease wall thickness, increase fractional cell content, contractile cell phenotype, cell alignment, and burst pressure in engineered vascular grafts.[18-21] Further, under loading conditions, cells can synthesize greater amounts of collagen more rapidly than when cultured statically. While some ECM molecules may take longer than one week to fully form, combining mechanical stimulation with growth factor supplementation may be able to increase the rate at which these molecules are deposited. Because our tissue rings are conducive to both growth factor supplementation and to mechanical stimulation, with the addition of cyclic mechanical loading, we may be able to force the cells to synthesize ECM faster leading to shorter production times for strong vascular tissue. Cell aggregated tissue rings are well suited for conditioning in a cyclic distension bioreactor. Many bioreactor designs include the distension of a silicone tube inside the vascular graft, leading to cyclic strains being applied on the tissue.[18,20,22] The tissue rings are conducive to mounting on silicone tubing (as early as one day in culture) as demonstrated throughout tube fusion. Therefore, cyclic loading could be considered as part of the culture regimen, to decrease thickness and increase collagen synthesis and burst strength so our vascular tissue more closely relates to that of native arteries.

Another means of increasing burst strength could be through the use of media supplements. All of the ring studies described in this thesis were cultured in standard growth media (DMEM with 10% FBS) and no media supplementation was used to increase mechanical strength. Work characterized by our lab suggests supplementation of our growth media with 50 μg/ml ascorbic acid appears to increase the ultimate tensile strength from 242 kPa to 402 kPa after 7 days in culture.[23] This culture regimen also increased collagen content.[23,24] Through increasing culture times and supplementing media with ascorbic acid, several groups developing tissue engineered blood vessels have shown that they can attain burst pressure strengths equal to saphenous vein.[19,25,26] Uniquely, this ring system allows for the screening of factors which promote ECM synthesis and lead to changes in mechanical properties. The rings can be cultured under various conditions and the structure and mechanics can be evaluated.

In addition to ECM within the tissues, it is important to also have circumferential alignment of the cells and contractility. Surprisingly, we did not observe alignment in any of our tissue rings. This result was surprising given that the cells self-assemble and contract to form tissue around the center post. In other cases of tissue remodeling around a central mandrel (such as cells in fibrin gels) the cells orient themselves circumferentially leading to an overall cellular alignment.[27,28] One reason that we did not

observe alignment could in part be due to the low stiffness of the agarose or the silicone tube, however further investigation would be required to determine if this is the only cause.

7.3 Benefits of tissue fusion

The second part of the thesis was focused on transforming the self-assembled rings into tissue tubes. We found that by culturing the rings in contact on silicone tube mandrels they fuse together to form tubes. Therefore, the rings can act as viable building blocks which can be used to generate larger tissues for further mechanical and functional analysis.[11,29] The concept of cell-derived building blocks has been established in the field of bioprinting,[7-9] where spheroid-shaped subunits were aggregated to fuse into larger tissues.[30] However, mechanical and functional testing cannot be performed on spherical sub-units. With the ring system, we can test tissue mechanical function on the individual sub-units without needing to fuse them into a larger structure first. This allows us to monitor how ring culture parameters affect tissue composition and function without the need to generate full sized tissue tubes, saving us time, materials, and reagents. But, ultimately, when parameters are established so that the desired mechanical properties are achieved, the rings can be fused into tubes, leading to the generation of strong vascular tissue tubes and ultimately vascular grafts.

Despite the clinical promise and increasing interest in cell-derived, scaffold-free tissue engineered vascular grafts; most existing approaches require long culture periods[13,14] or specialized equipment.[7,30] Generating tubes from ring-shaped building blocks, as described in this thesis, required little time and no expensive equipment. Currently, the method of stacking rings to fuse into tubes involves some manual manipulation of the tissue. However, modifications to the mandrel design (as described in Chapter 4) increased our efficiency and ease of transferring the rings from agarose onto the mandrels. Future work on this system may involve automation of ring stacking and tube generation to make this method more high throughput.

In this thesis we also described testing methods to assess the strength of fused tissue tubes. We demonstrated that tubes can be mounted onto a burst pressure testing device, filled with liquid and pressurized until failure. While the overall strength (n=1) of the tissue was far below what is required for implantation, dynamic conditioning or media supplementation may be added to the culture regimen to enhance their mechanical properties.[19,21,27,31-33]

We can compare the stresses we calculate through uniaxial tensile testing of ring-shaped structures to the burst pressure of tube-shaped tissues. To do this we must know the ring radius (r) as well as the wall

thickness (t, measured using the DVT). We also must follow the assumptions that the stresses in the tube wall are uniform, the external pressure is zero, and that the tube is thin-walled (wall thickness is approximately 1/10 that of the tube radius). With these assumptions, the ultimate tensile strength measured from uniaxial testing approximates the hoop stress (σ_h, circumferential stress) in the tube. Therefore, burst pressure (P) could be estimated using the following equation:

(Equation 1- hoop stress) $\qquad\qquad\qquad \sigma_h = Pr/t$

Because we conserved ring thickness by altering the initial cell seeding density based on the diameter of the ring (2, 4, or 6 mm), the thin-walled assumption did not hold true for all rings. Thick-walled tubes do not have equal stresses across the wall of the tube and therefore do not fit this equation. This could be one reason why the ultimate tensile strength decreased with smaller radius rings cultured for similar lengths.

Another difference to consider is whether the tissue tubes are weakest at the ring junction points. In this work we did not directly measure the strength of the ring junctions. However, the burst pressure results showed the failure mode as a longitudinal tear, suggesting the tubes were weaker in the longitudinal direction than circumferentially along the ring junctions. Mathematically one would expect the tubes to split longitudinally as the hoop stress is twice as much as the longitudinal stress (σ_l) in a cylinder.

(Equation 2 – longitudinal stress) $\qquad\quad \sigma_l = Pr/2t$
(Equation 3 – comparison of stresses) $\qquad \sigma_h = 2\sigma_l$

Another benefit to this modular ring fusion technique is our ability to maintain spatial retention of cell location within the tubes. We showed that the rings can fuse together, but the cells from each ring remain in their original location. Using genetic manipulation techniques or multiple cell types, we may now also be able to generate tubes with sections that differ in cellular origin, matrix composition, or mechanical properties from adjacent sections of the same tube. We may be able to exploit this for use in generating vascular disease models such as aneurysm where ECM and elastin in a specific region in the vessel degrades, leading to a decrease in local mechanical properties, and results in ballooning of the vessel.[34] If we can develop diseased tissues *in vitro*, we can then begin to study therapies which may help treat vascular diseases.

In addition to controlling cell location within our tissue tubes, we demonstrated that we can generate complex branched structures which may be used to model sections of the vasculature that are prone to

disease such as areas where atherosclerosis occurs and plaque builds-up.[35-37]   By placing the tissue rings on "Y"-shaped silicone mandrel, they fused together in a branched type structure. This may also offer a unique way to study the tissue remodeling at the site of anastomosis, another common location for graft failure.[38,39]   These regions are less studied due to the difficulty in building grafts with intricate structures even though they are some of the vascular region most prone to vessel diseases. The stacked ring method could supply the vascular biology field a much needed tool to begin to model flow patterns, vascular wall remodeling, and disease progression throughout branched regions.

7.4 Contribution to Science

The model system described in this thesis offers a method of rapidly generating ring-shaped or tube shaped tissue constructs that have many potential applications in the field of vascular tissue engineering and regenerative medicine. This platform technology can be used for more than just developing vascular grafts for *in vivo* use. Future studies can use this platform technology to screen the effects of soluble media components on ECM composition, mechanical properties, cell phenotype, and physiological contraction. Ultimately, we would like to be able to identify conditions that will enable us to "tune" the mechanical properties of cell-derived tissue for the generation of vascular grafts that are strong, stiff, and compliant, while maintaining ECM deposition rich in collagen and elastin and quiescent SMC phenotype.

Evaluation of the effect of soluble factors on the fusion of cell-aggregated tissues may lead us into a better understanding of optimal culturing techniques for vascular graft generation. Tissue tubes lend themselves nicely to culture with a combination of soluble factors and mechanical factors (such as cyclic distension, fluid flow, or both). We hope the combination of these culturing techniques may provide us with an environment to maintain tissues in culture for long periods of time so that we may study extracellular matrix synthesis and tissue remodeling in response to changes in environmental factors. Further, we could study the effect of changes in flow patterns at vascular branches and their contributions to vascular remodeling and disease progression.

This ring-based platform technology can also be used to help further our understanding of vascular diseases as well as facilitate pre-clinical screenings of vascular tissue response to pharmacological therapies. Most drug screening to date is developed through the use of animal studies where the findings do not necessarily correlate with drug effects on humans. A recent shift in the field has put more emphasis on developing in vitro screening tools to evaluate the effects of pharmacological agents prior to

pre-clinical animal studies.[40-46]   Although some progress has been made on this front, most screening tools lack the ability to quantitatively measure changes in mechanical or functional properties of the tissues.   The model tissue rings described in this thesis are ideally suited to the screening of pharmacological agents on tissue function (contraction or mechanics) and overall composition (ECM or cell phenotype). This could provide an additional experimental level that would decrease the quantity of animal studies.

Throughout this thesis we focused on the application of this system for *vascular* tissue engineering, however, this system could also be used to generate, screen growth conditions, and tune mechanical properties in a multitude of tissues types (such as cartilage, ligament, tendon, skeletal muscle, intestine, trachea, etc.).   In addition to mechanical testing, these rings are also conducive to other types of functional analysis such as myography to test contractile potential in tissues, which would be an important end point in any of the above mentioned contractile tissues.

In summary, we have developed a versatile approach to generating scaffold-free tissue that has applications in tissue engineering, regenerative biology, and biomechanics research. This model system can be utilized for not only tissue engineering applications, but also hypothesis-driven research aimed at discovering new mechanisms and soluble factors involved in controlling ECM synthesis, cell differentiation, and cell phenotype, and their effects on tissue remodeling and mechanical function.

7.5 References

1. Dean DM, Napolitano AP, Youssef J, Morgan JR. Rods, tori, and honeycombs: the directed self-assembly of microtissues with prescribed microscale geometries. FASEB J 2007;21(14):4005-12.
2. Livoti CM, Morgan JR. Self-assembly and tissue fusion of toroid-shaped minimal building units. Tissue Eng Part A 2010;16(6):2051-61.
3. Napolitano AP, Chai P, Dean DM, Morgan JR. Dynamics of the self-assembly of complex cellular aggregates on micromolded nonadhesive hydrogels. Tissue Eng 2007;13(8):2087-94.
4. Gentile C, Fleming PA, Mironov V, Argraves KM, Argraves WS, Drake CJ. VEGF-mediated fusion in the generation of uniluminal vascular spheroids. Dev Dyn 2008;237(10):2918-25.
5. Jakab K, Neagu A, Mironov V, Forgacs G. Organ printing: fiction or science. Biorheology 2004;41(3-4):371-5.
6. Jakab K, Norotte C, Damon B, Marga F, Neagu A, Besch-Williford CL, Kachurin A, Church KH, Park H, Mironov V and others. Tissue engineering by self-assembly of cells printed into topologically defined structures. Tissue Eng Part A 2008;14(3):413-21.
7. Norotte C, Marga FS, Niklason LE, Forgacs G. Scaffold-free vascular tissue engineering using bioprinting. Biomaterials 2009;30(30):5910-7.
8. Kelm JM, Lorber V, Snedeker JG, Schmidt D, Broggini-Tenzer A, Weisstanner M, Odermatt B, Mol A, Zünd G, Hoerstrup SP. A novel concept for scaffold-free vessel tissue engineering: self-assembly of microtissue building blocks. J Biotechnol 2010;148(1):46-55.

9.   Mironov V, Visconti RP, Kasyanov V, Forgacs G, Drake CJ, Markwald RR. Organ printing: tissue spheroids as building blocks. Biomaterials 2009;30(12):2164-74.

10.   L'Heureux N, Dusserre N, Konig G, Victor B, Keire P, Wight TN, Chronos NA, Kyles AE, Gregory CR, Hoyt G and others. Human tissue-engineered blood vessels for adult arterial revascularization. Nat Med 2006;12(3):361-5.

11.   Gwyther TA, Hu JZ, Christakis AG, Skorinko JK, Shaw SM, Billiar KL, Rolle MW. Engineered vascular tissue fabricated from aggregated smooth muscle cells. Cells Tissues Organs 2011;194(1):13-24.

12.   Youssef J, Bao B, Ferruccio T-M, Morgan J. Micromolded Nonadhesive Hydrogels for the Self-Assembly of Scaffold-Free 3D Cellular Microtissues. In: Berthiaume F, Morgan J, editors. Methods in Bioengineering: 3D Tissue Engineering. Norwood, MA: Artech House; 2010. p 151-166.

13.   L'Heureux N, Pâquet S, Labbé R, Germain L, Auger FA. A completely biological tissue-engineered human blood vessel. FASEB J 1998;12(1):47-56.

14.   L'Heureux N, McAllister TN, de la Fuente LM. Tissue-engineered blood vessel for adult arterial revascularization. N Engl J Med 2007;357(14):1451-3.

15.   Ahlfors JE, Billiar KL. Biomechanical and biochemical characteristics of a human fibroblast-produced and remodeled matrix. Biomaterials 2007;28(13):2183-91.

16.   Seliktar D, Black RA, Vito RP, Nerem RM. Dynamic mechanical conditioning of collagen-gel blood vessel constructs induces remodeling in vitro. Ann Biomed Eng 2000;28(4):351-62.

17.   Rowe SL, Stegemann JP. Interpenetrating collagen-fibrin composite matrices with varying protein contents and ratios. Biomacromolecules 2006;7(11):2942-8.

18.   Schutte SC, Chen Z, Brockbank KG, Nerem RM. Cyclic strain improves strength and function of a collagen-based tissue-engineered vascular media. Tissue Eng Part A 2010;16(10):3149-57.

19.   Niklason LE, Gao J, Abbott WM, Hirschi KK, Houser S, Marini R, Langer R. Functional arteries grown in vitro. Science 1999;284(5413):489-93.

20.   Isenberg BC, Tranquillo RT. Long-term cyclic distention enhances the mechanical properties of collagen-based media-equivalents. Ann Biomed Eng 2003;31(8):937-49.

21.   Syedain ZH, Weinberg JS, Tranquillo RT. Cyclic distension of fibrin-based tissue constructs: evidence of adaptation during growth of engineered connective tissue. Proc Natl Acad Sci U S A 2008;105(18):6537-42.

22.   Solan A, Dahl SL, Niklason LE. Effects of mechanical stretch on collagen and cross-linking in engineered blood vessels. Cell Transplant 2009;18(8):915-21.

23.   Hu J. Assmessent of Ascorbic Acid Effects on the Properties of Cell-Derived Tissue Rings. Worcester, MA: Worcester Polytechnic Institute (M.S. thesis); 2010.

24.   Adebayo O, Gwyther T, Hu J, Billiar K, Rolle M. Vascular smooth muscle cell derived tissue rings exhibit greater tensile strength than smooth muscle cells in fibrin or collagen gels. in submission.

25.   Dahl SL, Rhim C, Song YC, Niklason LE. Mechanical properties and compositions of tissue engineered and native arteries. Ann Biomed Eng 2007;35(3):348-55.

26.   Konig G, McAllister TN, Dusserre N, Garrido SA, Iyican C, Marini A, Fiorillo A, Avila H, Wystrychowski W, Zagalski K and others. Mechanical properties of completely autologous human tissue engineered blood vessels compared to human saphenous vein and mammary artery. Biomaterials 2009;30(8):1542-50.

27.   Syedain ZH, Meier LA, Bjork JW, Lee A, Tranquillo RT. Implantable arterial grafts from human fibroblasts and fibrin using a multi-graft pulsed flow-stretch bioreactor with noninvasive strength monitoring. Biomaterials 2011;32(3):714-22.

28.   Liu JY, Swartz DD, Peng HF, Gugino SF, Russell JA, Andreadis ST. Functional tissue-engineered blood vessels from bone marrow progenitor cells. Cardiovasc Res 2007;75(3):618-28.

29.   Gwyther TA, Hu JZ, Billiar KL, Rolle MW. Directed cellular self-assembly to fabricate cell-derived tissue rings for biomechanical analysis and tissue engineering. J Vis Exp 2011(57), doi: 10.3791/3366.

30.   Khatiwala C, Shepherd B, Romero M, Sorfman S, Marga F, Murphy K, Csete M. Fully Biological Multi-layered Vascular Grafts Generated with the NovoGen MMX Bioprinter. 2010 December 5-8; Orlando, FL.

31.   Zaucha MT, Raykin J, Wan W, Gauvin R, Auger FA, Germain L, Michaels TE, Gleason RL. A novel cylindrical biaxial computer-controlled bioreactor and biomechanical testing device for vascular tissue engineering. Tissue Eng Part A 2009;15(11):3331-40.

32.   Bjork JW, Tranquillo RT. Transmural flow bioreactor for vascular tissue engineering. Biotechnol Bioeng 2009;104(6):1197-206.

33.   Gong Z, Niklason LE. Small-diameter human vessel wall engineered from bone marrow-derived mesenchymal stem cells (hMSCs). FASEB J 2008;22(6):1635-48.

34. Nesi G, Anichini C, Tozzini S, Boddi V, Calamai G, Gori F. Pathology of the thoracic aorta: a morphologic review of 338 surgical specimens over a 7-year period. Cardiovasc Pathol 2009;18(3):134-9.
35. De Syo D, Franjić BD, Lovricević I, Vukelić M, Palenkić H. Carotid bifurcation position and branching angle in patients with atherosclerotic carotid disease. Coll Antropol 2005;29(2):627-32.
36. Chaniotis AK, Kaiktsis L, Katritsis D, Efstathopoulos E, Pantos I, Marmarellis V. Computational study of pulsatile blood flow in prototype vessel geometries of coronary segments. Phys Med 2010;26(3):140-56.
37. Tuinenburg JC, Koning G, Rareş A, Janssen JP, Lansky AJ, Reiber JH. Dedicated bifurcation analysis: basic principles. Int J Cardiovasc Imaging 2011;27(2):167-74.
38. S M, Ghista DN, Chua LP, Seng TY. Numerical investigation of blood flow in a sequential aorto-coronary bypass graft model. Conf Proc IEEE Eng Med Biol Soc 2006;1:875-8.
39. Roy-Chaudhury P, Wang Y, Krishnamoorthy M, Zhang J, Banerjee R, Munda R, Heffelfinger S, Arend L. Cellular phenotypes in human stenotic lesions from haemodialysis vascular access. Nephrol Dial Transplant 2009;24(9):2786-91.
40. Hansen A, Eder A, Bönstrup M, Flato M, Mewe M, Schaaf S, Aksehirlioglu B, Schwörer A, Uebeler J, Eschenhagen T. Development of a drug screening platform based on engineered heart tissue. Circ Res 2010;107(1):35-44.
41. L'Heureux N, Stoclet JC, Auger FA, Lagaud GJ, Germain L, Andriantsitohaina R. A human tissue-engineered vascular media: a new model for pharmacological studies of contractile responses. FASEB J 2001;15(2):515-24.
42. Tung YC, Hsiao AY, Allen SG, Torisawa YS, Ho M, Takayama S. High-throughput 3D spheroid culture and drug testing using a 384 hanging drop array. Analyst 2011;136(3):473-8.
43. Härmä V, Virtanen J, Mäkelä R, Happonen A, Mpindi JP, Knuuttila M, Kohonen P, Lötjönen J, Kallioniemi O, Nees M. A comprehensive panel of three-dimensional models for studies of prostate cancer growth, invasion and drug responses. PLoS One 2010;5(5):e10431.
44. Kloss D, Fischer M, Rothermel A, Simon JC, Robitzki AA. Drug testing on 3D in vitro tissues trapped on a microcavity chip. Lab Chip 2008;8(6):879-84.
45. Horning JL, Sahoo SK, Vijayaraghavalu S, Dimitrijevic S, Vasir JK, Jain TK, Panda AK, Labhasetwar V. 3-D tumor model for in vitro evaluation of anticancer drugs. Mol Pharm 2008;5(5):849-62.
46. Maguire TJ, Novik E, Chao P, Barminko J, Nahmias Y, Yarmush ML, Cheng KC. Design and application of microfluidic systems for in vitro pharmacokinetic evaluation of drug candidates. Curr Drug Metab 2009;10(10):1192-9.

Appendix A: Reprint permission for "Engineered vascular tissue fabricated from aggregated smooth muscle cells" (Chapter 3)

Dear Ms Gwyther,

thank you very much for your request.

As to it, kindly be informed that permission is granted to reuse your article

Gwyther, T.A. et al: Cells Tissues Organs 2011;194:13-24

in your PhD thesis, **provided that full credit is given to the original source and S. Karger AG, Basel is mentioned.**

Please note that any further distribution of this article requires written permission again and may be subject to a permission fee.

Hopefully, I have been of assistance to you.
Best regards,

Tatjana Sepin
Rights and Permissions

S. Karger AG
Medical and Scientific Publishers
Allschwilerstrasse 10
CH - 4009 Basel
Tel +41 61 306 12 88
Fax +41 61 306 12 34
E-Mail permission@karger.ch